ON THE STABILITY AND NUMBER OF STEADY STATES OF CHEMICAL REACTION NETWORKS

A Dissertation

by

NIDA KAZI OBATAKE

Submitted to the Office of Graduate and Professional Studies of
Texas A&M University
in partial fulfillment of the requirements for the degree of

DOCTOR OF PHILOSOPHY

Chair of Committee,	Anne Shiu
Committee Members,	Frank Sottile
	Sarah Witherspoon
	Irina Gaynanova
Head of Department,	Sarah Witherspoon

August 2021

Major Subject: Mathematics

ABSTRACT

Chemical reaction networks model the interactions of chemical substances. An important aim is to understand the long-term behaviors of these chemical reactions, which are called steady states. Interesting behaviors have implications in biology, such as in cell-signaling or regulatory processes. This motivates the need to predict if and when a network can exhibit interesting long-term behavior. Exact values of the physical parameters that describe these networks are often unknown. Because of this, the goal is to prove results based on a network's structure alone, independent of any specific numerical values. This dissertation harnesses theoretical mathematical techniques to investigate the number and stability of steady states of a chemical reaction network.

In this dissertation, we answer the following: Does a given chemical reaction network have the capacity for Hopf bifurcations (an important unstable steady state)? How many steady states can it have? Our first contribution is a novel procedure for constructing a Hopf bifurcation of a chemical reaction network. This algorithm gives an easy-to-check condition for the existence of a Hopf bifurcation and explicitly constructs one if it exists. Our second set of contributions are new upper bounds on the number of steady states of a chemical reaction network. These new numerical invariants are both quick to compute and are surprisingly good bounds on the number of steady states.

As the main application of our new tools, we analyze an important biological cell-signaling network called the Extracellular signal Regulated Kinase (ERK) network. Malfunctions in the ERK network are linked with human diseases, including cancers and developmental abnormalities, making it crucial to understand the ERK network's long-term behavior. We show how the ERK network has the capacity for different dynamic regimes, including multiple steady states, two stable steady states, simple Hopf bifurcations, and a unique, stable steady state. Applying our new tools, we directly relate each dynamic behavior to the network structure, specifically the presence of certain species or reactions.

DEDICATION

To my Puppa. Soar in peace, my forever guide.

ACKNOWLEDGEMENTS

The completion of my dissertation would not have been possible without the supportive mentoring of my advisor, Professor Anne Shiu. Thank you for your guidance, encouragement, and patience throughout our projects together. From you I learned great mathematics, and I witnessed firsthand what success looks like for a researcher and a mentor. Thank you for giving me the opportunity to learn and grow from you!

I would like to express my deepest appreciation to my committee, Professor Frank Sottile and Professor Sarah Witherspoon from the Department of Mathematics and Professor Irina Gaynanova from the Department of Statistics. Thank you for your insightful comments and patience through this research. In particular, I would like to extend my deepest gratitude to Frank Sottile for patiently giving me ample opportunities to further my research career.

Special thanks to my collaborators Xiaoxian Tang, Angélica Torres, Carsten Conradi, and Dilruba Sofia; it was my pleasure to work with each of you on this dissertation's published work.

Thank you to the Texas A&M University Department of Mathematics for being my stimulating home during this journey. My academic success would not have been possible without the support and nurturing of my mentors. I extend my sincere thanks to Professors Laura Matusevich, Dean Baskin, Peter Howard, Maurice Rojas, and Peter Kuchment for fostering my development as a mathematician. Thanks also to Professors Elizabeth Gross, Heather Harrington, Elena Dimitrova, Julia Plavnik, Fatma Terzioglu, Frank Farris, Glenn Appleby, and Tim Hsu for your unwavering support over the years.

I would also like to acknowledge the phenomenal staff in the Texas A&M Department of Mathematics, especially Monique Stewart, David Manuel, Sherry Floyd, Cara Barton, and Sharon Esparza. Mama Sherry, thank you for the prayers, hugs, and love. Monique, thank you, for your endless patience. The completion of this degree would not have been possible without you.

I am thankful for the mathematics community. I thank Elisenda Feliu, Carsten Conradi, Eliz-

abeth Gross, Cvetelina Hill, Maya Mincheva, Stanislav Shvartsman, Frank Sottile, Elise Walker, Timo de Wolff, Henry Mattingly, Stanislav Shvartsman, Sascha Timme, Angélica Torres, Emanuele Ventura, and Taylor Brysiewicz for helpful discussions. I am grateful for numerous anonymous referees, whose suggestions greatly improved the quality of this dissertation's published work. Many thanks also to my EDGE family for fostering a community of stellar womxn in mathematics.

Cheers to my colleagues who quickly became friends with whom I shared both success and struggle. In particular, I had the great pleasure of learning from Justin Owen, Byeongsu Yu, Jonathan Tyler, Alexander Ruys de Perez, Pablo Ocal, John Griffin, Konrad Wrobel, Hannah Solomon, and Mansi Bezbaruah.

I cannot begin to express my thanks to my friends who quickly became family. To Nate Snyder, Sean Plummer, and Megan Meyer: thank you for the laughs, games, and fun times. To my best friends Aleksandra Sobieska Snyder, Andrew Kimball, and Elise Walker: I am so blessed to have met you. Thank you for all the loving memories that I will cherish forever. Special thanks to my "partner in math", Ola, for being by my side every day through it all. There are no words to express how grateful I am for you so I will simply say this: love you, girl.

Finally, I would also like to extend my deepest gratitude to my family whose seemingly unsubstantiated confidence consistently lifted me up over the years.

Thank you to my in-laws, Andrew, Stephanie, and Mark Obatake for accepting me as one of your own. Thank you to my superstar sister, Akaxia Cruz, for always amping me up.

Thank you also to my son, Zaid, for the added challenge of writing a dissertation on minimal hours of sleep. I love you, light of my life, and I cannot imagine the end of this journey without you. Thanks for being my newest source of inspiration.

I will never be done thanking my siblings, who have supported me throughout their entire lives. Zeeshawn, I have laughed with you, cried with you, looked up to you, and sought out advice from you. Thanks for reminding me of the beauty and intricacies in the little things I would otherwise overlook. Love you, Zeeshawn. Zerreen, thank you for motivating me through any challenge. You have fueled my strength and power with which I can accomplish anything. Love you, Zerreen.

To my parents, Shehnaz and Phiroze Kazi, thank you for giving me life and for your unconditional love. Mom, thanks for being exactly what I needed at every step of the way. Thank you for being the best role model, problem solver, peace keeper, best friend, shoulder to cry on, and everything else in between. I love you beyond words, Mommy. Puppa, thanks for sparking my love of mathematics and for showing me what perseverance looks like. As you were always more than your physical presence, in every step, in every moment, without an iota of a doubt, you are with me. I love you, Puppa.

David, love of my life, we did it. Years ago when we started our life together you vowed your eternal support and I am forever grateful.

CONTRIBUTORS AND FUNDING SOURCES

Contributors

This work was supported by a dissertation committee consisting of Professor Shiu, Professor Sottile, and Professor Witherspoon of the Department of Mathematics and Professor Gaynanova of the Department of Statistics.

The research in Sections 3.1–3.3, Chapter 4, Sections 6.2–6.3, and Appendix A was conducted jointly with Anne Shiu, Xiaoxian Tang, and Angélica Torres. The research in Section 3.4, Chapter 5, and Appendix B was conducted jointly with Carsten Conradi, Anne Shiu, and Xiaoxian Tang. The research in Sections 6.4–6.5 was conducted jointly with Anne Shiu and Dilruba Sofia. The research in Chapter 7 and Appendix D was conducted jointly with Elise Walker. All other work conducted for the dissertation was completed by the student independently.

Funding Sources

Graduate study was supported by the H.B. Curtis Fellowship in Mathematics from Texas A&M University, NSF grant DMS-1752672, and an American Fellowship from AAUW.

TABLE OF CONTENTS

Page

LIST OF FIGURES

FIGURE Page

LIST OF TABLES

TABLE Page

1. INTRODUCTION

1.1 Overview

This dissertation concerns the mathematical study of chemical reaction networks. These networks model the interactions of chemical substances. An important aim is to understand the long-term behaviors of these chemical reactions. One can ask, for example, does the long-term behavior settle down in a *steady state*? Interesting behaviors – such as two stable steady states (called *bistability*) or certain unstable steady states (called *Hopf bifurcations*) – have implications in biology, such as in cell-signaling or regulatory processes. This motivates the need to predict if and when a network can exhibit such interesting long-term behavior.

One important network describes the activation of the extracellular signal-regulated kinase, called the *ERK network*. This kinase regulates many cellular activities including "mitosis, survival, apoptosis, differentiation, and metabolism" [14]. Malfunctions in the ERK network are linked with human diseases, including cancers and developmental abnormalities, making it crucial to understand the ERK network's long-term behavior. Furthermore, the ERK network is a prototype for more complicated networks. Despite its biological importance, the theoretical knowledge about the ERK network's dynamics is limited; prior to the work in this dissertation, most results about the behaviors of the ERK network were only experimental.

A theoretical understanding of chemical reaction networks will allow biochemists to better predict the results of their experiments. Indeed, understanding the long-term behavior of the ERK network will help researchers develop drugs to target parts of this network. Accordingly, this dissertation develops a mathematical framework for characterizing the behavior of signaling pathways modeled by polynomial dynamical systems by exploiting the information encoded in their polynomial structure. In particular, by identifying and understanding steady states mathematically, the methods developed here will predict the long-term behavior of chemical reactions without actually carrying out the reactions. Indeed, this dissertation contributes new algebraic-geometric methods

for predicting the number and stability of steady states of chemical reaction networks.

1.1.1 Outline of dissertation

This dissertation addresses the following questions.

Question 1.1.1. *Given a chemical reaction network:*

(A) How many steady states can the network have?

(B) Can the network have a Hopf bifurcation?

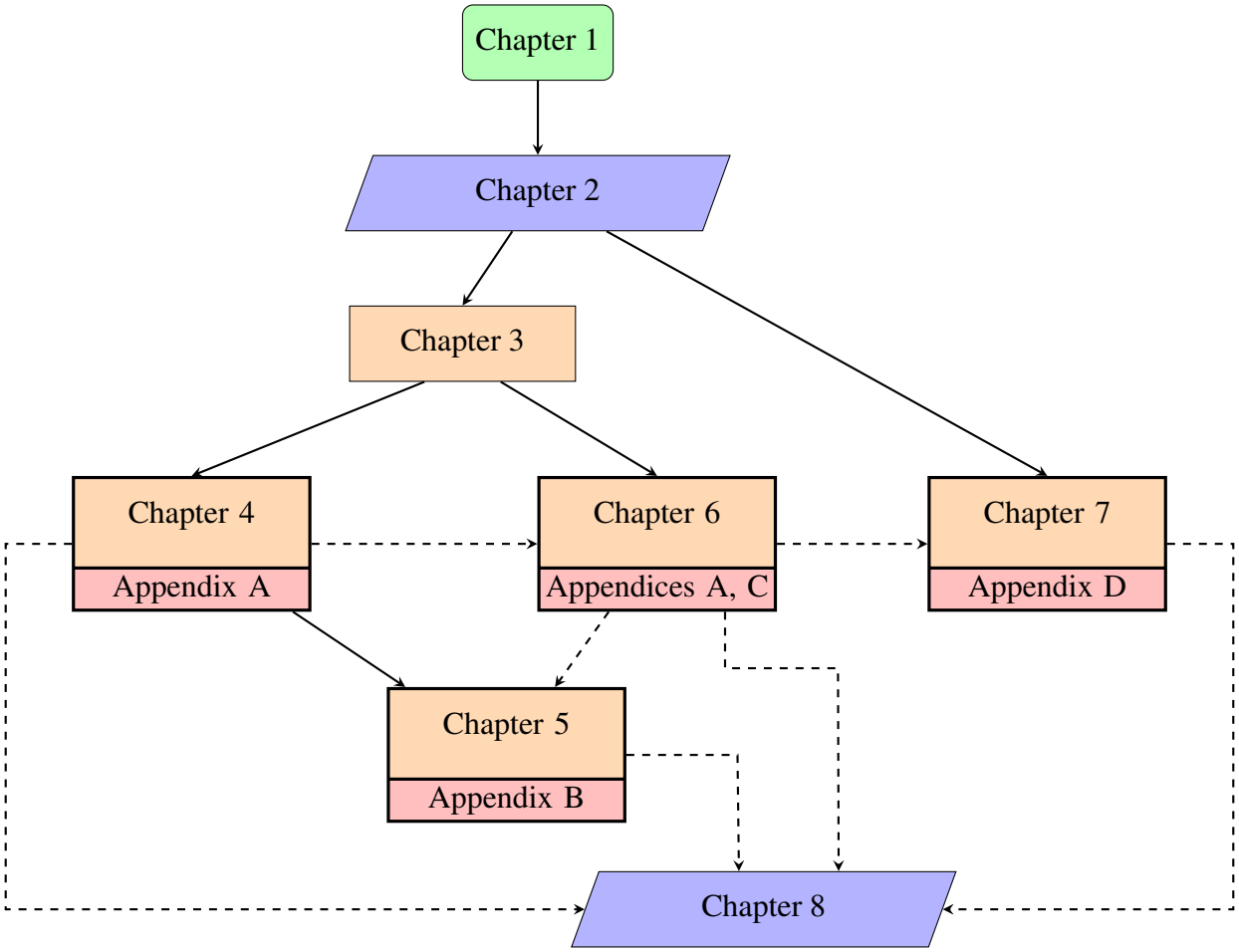

Figure 1.1: A flow chart of the interdependencies of this dissertation's chapters. Solid arrows indicate prerequisite material is required, and dashed arrows indicate prerequisite chapter is recommended but not strictly required.

In Chapter 2, we introduce chemical reaction network basics and recall core concepts from applied algebraic geometry. Chapter 3 sets up the mathematical formulation for the ERK networks that we will need in Chapters 4, 5, and 6.

The dynamics of ERK regulation is the focus of Chapters 4 and 5. Chapter 4 answers an open question about the dynamics of a model of ERK regulation, originally posed in [86]. Our partial answer to [86]'s question produced a surprising fact: the interesting dynamics of the ERK network are robust. Chapter 5 extends the existence results from Chapter 4 and explains the robustness of the dynamics exhibited by ERK subnetworks.

Chapter 6 introduces a chemical reaction network's mixed volume, a parameter-free numerical invariant that is an upper bound on the number of its steady states. We show that this numerical invariant is easy to compute and gives good bounds for many biological signalling networks, including the ERK networks from Chapter 3. In Chapter 7, we introduce another numerical invariant – the volume of the Newton-Okounkov body of a chemical reaction network. We include examples and investigate how the maximum number of steady states compares to the volume of its Newton-Okounkov body.

Finally, Chapter 8 poses open problems and future directions in chemical reaction network theory resulting from this dissertation. The appendices contain supplementary files for associated computations: Appendix A is associated with Chapter 4 and parts of Chapter 6, Appendix B with Chapter 5, Appendix C with Chapter 6, and Appendix D with Chapter 7.

The material in Chapter 3, Chapter 4, and Sections 6.2–6.3 of Chapter 6 is based on the published paper "Oscillations and bistability in a model of ERK regulation" [78], which was authored jointly with Anne Shiu, Xiaoxian Tang, and Angélica Torres. The material in Chapter 3 and Chapter 5 is based on the published paper "Dynamics of ERK regulation in the processive limit" [24], which was authored jointly with Carsten Conradi, Anne Shiu, and Xiaoxian Tang. Sections 6.4–6.5 of Chapter 6 are based on the published paper "Mixed volume of small reaction networks" [77], which is jointly authored with Anne Shiu and Dilruba Sofia. Section 6.6 of Chapter 6 contains new, unpublished material based on joint work with Anne Shiu. Finally, Chapter 7 contains new,

unpublished material based on joint work with Elise Walker.

The rest of this chapter concludes as follows. We translate the two guiding biological questions from Question 1.1.1 into mathematical questions. We explain the challenges associated with answering each mathematical question and intuitively explain the mathematical framework we develop in the main results chapter for answering these questions. Along the way, we highlight the main results of this dissertation.

1.2 Biological motivation: the ERK network

Theoretical results about chemical reaction networks explain qualitative information about their solutions. Our mathematical work expands upon biologist's experimental results. Models of phosphorylation cycles, an important family of biochemical reaction networks, have been studied by computational biologists since at least the early 2000s because they are minimal models of more complicated cell regulation systems. These model networks include the mixed-mechanism, processive, and distributive dual-site phosphorylation mechanisms and are summarized in [43]. Dual-site phosphorylation networks will serve as a case study for theoretical results presented in this thesis. Specifically, in this dissertation, we will analyze the ERK network and its subnetworks.

The *ERK network* depicted in Figure 1.2 is a model for the dual-site phosphorylation and dephosphorylation of extracellular signal-regulated kinase. This network involves 12 species participating in 18 reactions. The ERK network exhibits multiple steady states, is *bistable* (has at least two stable steady-states), and undergoes periodic oscillations for some choice of rate constants and total species concentrations [86]. However, these results were largely based on experimentation via parameter sampling. This method did not provide a rigorous insight into the occurrence of these phenomena.

The ERK network reduces to the fully processive (dual-site phosphorylation) network when all vertical reactions are omitted (those labeled by $k_{\text{on}}, k_{\text{off}}, m_1, m_2, m_3, \ell_{\text{on}}, \ell_{\text{off}}, n_1, n_2, n_3$). The fully processive network is known to have a unique, stable steady state [25, 35].

The stark contrast in the dynamics of the ERK network and the fully processive network begs the following natural question, originally posed in [86].

Question 1.2.1. *How are multiple steady states and oscillations lost as reactions are removed from the ERK network until it becomes the processive network? (See Figure 1.3.)*

More specifically, bistability is lost as reactions are removed and, moreover, the capacity for multiple steady states is also lost. How robust is bistability to existence of reactions and specific parameter values? Similarly, oscillations are lost as the reactions are removed and the network is simplified. How "close" to the limit (the fully processive network) can we get while still keeping the interesting dynamics of the ERK network?

By developing methods for solving the problems posed in Question 1.1.1, this dissertation provides a systematic way of understanding the dynamics between the ERK network and the fully processive network, thereby answering Question 1.2.1.

1.3 Methodology: algebraic-geometric methods for chemical reaction networks

As we will see in Section 2.2.1, chemical reaction networks are modeled mathematically by polynomial equations (2.1). Due to their ubiquity in modeling real-world phenomena, polyno-

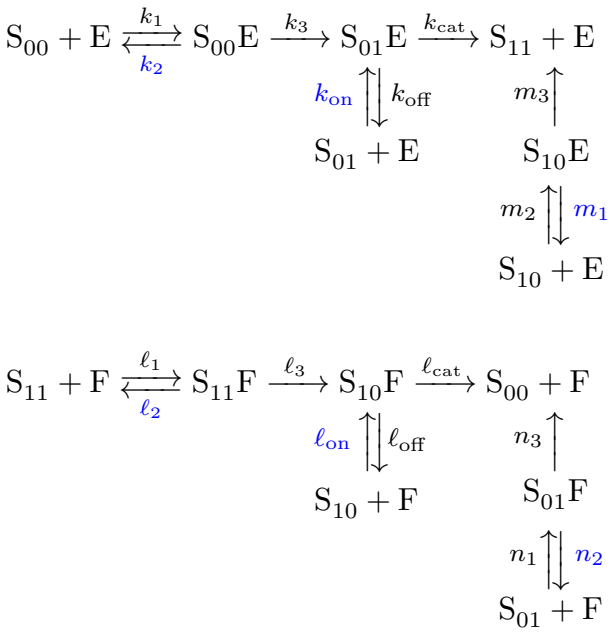

Figure 1.2: The ERK reaction network. Reprinted with permission from [78].

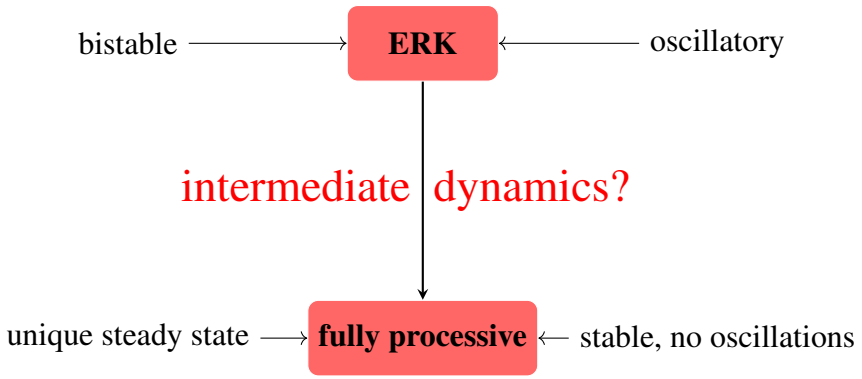

Figure 1.3: Known results on stability in the ERK network and its distinguished subnetwork, the fully processive network. Rubinstein et. al [86] showed that the full ERK network exhibits bistability and oscillations for specified rate constants, and [25, 35] showed that the fully processive network does *not* admit bistability nor oscillations, i.e. it can only have a unique, stable steady state.

mial equations are well-studied. There is an entire branch of mathematics dedicated to solving polynomial systems, called *(applied) algebraic geometry*. Moreover, in the biological context, all numerical quantities are real numbers. This brings us to the world of *real* algebraic geometry. Here, we can use algebraic and geometric techniques to solve real polynomial systems. If we further specialize to *positive* real algebraic geometry, we restrict to finding solutions that are biologically meaningful.

The broad goal in chemical reaction network theory is to predict a network's long-term dynamics from its structure alone. This means that we aim for results independent of specific numerical values. Using algebraic geometry, we take advantage of symbolic computations. As surveyed in [31], researchers have successfully used algebreo-geometric techniques for identifying: the capacity for multiple steady states, the stability of steady states, parameter regions where interesting dynamics can occur, steady-state invariants, etc.

In this dissertation, we will continue in this spirit. Our methodology to answer Question 1.1.1 will be the following: reframe biochemical questions as mathematical questions and use algebraic and geometric techniques to solve them.

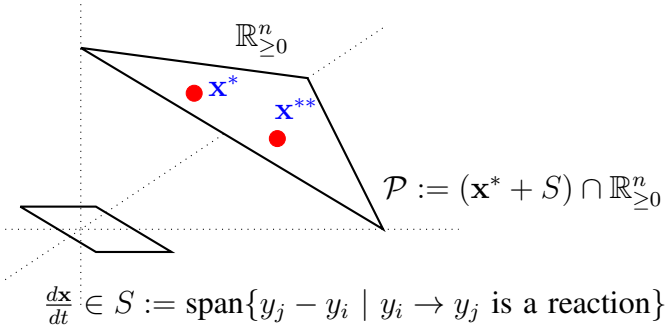

Figure 1.4: Two steady states, x^* and x^{**}, of a chemical reaction network.

1.3.1 Answering Question 1.1.1(A)

Chapters 6 and 7 address Question 1.1.1(A): counting the maximum number of steady states of a given network.

A steady state of a dynamical system is a set of initial conditions for which the species' concentrations remain constant, i.e., they do not change with time. See Figure 1.4 for a depiction of a chemical reaction network with multiple steady states x^* and x^{**}. Biologically, multiple steady states can be interpreted as a "switch": given a fixed set of parameters, the cell has a choice to converge to a state x^* or x^{**}.

Recall that a chemical reaction network's dynamical system is defined by a system of polynomials. Then finding steady states of a chemical reaction network amounts to solving a system of polynomial equations, where we restrict ourselves to solutions that lie in the real, positive orthant (they are biologically meaningful).

For general networks, much has been done for determining which networks admit multiple steady states – see e.g., [21, 28, 33, 37, 45, 65, 75] – but there are few techniques for determining a network's maximum number of steady states. To this end, we introduce two related measures of a network, the maximum number of complex-number steady states and the "mixed volume". We see that for many biological signaling networks, the mixed volume gives a good bound for its maximum number of steady states. Our new results extend techniques for deciding the existence of multistationarity by giving precise bounds on the maximum number of steady states. Moreover,

our results can be generalized to any parametrized polynomial dynamical system.

The Bernstein-Khovanskii-Kushnirenko (BKK) theorem (Proposition 6.2.2), a classical result in algebraic geometry, states that the maximum number of nonzero complex solutions to a polynomial system is given by the mixed volume of the Newton polytopes of its defining polynomials [8]. The mixed volume is a non-negative number assigned to a set of polytopes. The BKK theorem uses this geometric invariant, the mixed volume, associated to a polynomial system to convey algebraic information, namely its maximum number of nonzero solutions. Since any positive real steady state is also a complex steady state, Bernstein's theorem implies an upper bound on the number of biologically meaningful steady states of a network. How close is this bound to the actual number of steady states?

Accordingly, in Chapter 6, we propose a new definition of mixed volume of a chemical reaction network. In preliminary examples, we notice that the mixed volume is quick to compute since the polynomials defining a chemical reaction network are sparse and have low degree. When the mixed volume is equal to the maximum number of steady states of a network, this new tool will give a fast method for answering Question 1.1.1(A) for an arbitrary network. Moreover, the mixed volume depends only on the network's structure. This is a major plus: recall that our ultimate goal is to understand behaviors of a network without knowing exact numerical values of the parameters or species.

Recall that the ERK network (Figure 1.2) loses bistability and hence the capacity for multiple (stable) steady states as the vertical reactions are omitted; there is a change in the maximum number of steady states as we move from this network to its subnetwork. Can mixed volume predict this loss?

Our main results from Chapter 6 are as follows. For the ERK (sub)networks, the mixed volume does not greatly exceed the maximum number of steady states. Next, we completely classified the number of steady states for "small" reaction networks: In particular, 92% of all two-species, two-reaction networks have mixed volume equal to its maximum number of steady states. Thus, the mixed volume efficiently calculates the number of cell-states for these networks. Finally, we

compare related notions of mixed volume for reaction networks.

In Chapter 7, we introduce another numerical invariant – the volume of the Newton-Okounkov body of a chemical reaction network. By leveraging algebraic structure in a network's defining equations, the volume of the associated Newton-Okounkov body can improve the mixed volume bound. We include examples and investigate how the maximum number of steady states compares to the volume of its Newton-Okounkov body.

1.3.2 Answering Question 1.1.1(B)

Chapters 4 and 5 concern Question 1.1.1(B): whether a given network can have a Hopf bifurcation. Assume you have a steady state. How can you understand if it is a Hopf bifurcation?

A *Hopf bifurcation* is an unstable steady state that produces *oscillations* in the species' concentrations [70], as depicted in Figure 1.5.

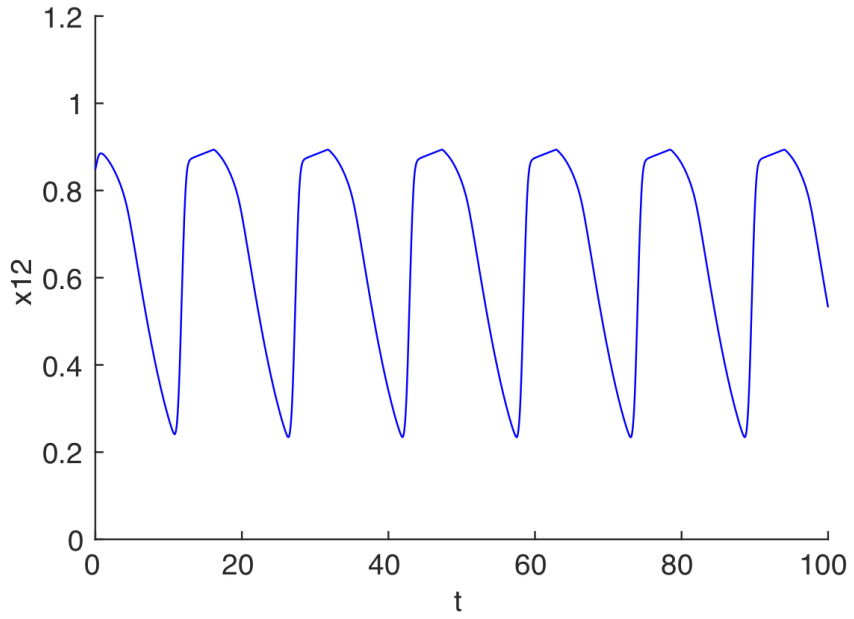

Figure 1.5: Periodic oscillations resulting from a Hopf bifurcation. The horizontal axis represents time and the vertical axis represents the concentration of a chemical species.

Recall, however, that exact numerical values are often unknown, so we cannot determine *a*

priori the eigenvalues' nature. To bypass this issue, we apply a criterion of Yang that characterizes Hopf bifurcations in terms of a system of polynomial inequalities and equations [106]. However, typical applications of Yang's criterion are to dynamical systems in 2-3 variables with one free parameter. Applying this criterion to chemical reaction networks – which involve tens of variables and even more parameters – turns the intractible problem of determining the nature of parametrized eigenvalues into a difficult, but theoretically possible problem of solving a system of polynomial inequalities.

To give an idea of the complexity of the system, we note that `Maple` cannot even compute the defining polynomials for Yang's criterion of the ERK network, which has 12 variables and 18 parameters: the computation times out.

This computational complexity arises because the polynomials defining these inequalities are

- numerous: there are at most as many polynomials as there are species in the network,
- large: they involve a number of variables equal to the number of species in the network, in addition to the number of reaction rate constants, and
- have high degree: they are obtained by taking determinants of *Hurwitz matrices*, which have as their entries coefficients of the determinant of the Jacobian matrix.

Even after some preprocessing and specialization of values, we reduce the system to 4 variables and 1 parameter, but still cannot solve this system with existing solvers.

We tackle this problem by generalizing the following classical result about polynomials. Given a univariate polynomial, the limit of the polynomial $f(x_1) = a_0 + a_1 x_1 + \ldots + a_n x_1^n$ (for $n \in \mathbb{N}$) as $x_1 \to \infty$ is $\text{sign}(a_n)\infty$, because as x_1 becomes large enough, $f(x_1) \approx a_n x_1^n$. That is, we force the polynomial to take the sign of its leading coefficient by setting the variable's value large enough. This naturally generalizes to multivariate polynomials; in this setting, the extreme terms that can dominate the polynomial are in bijection with the vertices of its Newton polytope. Simply put, we can use the geometric structure of a polynomial to pick a point in the positive orthant for which the polynomial achieves a desired sign, and so satisfies a desired inequality.

This dissertation will introduce a procedure that builds on this idea. Applying this procedure will solve the system of polynomial inequalities defining a Hopf bifurcation of a chemical reaction network and thus will (1) determine if there is a Hopf bifurcation, and (2) construct one, if it exists. In the case of the ERK network, this procedure may be used to construct a Hopf bifurcation of a subnetwork, giving a partial answer to Question 1.2.1.

The dynamics of ERK regulation is the focus of Chapters 4 and 5. Chapter 4 answers an open question about the dynamics of a model of ERK regulation, originally posed in [86]. Our partial answer to [86]'s question produced a surprising fact: the interesting dynamics of the ERK network are robust. In contrast to [86]'s parameter sampling methods, we employ symbolic methods to provide rigorous insight into the existence of these phenomena. We show that only two of the network's 18 parameters control bistability. Pivotal to this insight is a positive parametrization that gives us access to key parameters. Our oscillation results are aided by our new Newton-polytope method, a novel algorithm that combines control theory with convex geometry to construct a Hopf bifurcation (unstable steady state yielding oscillations in the solution). Chapter 5 extends the existence results from Chapter 4 and explains the robustness of the dynamics exhibited by ERK subnetworks.

2. PRELIMINARY DEFINITIONS

2.1 Overview of chemical reaction network theory

Chemical reaction network theory studies the interactions of chemical species [38]. Chemical reaction networks are known to exhibit wildly different dynamical behaviors, and when the interacting species are biochemical in nature, these dynamical behaviors have important biological consequences. A major goal in this area is to link a network's possible dynamics to its structure alone.

A toy example of a chemical reaction network is A + B $\xrightarrow{\kappa_1}$ AB. This network consists of a single *reaction*, where one unit each of two reacting *species*, A and B, react to produce one unit of the species AB. The nonnegative integer combination A + B of one unit of species A and one unit of species B (and zero units of AB) is called a chemical *complex*. The *reactant*, here A + B, is the chemical complex that is present at the start of the reaction, and the *product* is the complex that is present at the end of a chemical reaction, in this case AB. In this example, the *reaction rate constant* κ_1 is not specified, but it is assumed to be some nonnegative real number.

In general, we can model a chemical reaction by a finite, weighted, directed graph whose vertices are chemical complexes (which themselves are nonnegative integer combinations of chemical *species*) and whose directed edges are labeled by nonnegative real numbers, which we refer to as *reaction rate constants*. We provide these formal definitions in Section 2.2.1.

We want to understand the species' concentrations at any time t. Let

$$x(t) = (x_1(t), x_2(t), \ldots, x_s(t)) \in \mathbb{R}^s_{\geq 0}$$

denote the vector of the concentrations of the species $\{X_1, X_2, \ldots, X_s\}$ over time t. To mathematically model the species' concentrations of a network, we make the mild assumption that molecules are distributed throughout the system evenly. The law of mass-action kinetics, which dates back to the mid-1800s [38], is an intuitive law that states that the rate of a reaction is proportional to

the product of the concentrations of the species in the reactant. Mathematically, the law of mass-action implies that we can model the change over time of a network's species' concentrations by an *autonomous system of parametrized polynomial ordinary differential equations* – see (2.1).

Fully understanding a dynamical system would amount to finding a solution $x(t)$ of the system of ordinary differential equations. There are some techniques for solving systems of *linear* ordinary equations, but in general, very few *nonlinear* systems – as we have in the case of most chemical reaction networks – can be solved explicitly. Even numerical integration is computationally expensive, since parameters are numerous and have unknown or noisy values. Instead, we shift our attention to understanding, as best we can, the nature of the solutions. By understanding a system's steady states and their stability properties, we capture valuable qualitative information about the solution.

Perhaps the best known classical result in chemical reaction network theory is the *Deficiency Zero Theorem* [60, 61]. This theorem deduces the existence of a unique, stable steady state from easy-to-compute properties of a network – namely the number of stoichiometrically distinct complexes, the number of linkage classes, and the weak-reversibility of the network. It can be thought of as the "gold-standard" for results in chemical reaction network theory since it gives information about both the number and stability of steady states of a network, independent of any choice of parameter values or initial conditions. We aim for such results in this dissertation.

2.2 The mathematics of chemical reaction networks

In this section, we formally introduce chemical reaction networks and their dynamical systems (Section 2.2.1), steady states (Section 2.2.2), Hopf bifurcations – a distinguished unstable steady state – (Section 2.2.3), and steady-state parametrizations (Section 2.2.4). We refer the reader to [31, 38] for more on chemical reaction network theory. The interested reader is encouraged to seek out the forthcoming book of Dickenstein and Feliu for more on algebraic methods for biochemical reaction networks.

2.2.1 Chemical reaction networks and their dynamical systems

The notation in this dissertation closely matches that of [21, 33].

A reaction network G (or *network* for short) comprises a set of s species $\{X_1, X_2, \ldots, X_s\}$ and a set of m reactions:

$$\alpha_{1j}X_1 + \alpha_{2j}X_2 + \cdots + \alpha_{sj}X_s \xrightarrow{\kappa_j} \beta_{1j}X_1 + \beta_{2j}X_2 + \cdots + \beta_{sj}X_s\ , \qquad \text{for } j = 1, 2, \ldots, m\ ,$$

where each α_{ij} and β_{ij} is a non-negative integer called a stoichiometric coefficient and each κ_j is a nonnegative real number called a reaction rate constant. The stoichiometric matrix of G, denoted by N, is the $s \times m$ matrix with (i, j)-entry equal to $\beta_{ij} - \alpha_{ij}$. Let $d = s - \operatorname{rank}(N)$. The stoichiometric subspace, denoted by S, is the image of N, that is, S is the vector subspace of $\mathbb{R}^s$ generated by the columns of N. A conservation-law matrix of G, denoted by W, is a row-reduced $d \times s$-matrix whose rows form a basis of the orthogonal complement of S. If there exists a choice of W for which every entry is nonnegative and each column contains at least one nonzero entry (equivalently, each species occurs in at least one nonnegative conservation law), then G is conservative. A reaction network G is genuine if every species takes part in at least one reaction.

We denote the concentrations of the species $X_1, X_2, \ldots, X_s$ by $x_1, x_2, \ldots, x_s$, respectively. These concentrations, under the assumption of *mass-action kinetics*, evolve in time according to the following system of ordinary differential equations (ODEs):

$$\dot{x} \;=\; f(x) \;:=\; N \cdot \begin{pmatrix} \kappa_1\, x_1^{\alpha_{11}} x_2^{\alpha_{21}} \cdots x_s^{\alpha_{s1}} \\ \kappa_2\, x_1^{\alpha_{12}} x_2^{\alpha_{22}} \cdots x_s^{\alpha_{s2}} \\ \vdots \\ \kappa_m\, x_1^{\alpha_{1m}} x_2^{\alpha_{2m}} \cdots x_s^{\alpha_{sm}} \end{pmatrix}\ , \tag{2.1}$$

where $x = (x_1, x_2, \ldots, x_s)$, and each $\kappa_j \in \mathbb{R}_{>0}$. By considering the rate constants as a vector of parameters $\kappa = (\kappa_1, \kappa_2, \ldots, \kappa_m)$, we have polynomials $f_{\kappa,i} \in \mathbb{Q}[\kappa, x]$, for $i = 1, 2, \ldots, s$. For ease of notation, we often write f_i rather than $f_{\kappa,i}$.

A trajectory $x(t)$ beginning at a positive vector $x(0) = x^0 \in \mathbb{R}^s_{>0}$ remains, for all positive time, in the following stoichiometric compatibility class with respect to the total-constant vector $c \coloneqq Wx^0 \in \mathbb{R}^d$:

$$\mathcal{S}_c \coloneqq \{x \in \mathbb{R}^s_{\geq 0} \mid Wx = c\} . \tag{2.2}$$

Example 2.2.1. Consider the network $G = \{2\,\mathrm{A} \xrightarrow{k_1} 2\,\mathrm{B}\ ,\ \mathrm{B} \xrightarrow{k_2} \mathrm{A}\}$. This network comprises $s = 2$ species, A and B, and has $m = 2$ non-reversible reactions involving 4 distinct complexes – represented as vectors $(2,0),\ (0,2),\ (0,1),\ (1,0)$ Also, the network is genuine and at-most-bimolecular. The stoichiometric matrix of G is

$$\Gamma = \begin{bmatrix} -2 & 1 \\ 2 & -1 \end{bmatrix} .$$

The stoichiometric subspace S, which has dimension $d = 1$, is spanned by $(1,-1)^{\mathrm{T}}$, and a conservation-law matrix of G is $W = \begin{bmatrix} 1 & 1 \end{bmatrix}$. Let $x(t) = (x_1(t), x_2(t)) \in \mathbb{R}^2_{\geq 0}$ denote the vector of concentrations of species A and B. A conservation law for G is $x_1 + x_2 = c_1$ for $c_1 \in \mathbb{R}_{\geq 0}$. The chemical reaction system (2.1) of G arising from mass-action kinetics is

$$\dot{x} = \frac{dx}{dt} = \begin{pmatrix} -2k_1 x_1^2 + k_2 x_2 \\ 2k_1 x_1^2 - k_2 x_2 \end{pmatrix} .$$

2.2.2 Steady states

Recall from Section 2.1 that we will not attempt to find exact solutions to the ordinary differential equations (2.1). Instead, our strategy will be to study the fixed points of these differential equations, which we will call *steady states*[1]. By analyzing steady states and the local stability of the steady states, we can piece together an understanding of the possible, qualitatively different

[1] In the dynamical systems theory, a steady state is also called an *equilibrium solution* or a *fixed point*.

trajectories of the system (2.1). Our main tool for stability analysis will be the *Jacobian matrix*, which can be seen as a multivariable analog of the derivative. We refer the reader to the introductory text [94] for more on nonlinear dynamics with an emphasis on applications.

A steady state of (2.1) is a nonnegative concentration vector $x^* \in \mathbb{R}^s_{\geq 0}$ at which the right-hand sides of the ODEs (2.1) vanish: $f(x^*) = 0$. We distinguish between positive steady states $x^* \in \mathbb{R}^s_{>0}$ and boundary steady states $x^* \in \mathbb{R}^s_{\geq 0} \backslash \mathbb{R}^s_{>0}$.

The Jacobian matrix of a dynamical system is the matrix of all first-order partial derivatives of its defining functions. For example, the Jacobian matrix, $\mathrm{Jac}(f)$, of the system $\dot{x} = f(x)$ (2.1) with respect to x is the $s \times s$ matrix with (i, j) entry $\frac{\partial f_{\kappa,i}(x)}{\partial x_j}$. Recall that the behavior of a (differentiable) function around a point is approximated by its tangent line at that point. Analogously, we can use the Jacobian matrix of a dynamical system at a steady state to understand the local behavior of the corresponding nonlinear dynamical system nearby.

A steady state x^* is nondegenerate if $\mathrm{Im}\,(\mathrm{Jac}(f)(x^*)|_S)$ is the stoichiometric subspace S. (Here, $\mathrm{Jac}(f)(x^*)$ is the Jacobian matrix of f, with respect to x, at x^*.) A nondegenerate steady state is exponentially stable if each of the $\dim(S)$ nonzero eigenvalues of $\mathrm{Jac}(f)(x^*)$ has negative real part.

A network is multistationary if there exists a positive rate-constant vector $\kappa \in \mathbb{R}^m_{>0}$ such that there exist two or more positive steady states of (2.1) in some stoichiometric compatibility class (2.2). Similarly, a network is bistable if there exists a positive rate-constant vector $\kappa \in \mathbb{R}^m_{>0}$ such that there exists two or more *exponentially stable* positive steady states of (2.1) in some stoichiometric compatibility class (2.2). Thus, every bistable network is multistationary. A network is monostationary[2] if, for every choice of positive rate constants, there is exactly one positive steady state in every stoichiometric compatibility class.

To analyze steady states within a stoichiometric compatibility class, we will use conservation laws in place of linearly dependent steady-state equations, as follows. Let $I = \{i_1 < i_2 < \cdots < i_d\}$ denote the indices of the first nonzero coordinate of the rows of conservation-law matrix W.

[2]Some authors define *monostationary* to be non-multistationary; the two definitions are equivalent for the ERK networks in this dissertation.

Consider the function $f_{c,\kappa} : \mathbb{R}^s_{\geq 0} \to \mathbb{R}^s$ defined by

$$f_{c,\kappa,i} = f_{c,\kappa}(x)_i := \begin{cases} f_i(x) & \text{if } i \notin I, \\ (Wx - c)_k & \text{if } i = i_k \in I. \end{cases} \tag{2.3}$$

We call system (2.3), the system augmented by conservation laws or just the augmented system. By construction, positive roots of the system of polynomial equations $f_{c,\kappa} = 0$ are precisely the positive steady states of (2.1) in the stoichiometric compatibility class (2.2) defined by the total-constant vector c.

2.2.3 Hopf bifurcations

A simple Hopf bifurcation is a bifurcation in which a single complex-conjugate pair of eigenvalues of the Jacobian matrix crosses the imaginary axis as some system parameter varies, while all other eigenvalues remain with negative real parts. Such a bifurcation generates oscillations or periodic orbits [70]. Figure 2.1 depicts oscillations resulting from a Hopf bifurcation. In this dissertation, we will only consider simple Hopf bifurcations, so we will use Hopf bifurcation to mean a simple Hopf bifurcation.

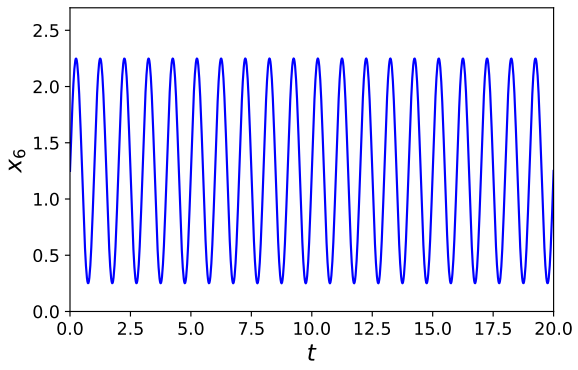

Figure 2.1: Periodic oscillations resulting from a Hopf bifurcation. The horizontal axis represents time and the vertical axis represents the concentration of a chemical species.

To detect simple Hopf bifurcations, we will use a criterion of Yang [106] that characterizes Hopf bifurcations in terms of *Hurwitz-matrix* determinants (Proposition 2.2.3).

Definition 2.2.2. The i-th Hurwitz matrix of a univariate polynomial $p(\lambda) = b_0\lambda^n + b_1\lambda^{n-1} + \cdots + b_n$ is the following $i \times i$ matrix:

$$H_i \;=\; \begin{pmatrix} b_1 & b_0 & 0 & 0 & 0 & \cdots & 0 \\ b_3 & b_2 & b_1 & b_0 & 0 & \cdots & 0 \\ \vdots & \vdots & \vdots & \vdots & \vdots & & \vdots \\ b_{2i-1} & b_{2i-2} & b_{2i-3} & b_{2i-4} & b_{2i-5} & \cdots & b_i \end{pmatrix},$$

in which the (k,l)-th entry is b_{2k-l} as long as $n \geq 2k - l \geq 0$, and 0 otherwise.

Consider an ODE system parametrized by $\mu \in \mathbb{R}$:

$$\dot{x} \;=\; g_\mu(x)\,,$$

where $x \in \mathbb{R}^n$, and $g_\mu(x)$ varies smoothly in μ and x. Assume that $x^0 \in \mathbb{R}^n$ is a steady state of the system defined by μ_0, that is, $g_{\mu_0}(x^0) = 0$. Assume, furthermore, that we have a smooth curve of steady states:

$$\mu \;\mapsto\; x(\mu)$$

(that is, $g_\mu\left(x(\mu)\right) = 0$ for all μ) and that $x(\mu_0) = x^0$. Denote the characteristic polynomial of the Jacobian matrix of g_μ, evaluated at $x(\mu)$, as follows:

$$p_\mu(\lambda) \;:=\; \det\left(\lambda I - \operatorname{Jac} g_\mu\right)|_{x=x(\mu)} \;=\; \lambda^n + b_1(\mu)\lambda^{n-1} + \cdots + b_n(\mu)\,,$$

and, for $i = 1, \ldots, n$, define $H_i(\mu)$ to be the i-th Hurwitz matrix of $p_\mu(\lambda)$.

Proposition 2.2.3 (Yang's criterion [106])**.** *Assume the above setup. Then, there is a simple Hopf bifurcation at x_0 with respect to μ if and only if the following hold:*

(i) $b_n(\mu_0) > 0$,

(ii) $\det H_1(\mu_0) > 0$, $\det H_2(\mu_0) > 0$, $\ldots$, $\det H_{n-2}(\mu_0) > 0$, *and*

(iii) $\det H_{n-1}(\mu_0) = 0$ *and* $\frac{d(\det H_{n-1}(\mu))}{d\mu}|_{\mu=\mu_0} \neq 0$.

2.2.4 Steady-state parametrizations

Here we introduce steady-state parametrizations (Definition 2.2.5) and recall from [33] how to use them to determine whether a network is multistationary (Proposition 2.2.7). Later we will see how to use these parametrizations to detect Hopf bifurcations (Proposition 4.2.1).

Definition 2.2.4. Let G be a network with m reactions and s species, and let $\dot{x} = f(x)$ denote the resulting mass-action system. Denote by W a $d \times s$ row-reduced conservation-law matrix and by I the set of indices of the first nonzero coordinates of its rows. Enumerate the complement of I as follows: $[s] \setminus I = \{j_1 < j_2 < \cdots < j_{s-d}\}$. A set of effective parameters for G is formed by polynomials $\bar{a}_1(\kappa), \bar{a}_2(\kappa), \ldots, \bar{a}_{\bar{m}}(\kappa) \in \mathbb{Q}(\kappa)$ for which the following hold:

(i) $\bar{a}_i(\kappa^*)$ is defined and, moreover, $\bar{a}_i(\kappa^*) > 0$ for every $i = 1, 2, \ldots, \bar{m}$ and for all $\kappa^* \in \mathbb{R}^m_{>0}$,

(ii) the reparametrization map below is surjective:

$$\begin{aligned} \bar{a} \;:\; \mathbb{R}^m_{>0} &\to \mathbb{R}^{\bar{m}}_{>0} \\ \kappa &\mapsto (\bar{a}_1(\kappa), \bar{a}_2(\kappa), \ldots, \bar{a}_{\bar{m}}(\kappa)) \,, \end{aligned} \tag{2.4}$$

(iii) there exists an $(s-d) \times (s-d)$ matrix $M(\kappa)$ with entries in $\mathbb{Q}(\kappa) := \mathbb{Q}(\kappa_1, \kappa_2, \ldots, \kappa_m)$ such that:

(a) for all $\kappa^* \in \mathbb{R}^m_{>0}$, the matrix $M(\kappa^*)$ is defined and, moreover, $\det M(\kappa^*) > 0$, and

(b) letting $(\bar{h}_{j_\ell})$ denote the functions obtained from (f_{j_ℓ}) as follows:

$$(\bar{h}_{j_1}, \bar{h}_{j_2}, \ldots, \bar{h}_{j_{s-d}})^\top \quad := \quad M(\kappa)\,(f_{j_1}, f_{j_2}, \ldots, f_{j_{s-d}})^\top \,, \tag{2.5}$$

every nonconstant coefficient in every $\bar{h}_{j_\ell}$ is equal to a rational-number multiple of some $\bar{a}_i(\kappa)$.

Given such a set of effective parameters, we consider for $\ell = 1, 2, \ldots, s - d$, polynomials $h_{j_\ell} = h_{j_\ell}(a; x) \in \mathbb{Q}[a_1, a_2, \ldots, a_{\bar{m}}][x]$ (here, the a_i's are indeterminates) such that:

$$\bar{h}_{j_\ell} \;=\; h_{j_\ell}|_{a_1=\bar{a}_1(\kappa),\ \ldots\ ,\ a_{\bar{m}}=\bar{a}_{\bar{m}}(\kappa)}\ . \tag{2.6}$$

For $i = 1, 2, \ldots, s$ and any choice of $c \in \mathbb{R}^d_{>0}$ and $a \in \mathbb{R}^{\bar{m}}_{>0}$, set

$$h_{c,a}(x)_i \;:=\; \begin{cases} h_i(a; x) & \text{if } i \notin I \\ (Wx - c)_k & \text{if } i = i_k \in I. \end{cases} \tag{2.7}$$

We call the function $h_{c,a} : \mathbb{R}^s_{>0} \to \mathbb{R}^s$ an effective steady-state function of G.

The "steady-state parametrizations" that we will use in this dissertation belong to a subclass of the ones introduced by [33]. Thus, for simplicity, Definition 2.2.5 below is more restrictive than [33, Definition 3.6]. Specifically, our parametrizations have the form $\phi(\hat{a}; x)$, while those of [33] are of the form $\phi(\hat{a}; \hat{x})$.

Definition 2.2.5. Let G be a network with m reactions, s species, and conservation-law matrix W. Let $f_{c,\kappa}$ arise from G and W as in (2.3). Suppose that $h_{c,a}$ is an effective steady-state function of G, as in (2.7), arising from a matrix $M(\kappa)$, as in (2.5), a reparametrization map $\bar{a}$, as in (2.4), and polynomials h_{j_ℓ}'s as in (2.6). The positive steady states of G admit a positive parametrization with respect to $h_{c,a}$ if there exists a function $\phi : \mathbb{R}^{\hat{m}}_{>0} \times \mathbb{R}^s_{>0} \to \mathbb{R}^{\bar{m}}_{>0} \times \mathbb{R}^s_{>0}$, for some $\hat{m} \leq \bar{m}$, which we denote by $(\hat{a}; x) \mapsto \phi(\hat{a}; x)$, such that:

(i) $\phi(\hat{a}; x)$ extends the vector $(\hat{a}; x)$. More precisely, there exists a natural projection $\pi : \mathbb{R}^{\bar{m}}_{>0} \times \mathbb{R}^s_{>0} \to \mathbb{R}^{\hat{m}}_{>0} \times \mathbb{R}^s_{>0}$ such that $\pi \circ \phi$ is equal to the identity map.

(ii) Consider any $(a; x) \in \mathbb{R}^{\bar{m}}_{>0} \times \mathbb{R}^s_{>0}$. Then, the equality $h_i(a; x) = 0$ holds for every $i \notin I$ if and only if there exists $\hat{a}^* \in \mathbb{R}^{\hat{m}}_{>0}$ such that $(a; x) = \phi(\hat{a}^*; x)$.

We call ϕ a positive parametrization or a steady-state parametrization.

Definition 2.2.6. Under the notation and hypotheses of Definition 2.2.5, assume that the steady states of G admit a positive parametrization with respect to $h_{c,a}$. For such a positive parametrization ϕ, the critical function $C : \mathbb{R}^{\hat{m}}_{>0} \times \mathbb{R}^{s}_{>0} \to \mathbb{R}$ is given by:

$$C(\hat{a}; x) \quad = \quad (\det \operatorname{Jac} h_{c,a})\,|_{(a;x)=\phi(\hat{a};x)} \ ,$$

where $\operatorname{Jac}(h_{c,a})$ denotes the Jacobian matrix of $h_{c,a}$ with respect to x.

The following result is a specialization[3] of [33, Theorem 3.12]:

Proposition 2.2.7. *Under the notation and hypotheses of Definitions 2.2.4–2.2.6, assume also that G is a conservative network without boundary steady states in any compatibility class. Let N denote the stoichiometric matrix of G.*

(A) **Multistationarity.** *G is multistationary if there exists $(\hat{a}^*; x^*) \in \mathbb{R}^{\hat{m}}_{>0} \times \mathbb{R}^{s}_{>0}$ such that*

$$\operatorname{sign}(C(\hat{a}^*; x^*)) \ = \ (-1)^{\operatorname{rank}(N)+1} \ .$$

(B) **Monostationarity.** *G is monostationary if for all $(\hat{a}; x) \in \mathbb{R}^{\hat{m}}_{>0} \times \mathbb{R}^{s}_{>0}$,*

$$\operatorname{sign}(C(\hat{a}; x)) \ = \ (-1)^{\operatorname{rank}(N)} \ .$$

2.3 Applied algebraic geometry

Since the differential equations that model chemical reaction systems are given by parametrized polynomial systems, we will benefit from the rich theory for solving systems of polynomial equations from computational algebraic geometry. We refer the reader to Dickenstein's survey on algebraic-geometric methods in the study of biochemical reaction networks [32].

[3] As noted earlier, here we consider parametrizations of the form $\phi(\hat{a}; x)$, while [33] allowed those of the form $\phi(\hat{a}; \hat{x})$. Also, "conservative" in Proposition 2.2.7 can be generalized to "dissipative" [33].

In this section, we recall the essential definitions from algebraic geometry that we will need for this dissertation. We refer the reader to the accessible texts [27] and [92] for the fundamentals of computational algebraic geometry and real algebraic geometry, respectively.

2.3.1 Computational algebraic geometry basics

We recall some basic definitions from computational algebraic geometry.

A polynomial is a function $f(x) := f(x_1, \ldots, x_n) = \sum_{\alpha \in \mathcal{A}} c_\alpha x^\alpha$, where $\mathcal{A} \subset \mathbb{Z}^n_{\geq 0}$ is a finite set called the support of f and the c_α are its coefficients, and $x^\alpha := x_1^{\alpha_1} \cdots x_n^{\alpha_n}$. When the coefficients $c_\alpha(\kappa)$ are themselves functions of some parameters $\kappa = (\kappa_1, \ldots, \kappa_m)$, we call f a parametrized polynomial. The Newton polytope of f is the convex hull of its support, that is, the smallest convex set containing each exponent vector α of f. In other words, the Newton polytope of a polynomial is a geometric object that records the monomial structure of the polynomial.

Definition 2.3.1. For a polynomial $f = b_1 x^{\sigma_1} + b_2 x^{\sigma_2} + \cdots + b_\ell x^{\sigma_\ell} \in \mathbb{C}[x_1, x_2, \ldots, x_s]$, where the exponent vectors $\sigma_i \in \mathbb{Z}^s$ are distinct and $b_i \neq 0$ for all i, the Newton polytope of f is the convex hull of its exponent vectors: $\mathrm{Newt}(f) := \mathrm{conv}\{\sigma_1, \sigma_2, \ldots, \sigma_\ell\} \subseteq \mathbb{R}^s$. A vertex of a Newton polytope is an extreme point of the polytope.

Example 2.3.2. Figure 2.2 shows the Newton polytopes of $f_1(x_1, x_2) = \kappa_1 x_1 + \kappa_2 x_1 x_2$ (in red) and $f_2(x_1, x_2) = c_{(2,0)} x_1^2 + c_{(1,0)} x_1 + c_{(0,1)} x_2 + c_{(0,0)}$ (in blue). The Newton polytope of f_1 has 3 vertices; the point $(0, 1)$ corresponding to the monomial x_1 is not an extremal point of the polytope.

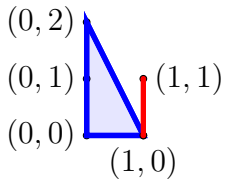

Figure 2.2: The Newton polytopes of $f_1(x_1, x_2) = \kappa_1 x_1 + \kappa_2 x_1 x_2$ (in red) and $f_2(x_1, x_2) = c_{(2,0)} x_1^2 + c_{(1,0)} x_1 + c_{(0,1)} x_2 + c_{(0,0)}$ (in blue).

Remark 2.3.3. Connecting back to chemical reaction networks, we note that the Newton polytope is blind to the coefficients of the polynomial. Then, any tools we develop using Newton polytopes – e.g., the Newton-polytope method developed in Section 4.3 – will be parameter-independent, aligning with our original goals.

2.3.2 Counting solutions of real univariate polynomials

In this subsection, we collect definitions related to counting solutions of real, univariate polynomials that we will need in Chapters 4–6.

The sign of a real number $a \in \mathbb{R}$ is

$$\text{sign}(a) := \begin{cases} + & \text{if } a > 0 \\ 0 & \text{if } a = 0 \\ - & \text{if } a < 0 \,. \end{cases}$$

The sign of a vector $x \in \mathbb{R}^s$ is subsequently defined component-wise:

$$\text{sign}(x) := (\text{sign}(x_1), \text{sign}(x_2), \ldots, \text{sign}(x_s)) \in \{+, 0, -\}^s \,.$$

The number of sign changes in such a vector of signs $v \in \{+, 0, -\}^s$ is obtained by first removing all 0's from v and then counting the number of times in the resulting vector a coordinate switches from $+$ to $-$ or from $-$ to $+$. For instance, the vector $(+, -, -, 0, -, 0, +)$ has two sign changes.

The classical *Descartes' rule of signs* counts positive real roots of a univariate polynomial.

Proposition 2.3.4 (Descartes' rule of signs [47])**.** *Given a nonzero univariate real polynomial $f(x) = c_0 + c_1 x + \cdots + c_r x^r$, the number of positive real roots of f, counted with multiplicity, is bounded above by the number of sign variations in the ordered sequence of the coefficients $sign(c_0), \ldots, sign(c_r)$.*

In fact, for polynomials whose coefficients alternate in sign, the bound from Descartes' rule can be achieved by some choice of coefficients [47].

Lemma 2.3.5 ([47]). *For $0 < l_1 < l_2 < \cdots < l_q$, consider the polynomial $P(x) := 1 - k_1 x^{l_1} + k_2 x^{l_2} - \cdots + (-1)^q k_q x^{l_q}$. Then there exist $k_1 > 0, k_2 > 0, \ldots, k_q > 0$ such that $P(x)$ has q positive roots $0 < x_1^* < x_2^* < \cdots < x_q^*$, and $P'(x_i^*) < 0$ for i odd and $P'(x_i^*) > 0$ for i even.*

Although Descartes' rule of signs bounds the number of positive real solutions of a univariate polynomial, it does not generalize easily to multivariate polynomial systems. In Chapter 6 and Chapter 7 we will employ more sophisticated algebraic-geometric methods for root-counting for such systems.

3. MATHEMATICAL FORMULATION OF ERK NETWORKS*

In this chapter, we introduce the graphical models, defining differential equations, and steady-state parametrizations for the full ERK network (Section 3.1) and also irreducible and reduced versions of the network (Sections 3.2–3.4). We will analyze the dynamics of the networks defined here in Chapters 4, 5, and 6.

3.1 The full ERK network

Figure 3.1 depicts a model of ERK regulation by the dual-site phosphorylation by the kinase E and dephosphorylation by the kinase F. Throughout this dissertation, we will refer to this network as the full ERK network.

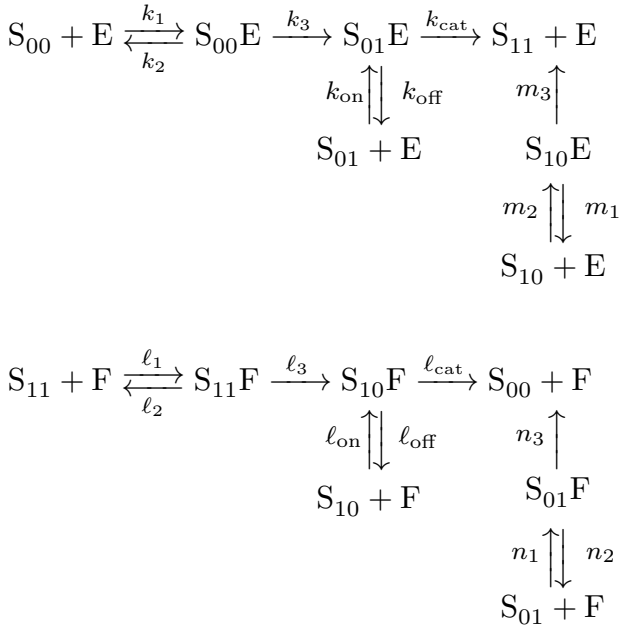

Figure 3.1: Full ERK network. Reprinted with permission from [78].

*Part of this chapter is reprinted from [78] by permission from Springer Nature Customer Service Centre GmbH: Springer *Journal of Mathematical Biology* "Oscillations and bistability in a model of ERK regulation", Nida Obatake, Anne Shiu, Xiaoxian Tang, and Angélica Torres, Copyright 2019). Part of this chapter is reprinted from [24] by permission from Springer Nature Customer Service Centre GmbH: Springer *Journal of Mathematical Biology* "Dynamics of ERK regulation in the processive limit", Carsten Conradi, Anne Shiu, and Xiaoxiang Tang, Copyright (2020).

x_1	x_2	x_3	x_4	x_5	x_6	x_7	x_8	x_9	x_{10}	x_{11}	x_{12}
S_{00}	E	F	$S_{11}F$	$S_{10}F$	$S_{01}F$	$S_{01}E$	$S_{10}E$	S_{01}	S_{10}	$S_{00}E$	S_{11}

Table 3.1: Assignment of variables to species for the full ERK network in Figure 3.1.

For the full ERK network shown in Figure 3.1, we let $x_1, x_2, \ldots, x_{12}$ denote the concentrations of the species in the order given in Table 3.1. The resulting ODE system (2.1) is as follows:

$$\begin{aligned}
\dot{x_1} &= -k_1 x_1 x_2 + k_2 x_{11} + \ell_{\text{cat}} x_5 + n_3 x_6 \\
\dot{x_2} &= -k_1 x_1 x_2 - k_{\text{on}} x_2 x_9 - m_2 x_2 x_{10} + k_2 x_{11} + k_{\text{cat}} x_7 + k_{\text{off}} x_7 + m_1 x_8 + m_3 x_8 \\
\dot{x_3} &= -\ell_1 x_3 x_{12} - \ell_{\text{on}} x_3 x_{10} - n_1 x_3 x_9 + \ell_2 x_4 + \ell_{\text{cat}} x_5 + \ell_{\text{off}} x_5 + n_2 x_6 + n_3 x_6 \\
\dot{x_4} &= \ell_1 x_3 x_{12} - \ell_2 x_4 - \ell_3 x_4 \\
\dot{x_5} &= \ell_{\text{on}} x_3 x_{10} + \ell_3 x_4 - \ell_{\text{cat}} x_5 - \ell_{\text{off}} x_5 \\
\dot{x_6} &= n_1 x_3 x_9 - n_2 x_6 - n_3 x_6 \\
\dot{x_7} &= k_{\text{on}} x_2 x_9 + k_3 x_{11} - k_{\text{cat}} x_7 - k_{\text{off}} x_7 \\
\dot{x_8} &= m_2 x_2 x_{10} - m_1 x_8 - m_3 x_8 \\
\dot{x_9} &= -k_{\text{on}} x_2 x_9 - n_1 x_3 x_9 + k_{\text{off}} x_7 + n_2 x_6 \\
\dot{x_{10}} &= -\ell_{\text{on}} x_3 x_{10} - m_2 x_2 x_{10} + \ell_{\text{off}} x_5 + m_1 x_8 \\
\dot{x_{11}} &= k_1 x_1 x_2 - k_2 x_{11} - k_3 x_{11} \\
\dot{x_{12}} &= -\ell_1 x_3 x_{12} + k_{\text{cat}} x_7 + \ell_2 x_4 + m_3 x_8
\end{aligned} \tag{3.1}$$

There are 18 rate constants k_i, ℓ_i, m_i, n_i. The 3 conservation laws correspond to the total amounts of substrate S, kinase E, and phosphatase F, respectively:

$$\begin{aligned}
x_1 + x_4 + x_5 + x_6 + x_7 + x_8 + x_9 + x_{10} + x_{11} + x_{12} &= \text{S}_{\text{tot}} =: c_1 \\
x_2 + x_7 + x_8 + x_{11} &= \text{E}_{\text{tot}} =: c_2 \\
x_3 + x_4 + x_5 + x_6 &= \text{F}_{\text{tot}} =: c_3 \,.
\end{aligned} \tag{3.2}$$

A steady-state parametrization for the full ERK network was given by [33, Examples 3.1 and 3.7]. That parametrization, however, cannot specialize to accommodate irreversible versions of the network (in the effective parameters given by [33], two of the denominators are k_{on} and ℓ_{on}, so we can not set those rate constants to 0). So, in the next section, we give an alternate steady-state parametrization that, although quite similar to the one of [33], specializes when considering irreversible versions of the network (see Proposition 3.2.1).

3.2 Irreversible versions of the ERK network

Here we consider networks obtained from the full ERK network (Figure 3.1) by making some reversible reactions irreversible. Specifically, we delete one or more of the reactions marked in blue from Figure 3.2.

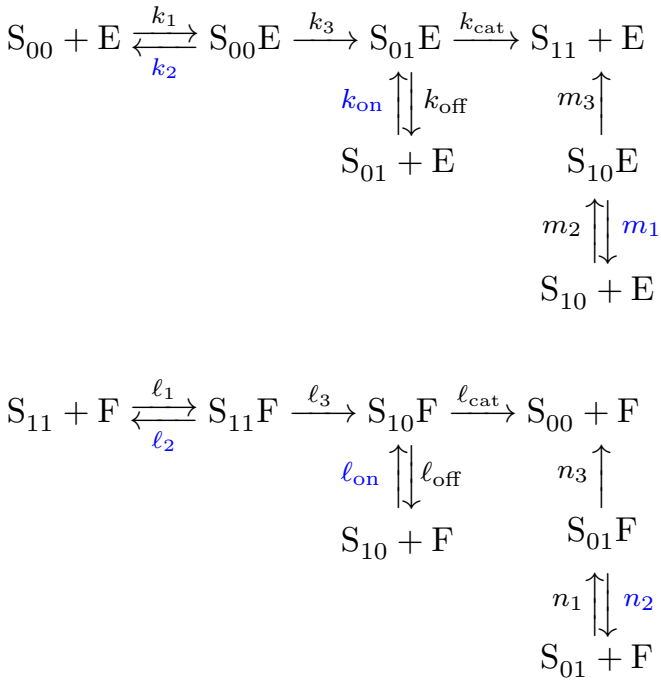

Figure 3.2: Irreversible versions of the ERK network are obtained by deleting some of the reactions labeled $k_2, k_{\text{on}}, m_1, l_2, \ell_{\text{on}}, n_2$ (in blue) from the full ERK network. In particular, deleting all six of those reactions yields the fully irreversible ERK network. Reprinted with permission from [78].

Our motivation for removing those specific reactions (the ones with rate constants k_2, k_{on}, m_1, ℓ_2, ℓ_{on}, n_2) rather than any of their opposite reactions is to preserve the main reaction pathways (from S_{00} to S_{11}, as well as S_{10} to S_{11}, S_{11} to S_{00}, and S_{01} to S_{00}). At the same time, we do not remove the reactions for k_{off} or ℓ_{off}, so that we can still pursue Question 1.2.1 (which involves k_{off} and ℓ_{off}) in a model with fewer reactions. We instead allow the removal of reactions k_{on} and ℓ_{on}.

Proposition 3.2.1 (Steady-state parametrization for full and irreversible ERK networks)**.** *Let $\mathcal{N}$ be the full ERK network or any network obtained from the full ERK network by deleting one or more the reactions corresponding to rate constants $k_2, k_{\text{on}}, m_1, \ell_2, \ell_{\text{on}}, n_2$ (marked in blue in Figure 3.2). Let $\mathbb{1}_{k_2}$ denote the indicator function that is 1 if the reaction labeled by k_2 is in $\mathcal{N}$ and 0 otherwise; analogously, we also define $\mathbb{1}_{k_{\text{on}}}$, $\mathbb{1}_{m_1}$, $\mathbb{1}_{\ell_2}$, $\mathbb{1}_{\ell_{\text{on}}}$, and $\mathbb{1}_{n_2}$. Also, define $\hat{a} := (a_2, a_4, a_6, a_8)$ if $\mathcal{N}$ contains the reactions labeled by k_{on} and ℓ_{on}, and $\hat{a} := (a_2, a_4, a_6)$ if $\mathcal{N}$ contains the reaction ℓ_{on} but not k_{on}, and $\hat{a} := (a_2, a_4, a_8)$ if $\mathcal{N}$ contains k_{on} but not ℓ_{on}, and $\hat{a} := (a_2, a_4)$ if $\mathcal{N}$ contains neither k_{on} nor ℓ_{on}. Then $\mathcal{N}$ admits an effective steady-state function $h_{c,a} : \mathbb{R}^{12}_{>0} \to \mathbb{R}^{12}$ given by:*

$$
\begin{aligned}
h_{c,a,1} &= x_1 + x_4 + x_5 + x_6 + x_7 + x_8 + x_9 + x_{10} + x_{11} + x_{12} - c_1 \,, \\
h_{c,a,2} &= x_2 + x_7 + x_8 + x_{11} - c_2 \,, \\
h_{c,a,3} &= x_3 + x_4 + x_5 + x_6 - c_3 \,, \\
h_{c,a,4} &= a_{12} x_3 x_{12} - x_4 \,, \\
h_{c,a,5} &= a_3 x_4 - x_5 - a_2 x_8 \,, \\
h_{c,a,6} &= a_{13} x_3 x_9 - x_6 \,, \\
h_{c,a,7} &= a_5 x_{11} - a_4 x_6 - x_7 \,, \\
h_{c,a,8} &= a_{11} x_2 x_{10} - x_8 \,, \\
h_{c,a,9} &= a_9 x_7 - \mathbb{1}_{k_{\text{on}}} a_8 x_2 x_9 - x_6 \,, \\
h_{c,a,10} &= a_7 x_5 - \mathbb{1}_{\ell_{\text{on}}} a_6 x_3 x_{10} - x_8 \,, \\
h_{c,a,11} &= a_{10} x_1 x_2 - x_{11} \,, \\
h_{c,a,12} &= x_7 - a_1 x_5 \,.
\end{aligned}
\tag{3.3}
$$

Moreover, with respect to this effective steady-state function, the positive steady states of $\mathcal{N}$ admit the following positive parametrization:

$$\begin{aligned}\phi : \mathbb{R}_{>0}^{2+\mathbb{1}_{k_{\text{on}}}+\mathbb{1}_{\ell_{\text{on}}}+12} &\to \mathbb{R}_{>0}^{13+12}\\ (\hat{a};\ x_1, x_2, \ldots, x_{12}) &\mapsto (a_1, a_2, \ldots, a_{13},\ x_1, x_2, \ldots, x_{12})\,,\end{aligned}$$

given by

$$\begin{aligned}
a_1 &:= \frac{x_7}{x_5} & a_3 &:= \frac{a_2x_8 + x_5}{x_4} & a_5 &:= \frac{a_4x_6 + x_7}{x_{11}}\\
a_7 &:= \frac{\mathbb{1}_{\ell_{\text{on}}}a_6x_3x_{10} + x_8}{x_5} & a_9 &:= \frac{\mathbb{1}_{k_{\text{on}}}a_8x_2x_9 + x_6}{x_7} & a_{10} &:= \frac{x_{11}}{x_1x_2}\\
a_{11} &:= \frac{x_8}{x_2x_{10}} & a_{12} &:= \frac{x_4}{x_3x_{12}} & a_{13} &:= \frac{x_6}{x_3x_9}\,.
\end{aligned} \tag{3.4}$$

Proof. We will show that the map $\bar{a} : \mathbb{R}_{>0}^{12+\mathbb{1}_{k_2}+\mathbb{1}_{k_{\text{on}}}+\mathbb{1}_{m_1}+\mathbb{1}_{\ell_2}+\mathbb{1}_{\ell_{\text{on}}}+\mathbb{1}_{n_2}} \to \mathbb{R}_{>0}^{11+\mathbb{1}_{k_{\text{on}}}+\mathbb{1}_{\ell_{\text{on}}}}$, defined as follows, is a reparametrization map as in (2.4):

$$\begin{aligned}
&\bar{a}_1 = \tfrac{\ell_{cat}}{k_{\text{cat}}}, && \bar{a}_2 = \tfrac{m_3}{\ell_{\text{cat}}}, && \bar{a}_3 = \tfrac{\ell_3}{\ell_{\text{cat}}}, && \bar{a}_4 = \tfrac{n_3}{k_{\text{cat}}}, && \bar{a}_5 = \tfrac{k_3}{k_{\text{cat}}},\\
&\bar{a}_6 = \tfrac{\mathbb{1}_{\ell_{\text{on}}}\ell_{\text{on}}}{m_3}, && \bar{a}_7 = \tfrac{\ell_{\text{off}}}{m_3}, && \bar{a}_8 = \tfrac{\mathbb{1}_{k_{\text{on}}}k_{\text{on}}}{n_3}, && \bar{a}_9 = \tfrac{k_{\text{off}}}{n_3}, && \bar{a}_{10} = \tfrac{k_1}{\mathbb{1}_{k_2}k_2+k_3},\\
&\bar{a}_{11} = \tfrac{m_2}{\mathbb{1}_{m_1}m_1+m_3}, && \bar{a}_{12} = \tfrac{\ell_1}{\mathbb{1}_{\ell_2}\ell_2+\ell_3}, && \bar{a}_{13} = \tfrac{n_1}{\mathbb{1}_{n_2}n_2+n_3}.
\end{aligned} \tag{3.5}$$

In particular, we remove the effective parameter $\bar{a}_6$ (respectively, $\bar{a}_8$) if $\mathbb{1}_{\ell_{\text{on}}} = 0$ (respectively, $\mathbb{1}_{k_{\text{on}}} = 0$). Notice that each $\bar{a}_i$ (if it is not removed) is defined and positive for all $\kappa = (k_1, \ldots, n_3) \in \mathbb{R}_{>0}^{12+\mathbb{1}_{k_2}+\mathbb{1}_{k_{\text{on}}}+\mathbb{1}_{m_1}+\mathbb{1}_{\ell_2}+\mathbb{1}_{\ell_{\text{on}}}+\mathbb{1}_{n_2}}$.

We must show that the map $\bar{a}$ is surjective. Indeed, given $a \in \mathbb{R}_{>0}^{11+\mathbb{1}_{k_{\text{on}}}+\mathbb{1}_{\ell_{\text{on}}}}$, it is easy to check that a is the image under $\bar{a}$ of the vector obtained by removing every 0 coordinate from the following vector: $(k_1, k_2, k_3, k_{\text{cat}}, k_{\text{on}}, k_{\text{off}}, \ell_1, \ell_2, \ell_3, \ell_{\text{cat}}, \ell_{\text{on}}, \ell_{\text{off}}, m_1, m_2, m_3, n_1, n_2, n_3)$

$$\begin{aligned}
= \Big(&(\mathbb{1}_{k_2} + a_5)a_{10}, \mathbb{1}_{k_2}, a_5, 1, \mathbb{1}_{k_{\text{on}}}a_4a_8, a_4a_9, (\mathbb{1}_{\ell_2} + a_1a_3)a_{12}, \mathbb{1}_{\ell_2}, a_1a_3, a_1, \mathbb{1}_{\ell_{\text{on}}}a_1a_2a_6, a_1a_2a_7, \mathbb{1}_{m_1},\\
&(\mathbb{1}_{m_1} + a_1a_2)a_{11}, a_1a_2, (\mathbb{1}_{n_2} + a_4)a_{13}, \mathbb{1}_{n_2}, a_4\Big)\,.
\end{aligned}$$

With an eye toward applying Definition 2.2.4, consider the following 9×9 matrix:

$$M(\kappa) := \begin{pmatrix} \frac{1}{\mathbb{1}_{\ell_2}\ell_2+\ell_3} & 0 & 0 & 0 & 0 & 0 & 0 & 0 & 0 \\ 0 & \frac{1}{\ell_{\rm cat}} & 0 & 0 & \frac{1}{\ell_{\rm cat}} & 0 & \frac{1}{\ell_{\rm cat}} & 0 & 0 \\ 0 & 0 & \frac{1}{\mathbb{1}_{n_2}n_2+n_3} & 0 & 0 & 0 & 0 & 0 & 0 \\ 0 & 0 & \frac{1}{k_{\rm cat}} & \frac{1}{k_{\rm cat}} & 0 & \frac{1}{k_{\rm cat}} & 0 & 0 & 0 \\ 0 & 0 & 0 & 0 & \frac{1}{\mathbb{1}_{m_1}m_1+m_3} & 0 & 0 & 0 & 0 \\ 0 & 0 & \frac{1}{n_3} & 0 & 0 & \frac{1}{n_3} & 0 & 0 & 0 \\ 0 & 0 & 0 & 0 & \frac{1}{m_3} & 0 & \frac{1}{m_3} & 0 & 0 \\ 0 & 0 & 0 & 0 & 0 & 0 & 0 & \frac{1}{\mathbb{1}_{k_2}k_2+k_3} & 0 \\ \frac{1}{k_{\rm cat}} & \frac{1}{k_{\rm cat}} & 0 & 0 & \frac{1}{k_{\rm cat}} & 0 & \frac{1}{k_{\rm cat}} & 0 & \frac{1}{k_{\rm cat}} \end{pmatrix}. \tag{3.6}$$

It is straightforward to check that $\det M(\kappa)$ is the product of all diagonal terms, and hence is positive for all $\kappa \in \mathbb{R}^{12+\mathbb{1}_{k_2}+\mathbb{1}_{k_{\rm on}}+\mathbb{1}_{m_1}+\mathbb{1}_{\ell_2}+\mathbb{1}_{\ell_{\rm on}}+\mathbb{1}_{n_2}}_{>0}$.

The mass-action ODEs of $\mathcal{N}$ are obtained from those (3.1) of the full ERK network by replacing the rate constants $k_2, k_{\rm on}, m_1, \ell_2, \ell_{\rm on}, n_2$, respectively, by $\mathbb{1}_{k_2}k_2$, $\mathbb{1}_{k_{\rm on}}k_{\rm on}$, $\mathbb{1}_{m_1}m_1$, $\mathbb{1}_{\ell_2}\ell_2$, $\mathbb{1}_{\ell_{\rm on}}\ell_{\rm on}$, and $\mathbb{1}_{n_2}n_2$, respectively. To the right-hand sides of these ODEs, we apply the recipe given in equations (2.5)–(2.7), using the effective parameters $\bar{a}_i$ in (3.5), the matrix $M(\kappa)$ in (3.6), and the conservation-law matrix W arising from the conservation laws (3.2). It is straightforward to check that the result is the function $h_{c,a}(x)$ given in (3.3).

Observe that, for the non-conservation-law equations $h_{c,a,4}, \ldots, h_{c,a,12}$ in (3.3), each non-constant coefficient is, up to sign, one of the a_i's. Hence, the $\bar{a}_i$'s in (3.5) are effective parameters, and the function in (3.3) is an effective steady-state function. Finally, the fact that ϕ is a positive parametrization with respect to (3.3) (as in Definition 2.2.5) follows directly from comparing equations (3.3) and (3.4). □

Remark 3.2.2 (Multistationarity depends on only $k_{\rm on}$ and $\ell_{\rm on}$)**.** Proposition 3.2.1 considers any network obtained by deleting any (or none) of the six reactions labeled by k_2, $k_{\rm on}$, m_1, ℓ_2, $\ell_{\rm on}$, n_2. Nonetheless, the resulting steady-state parametrization (3.4) depends on $k_{\rm on}$ and $\ell_{\rm on}$ but not any of the other rate constants. Thus, multistationarity for these irreversible networks depends only on whether the network contains $k_{\rm on}$ and $\ell_{\rm on}$ (see Theorem 4.2.6).

3.3 The reduced ERK network

In the previous section, we consider irreversible versions of the ERK network. Now we further reduce the network by additionally removing some "intermediate complexes" (namely, $S_{10}E$ and $S_{01}F$). These operations yield the reduced ERK network in Figure 3.3. Note that in the process of removing intermediates, the reactions m_2 and m_3 (similarly, n_1 and n_3) are collapsed into a single reaction labeled m (respectively, n). A biological motivation for collapsing these reactions is the fact that intermediates are usually short-lived, so the simpler model may approximate the dynamics well.

$$\begin{array}{ccccccc} \mathrm{S_{00}} + \mathrm{E} & \xrightarrow{k_1} & \mathrm{S_{00}E} & \xrightarrow{k_3} & \mathrm{S_{01}E} & \xrightarrow{k_{\mathrm{cat}}} & \mathrm{S_{11}} + \mathrm{E} \\ & & & & \downarrow{\scriptstyle k_{\mathrm{off}}} & & \uparrow{\scriptstyle m} \\ & & & & \mathrm{S_{01}} + \mathrm{E} & & \mathrm{S_{10}} + \mathrm{E} \end{array}$$

$$\begin{array}{ccccccc} \mathrm{S_{11}} + \mathrm{F} & \xrightarrow{\ell_1} & \mathrm{S_{11}F} & \xrightarrow{\ell_3} & \mathrm{S_{10}F} & \xrightarrow{\ell_{\mathrm{cat}}} & \mathrm{S_{00}} + \mathrm{F} \\ & & & & \downarrow{\scriptstyle \ell_{\mathrm{off}}} & & \uparrow{\scriptstyle n} \\ & & & & \mathrm{S_{10}} + \mathrm{F} & & \mathrm{S_{01}} + \mathrm{F} \end{array}$$

Figure 3.3: Reduced ERK network. Reprinted with permission from [78].

Our notion of removing intermediates matches that of [40], who initiated the recent interest in the question of when dynamical properties are preserved when intermediates are added or removed (e.g., $S_{10} + E \leftrightarrows S_{10}E \to S_{11} + E$ versus $S_{10} \to S_{11}$). Our work, therefore, fits into this circle of ideas [16, 74, 87].

In the reduced ERK network, the remaining 10 rate constants are as follows: k_1, k_3, k_{cat}, k_{off}, m, ℓ_1, ℓ_3, ℓ_{cat}, ℓ_{off}, n. Letting $x_1, x_2, \ldots, x_{10}$ denote the species concentrations in the order given

x_1	x_2	x_3	x_4	x_5	x_6	x_7	x_8	x_9	x_{10}
S_{00}	E	$S_{00}E$	$S_{01}E$	S_{11}	S_{01}	S_{10}	F	$S_{11}F$	$S_{10}F$

Table 3.2: Assignment of variables to species for the reduced ERK network in Figure 3.3. (Many of the variables that are also in the full ERK, in Table 3.1, have been relabeled.)

in Table 3.2, the resulting mass-action kinetics ODEs are as follows:

$$\begin{aligned}
\dot{x_1} &= -k_1x_1x_2 + nx_6x_8 + \ell_{\text{cat}}x_{10} &=: f_1\\
\dot{x_2} &= -k_1x_1x_2 + k_{\text{cat}}x_4 + k_{\text{off}}x_4 &=: f_2\\
\dot{x_3} &= k_1x_1x_2 - k_3x_3 &=: f_3\\
\dot{x_4} &= k_3x_3 - k_{\text{cat}}x_4 - k_{\text{off}}x_4 &=: f_4\\
\dot{x_5} &= mx_2x_7 - \ell_1x_5x_8 + k_{\text{cat}}x_4 &=: f_5\\
\dot{x_6} &= -nx_6x_8 + k_{\text{off}}x_4 &=: f_6\\
\dot{x_7} &= -mx_2x_7 + \ell_{\text{off}}x_{10} &=: f_7\\
\dot{x_8} &= -\ell_1x_5x_8 + \ell_{\text{off}}x_{10} + \ell_{\text{cat}}x_{10} &=: f_8\\
\dot{x_9} &= \ell_1x_5x_8 - \ell_3x_9 &=: f_9\\
\dot{x_{10}} &= -\ell_{\text{off}}x_{10} + \ell_3x_9 - \ell_{\text{cat}}x_{10} &=: f_{10}.
\end{aligned} \tag{3.7}$$

The 3 conservation equations are:

$$\begin{aligned}
x_1 + x_3 + x_4 + x_5 + x_6 + x_7 + x_9 + x_{10} &= S_{\text{tot}} =: c_1\\
x_2 + x_3 + x_4 &= E_{\text{tot}} =: c_2\\
x_8 + x_9 + x_{10} &= F_{\text{tot}} =: c_3.
\end{aligned} \tag{3.8}$$

Proposition 3.3.1 (Steady-state parametrization for reduced ERK network)**.** *The reduced ERK network (Figure 3.3) admits an effective steady-state function* $h_{c,a} : \mathbb{R}^{10}_{>0} \to \mathbb{R}^{10}$ *given by:*

$$
\begin{aligned}
h_{c,a,1} &= x_1 + x_3 + x_4 + x_5 + x_6 + x_7 + x_9 + x_{10} - c_1, & h_{c,a,2} &= x_2 + x_3 + x_4 - c_2,\\
h_{c,a,3} &= -(k_{\text{cat}} + k_{\text{off}})\ell_{\text{cat}} x_{10} + k_1 k_{\text{cat}} x_1 x_2, & h_{c,a,4} &= k_3 x_3 - (k_{\text{cat}} + k_{\text{off}}) x_4,\\
h_{c,a,5} &= \ell_{\text{off}} x_{10} - m x_2 x_7, & h_{c,a,6} &= \ell_1 x_5 x_8 - (\ell_{\text{cat}} + \ell_{\text{off}}) x_{10},\\
h_{c,a,7} &= \ell_3 x_9 - (\ell_{\text{cat}} + \ell_{\text{off}}) x_{10}, & h_{c,a,8} &= x_8 + x_9 + x_{10} - c_3,\\
h_{c,a,9} &= k_{\text{cat}} x_4 - \ell_{\text{cat}} x_{10}, & h_{c,a,10} &= k_{\text{off}} \ell_{\text{cat}} x_{10} - k_{\text{cat}} n x_6 x_8.
\end{aligned}
\tag{3.9}
$$

Moreover, with respect to this effective steady-state function, the positive steady states admit the following positive parametrization:

$$
\begin{aligned}
\phi : \mathbb{R}_{>0}^{3+10} &\to \mathbb{R}_{>0}^{10+10} \\
(k_{\text{cat}}, k_{\text{off}}, \ell_{\text{off}},\ x_1, x_2, \ldots, x_{10}) &\mapsto (k_1, k_3, k_{\text{cat}}, k_{\text{off}}, m, \ell_1, \ell_3, \ell_{\text{cat}}, \ell_{\text{off}}, n,\ x_1, x_2, \ldots, x_{10}),
\end{aligned}
\tag{3.10}
$$

given by

$$
\begin{aligned}
k_1 &:= \frac{(k_{\text{cat}} + k_{\text{off}}) x_4}{x_1 x_2} & k_3 &:= \frac{(k_{\text{cat}} + k_{\text{off}}) x_4}{x_3} & m &:= \frac{\ell_{\text{off}} x_{10}}{x_2 x_7} & \ell_1 &:= \frac{\ell_{\text{off}} x_{10} + k_{\text{cat}} x_4}{x_5 x_8}\\
\ell_3 &:= \frac{\ell_{\text{off}} x_{10} + k_{\text{cat}} x_4}{x_9} & \ell_{\text{cat}} &:= \frac{k_{\text{cat}} x_4}{x_{10}} & n &:= \frac{k_{\text{off}} x_4}{x_6 x_8}.
\end{aligned}
\tag{3.11}
$$

In particular, the image of ϕ is the following set of pairs of positive steady states and rate constants:

$$
\{(k^*; x^*) \in \mathbb{R}_{>0}^{10+10} \mid x^* \textit{ is a steady state of } (3.7) \textit{ when } k = k^*\}\ .
$$

Here, k denotes the vector $(k_1, k_3, k_{\text{cat}}, k_{\text{off}}, m, \ell_1, \ell_3, \ell_{\text{cat}}, \ell_{\text{off}}, n)$.

Proof. Let W denote the conservation-law matrix arising from the conservation laws (3.8) for the reduced ERK network. Then $I = \{1, 2, 8\}$ is the set of indices of the first nonzero coordinates of the rows of W. We take $\mathbb{Q}(k_{\text{cat}}, k_{\text{off}})$-linear combinations of the f_i's in (3.7), where $i \notin I$, to obtain

the following binomials in the x_i's:

$$\begin{aligned}
h_3 &:= (k_{\text{cat}} + k_{\text{off}})(f_5 + f_7 + f_9 + f_{10}) + k_{\text{cat}}(f_3 + f_4) &&= -(k_{\text{cat}} + k_{\text{off}})\ell_{\text{cat}} x_{10} + k_1 k_{\text{cat}} x_1 x_2 \\
h_4 &:= f_4 &&= k_3 x_3 - (k_{\text{cat}} + k_{\text{off}}) x_4 \\
h_5 &:= f_7 &&= \ell_{\text{off}} x_{10} - m x_2 x_7 \\
h_6 &:= f_9 + f_{10} &&= \ell_1 x_5 x_8 - (\ell_{\text{cat}} + \ell_{\text{off}}) x_{10} \\
h_7 &:= f_{10} &&= \ell_3 x_9 - (\ell_{\text{cat}} + \ell_{\text{off}}) x_{10} \\
h_9 &:= f_5 + f_7 + f_9 + f_{10} &&= k_{\text{cat}} x_4 - \ell_{\text{cat}} x_{10} \\
h_{10} &:= k_{\text{cat}} f_6 - k_{\text{off}}(f_5 + f_7 + f_9 + f_{10}) &&= k_{\text{off}} \ell_{\text{cat}} x_{10} - k_{\text{cat}} n x_6 x_8.
\end{aligned}$$

Consider the (above) linear transformation from f_i to h_i ($i \notin I$). Let M denote the corresponding matrix representation (M plays the role of the matrix denoted by $M(\kappa)$ in Definition 2.2.4). It is straightforward to check that $\det M = k_{\text{cat}}^2$, which is positive when $k_{\text{cat}} > 0$.

Consider the reparametrization map $\bar{a} : \mathbb{R}^{10} \to \mathbb{R}^{10}$ defined by the identity map (and so is surjective). Then $\bar{a}$, together with the conservation-law matrix W and the matrix M, yield (as in Definition 2.2.4[2]) the effective steady-state function $h_{c,a}(x)$ given in (3.9).

To show that ϕ is a positive steady-state parametrization with respect to (3.9), as in Definition 2.2.5, it suffices to show the following claim:

Claim: For every $(k^*; x^*) \in \mathbb{R}^{10+10}_{>0}$, the steady-state condition holds – namely, $h_i(k^*; x^*) = 0$ for all $i \in \{3, 4, 5, 6, 7, 9, 10\}$ – if and only if $\phi(k^*_{\text{cat}}, k^*_{\text{off}}, \ell^*_{\text{off}}; x^*) = (k^*; x^*)$.

For the "⇒" direction, assume $h_i(k^*; x^*) = 0$ for all i. Then $h_9(k^*; x^*) = 0$ implies that

$$\ell^*_{\text{cat}} \;=\; \frac{k^*_{\text{cat}} x^*_4}{x^*_{10}}\,. \tag{3.12}$$

[2]In this case, Definition 2.2.4(iii)(b) requires every nonconstant coefficient in the effective steady-state function (3.9) to be a rational-number multiple of one of the rate constants. However, for the non-conservation-law equations in (3.9), many of the non-constant coefficients – such as $k_{\text{off}}\ell_{\text{cat}}$ – are not rational-number multiples of one of the rate constants. Nonetheless, these coefficients are all polynomials in the rate constants, and the relevant results by [33] hold in that generality.

In other words, λ_{cat} – when evaluated at $(k_{\text{cat}}, k_{\text{off}}, \ell_{\text{off}}; x) = (k^*_{\text{cat}}, k^*_{\text{off}}, \ell^*_{\text{off}}; x^*)$ – equals ℓ^*_{cat}. Next, the equality $h_3(k^*; x^*) = 0$ implies that

$$k_1^* \;=\; \frac{(k^*_{\text{cat}} + k^*_{\text{off}})\ell^*_{\text{cat}} x^*_{10}}{k^*_{\text{cat}} x^*_1 x^*_2} \;=\; \frac{(k^*_{\text{cat}} + k^*_{\text{off}}) x^*_4}{x^*_1 x^*_2}\,, \tag{3.13}$$

where the final equality follows from equation (3.12). Thus, the expression for k_1 given after (3.11) – when evaluated at $(k_{\text{cat}}, k_{\text{off}}, \ell_{\text{off}}; x) = (k^*_{\text{cat}}, k^*_{\text{off}}, \ell^*_{\text{off}}; x^*)$ – equals k_1^*.

Similarly, the equality $h_4(k^*; x^*) = 0$ (respectively, $h_5(k^*; x^*) = 0$, $h_6(k^*; x^*) = 0$, $h_7(k^*; x^*) = 0$, or $h_{10}(k^*; x^*) = 0$) implies that κ_3 (respectively, m, ℓ_1, ℓ_3, or n) – evaluated at $(k_{\text{cat}}, k_{\text{off}}, \ell_{\text{off}}; x) = (k^*_{\text{cat}}, k^*_{\text{off}}, \ell^*_{\text{off}}; x^*)$ – equals k_3^* (respectively, m^*, ℓ_1^*, ℓ_3^*, or n^*). Thus, $\phi(k^*_{\text{cat}}, k^*_{\text{off}}, \ell^*_{\text{off}}; x^*) = (k^*; x^*)$.

The "$\Leftarrow$" direction is similar. Assume $\phi(k^*_{\text{cat}}, k^*_{\text{off}}, \ell^*_{\text{off}}; x^*) = (k^*; x^*)$. That is, the expressions for k_1, k_3, m, ℓ_1, ℓ_3, ℓ_{cat}, and n evaluate to, respectively, k_1^*, k_3^*, m^*, ℓ_1^*, ℓ_3^*, ℓ^*_{cat}, and n^*, when $(k_{\text{cat}}, k_{\text{off}}, \ell_{\text{off}}; x) = (k^*_{\text{cat}}, k^*_{\text{off}}, \ell^*_{\text{off}}; x^*)$. In particular, equation (3.12) holds, and so $h_9(k^*; x^*) = 0$. Similarly, $h_i(k^*; x^*) = 0$ for all other i (here we also use equation (3.12)). □

Remark 3.3.2. The proof of Proposition 3.3.1 proceeds by performing linear operations on the steady-state polynomials to yield binomials g_i, and then solving for one k_j from each binomial to obtain the parametrization (3.10). This is similar in spirit to – but more general than – the approach prescribed in [33, §4] for "linearly binomial" networks. Also, our linear operations were found "by hand", and so an interesting future direction is to develop efficient and systematic approaches to finding such operations leading to binomials.

Remark 3.3.3. The proof of Proposition 3.3.1 shows that the "steady-state ideal" (the ideal generated by the right-hand sides of the ODEs) of the reduced ERK network is generated by the binomials g_i. This network, therefore has, "toric steady states" [81]. In contrast, the steady-state ideal of the full ERK network is not a binomial ideal (it is straightforward to check this computationally, e.g., using the `Binomials` package in `Macaulay2` [48]). As for the irreversible versions of the ERK network, when the reactions with rate constants k_{on} and ℓ_{on} are deleted, we see from (3.3)

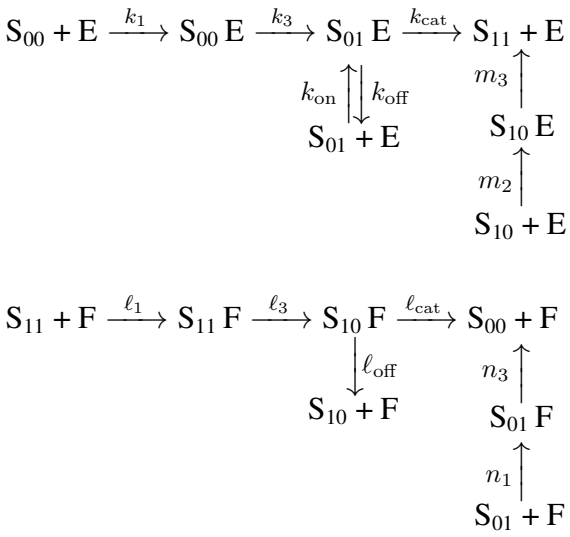

Figure 3.4: Minimally bistable ERK subnetwork

that the steady-state ideal becomes binomial. Hence, irreversible ERK networks that are missing both k_{on} and ℓ_{on} are "linearly binomial" as defined by [33].

Remark 3.3.4. All networks considered in this section are conservative, which can be seen from the conservation laws (3.2) for the full and irreversible ERK networks, and (3.8) for the reduced ERK network. Also for these networks, there are no boundary steady states in any compatibility class (it is straightforward to check this using results from [1] or [91]).

3.4 Minimally bistable ERK subnetwork

We will show in Chapter 4 that bistability persists when reactions in the ERK network are made irreversible, provided that at least one of the reactions labeled by k_{on} and ℓ_{on} is preserved. The minimally bistable ERK subnetwork is thus defined as the network obtained by deleting the reactions labeled $k_2, m_1, \ell_2, \ell_{\text{on}}, n_2$ from the ERK network. We conclude this section with a steady-state parametrization for the minimally bistable ERK subnetwork (Proposition 3.4.1).

For the minimally bistable ERK subnetwork, let $x_1, x_2, \ldots, x_{12}$ denote the concentrations of the species in the order given in Table 3.3. We obtain the following ODE system (2.1):

x_1	x_2	x_3	x_4	x_5	x_6	x_7	x_8	x_9	x_{10}	x_{11}	x_{12}
S_{00}	E	F	$S_{11}F$	$S_{10}F$	$S_{01}F$	$S_{01}E$	$S_{10}E$	S_{01}	S_{10}	$S_{00}E$	S_{11}

Table 3.3: Assignment of variables to species for the minimally bistable ERK subnetwork.

$$
\begin{aligned}
\dot{x_1} &= -k_1x_1x_2 + \ell_{\text{cat}}x_5 + n_3x_6 &&=: f_1\\
\dot{x_2} &= -k_1x_1x_2 - k_{\text{on}}x_2x_9 - m_2x_{10}x_2 + k_{\text{cat}}x_7 + k_{\text{off}}x_7 + m_3x_8 &&=: f_2\\
\dot{x_3} &= -\ell_1x_3x_{12} - n_1x_3x_9 + \ell_{\text{cat}}x_5 + \ell_{\text{off}}x_5 + n_3x_6 &&=: f_3\\
\dot{x_4} &= \ell_1x_3x_{12} - \ell_3x_4 &&=: f_4\\
\dot{x_5} &= \ell_3x_4 - \ell_{\text{cat}}x_5 - \ell_{\text{off}}x_5 &&=: f_5\\
\dot{x_6} &= n_1x_3x_9 - n_3x_6 &&=: f_6\\
\dot{x_7} &= k_{\text{on}}x_2x_9 + k_3x_{11} - k_{\text{cat}}x_7 - k_{\text{off}}x_7 &&=: f_7\\
\dot{x_8} &= m_2x_2x_{10} - m_3x_8 &&=: f_8\\
\dot{x_9} &= -k_{\text{on}}x_2x_9 - n_1x_3x_9 + k_{\text{off}}x_7 &&=: f_9\\
\dot{x_{10}} &= -m_2x_2x_{10} + \ell_{\text{off}}x_5 &&=: f_{10}\\
\dot{x_{11}} &= k_1x_1x_2 - k_3x_{11} &&=: f_{11}\\
\dot{x_{12}} &= -\ell_1x_3x_{12} + k_{\text{cat}}x_7 + m_3x_8 &&=: f_{12}
\end{aligned}
\tag{3.14}
$$

The 3 conservation equations correspond to the total amounts of substrate, kinase E, and phosphatase F, respectively:

$$
\begin{aligned}
x_1 + x_4 + x_5 + x_6 + x_7 + x_8 + x_9 + x_{10} + x_{11} + x_{12} &= S_{\text{tot}} =: c_1\\
x_2 + x_7 + x_8 + x_{11} &= E_{\text{tot}} =: c_2\\
x_3 + x_4 + x_5 + x_6 &= F_{\text{tot}} =: c_3.
\end{aligned}
\tag{3.15}
$$

This network admits a steady-state parametrization (Proposition 3.4.1 below). Another parametrization for this network was given in Section 3.2, involving "effective parameters" (replacing, for instance, $\ell_{\text{cat}}/k_{\text{cat}}$ by a new parameter a_1). That parametrization, however, does not give (direct) access to the rate constants $k_{\text{cat}}, \ell_{\text{cat}}, k_{\text{off}}, \ell_{\text{off}}$ involved in processivity levels. We therefore need a new parametrization, as follows.

Proposition 3.4.1 (Steady-state parametrization for minimally bistable ERK subnetwork)**.** *For the minimally bistable ERK subnetwork, with rate-constant vector denoted by* $\kappa := (k_1, k_3, k_{\text{cat}}, k_{\text{on}}, k_{\text{off}}, \ell_1, \ell_3, \ell_{\text{cat}}, \ell_{\text{off}}, m_2, m_3, n_1, n_3)$*, a steady-state parametrization is given by:*

$$\begin{aligned} \phi : \mathbb{R}^{13}_{>0} \times \mathbb{R}^{3}_{>0} &\to \mathbb{R}^{13}_{>0} \times \mathbb{R}^{12}_{>0} \\ (\kappa;\ x_1, x_2, x_3) &\mapsto (\kappa;\ x_1, x_2, \ldots, x_{12}) \,, \end{aligned}$$

where

$$\begin{aligned} x_4 &= \tfrac{k_1 k_{\text{cat}}(\ell_{\text{cat}}+\ell_{\text{off}})(k_{\text{on}}x_2+n_1x_3)x_1x_2}{\ell_3\ell_{\text{cat}}(k_{\text{cat}}k_{\text{on}}x_2+k_{\text{cat}}n_1x_3+k_{\text{off}}n_1x_3)}, & x_5 &= \tfrac{k_1 k_{\text{cat}}(k_{\text{on}}x_2+n_1x_3)x_1x_2}{\ell_{\text{cat}}(k_{\text{cat}}k_{\text{on}}x_2+k_{\text{cat}}n_1x_3+k_{\text{off}}n_1x_3)} \\ x_6 &= \tfrac{n_1 k_1 k_{\text{off}} x_1x_2x_3}{n_3(k_{\text{cat}}k_{\text{on}}x_2+k_{\text{cat}}n_1x_3+k_{\text{off}}n_1x_3)}, & x_7 &= \tfrac{k_1(k_{\text{on}}x_2+n_1x_3)x_1x_2}{k_{\text{cat}}k_{\text{on}}x_2+k_{\text{cat}}n_1x_3+k_{\text{off}}n_1x_3}, \\ x_8 &= \tfrac{k_1 k_{\text{cat}}\ell_{\text{off}}(k_{\text{on}}x_2+n_1x_3)x_1x_2}{\ell_{\text{cat}}m_3(k_{\text{cat}}k_{\text{on}}x_2+k_{\text{cat}}n_1x_3+k_{\text{off}}n_1x_3)}, & x_9 &= \tfrac{k_1 k_{\text{off}} x_1x_2}{k_{\text{cat}}k_{\text{on}}x_2+k_{\text{cat}}n_1x_3+k_{\text{off}}n_1x_3}, \\ x_{10} &= \tfrac{k_1 k_{\text{cat}}\ell_{\text{off}}(k_{\text{on}}x_2+n_1x_3)x_1}{\ell_{\text{cat}}m_2(k_{\text{cat}}k_{\text{on}}x_2+k_{\text{cat}}n_1x_3+k_{\text{off}}n_1x_3)}, & x_{11} &= \tfrac{k_1x_1x_2}{k_3}, \\ x_{12} &= \tfrac{k_1 k_{\text{cat}}(\ell_{\text{cat}}+\ell_{\text{off}})(k_{\text{on}}x_2+n_1x_3)x_1x_2}{\ell_{\text{cat}}\ell_1(k_{\text{cat}}k_{\text{on}}x_2+k_{\text{cat}}n_1x_3+k_{\text{off}}n_1x_3)x_3}. \end{aligned} \tag{3.16}$$

Proof. Due to the conservation laws (3.15), it suffices to show that by solving the equations $f_i = 0$ from (3.14), for all $i \neq 2, 3, 12$, we obtain the expressions in (3.16). We accomplish this as follows. By solving for x_{11} in the equation $f_{11} = 0$, we obtain the desired expression for x_{11}. Next, we solve for x_7 and x_9 in $f_7 = f_9 = 0$, and use the expression for x_{11}, plus the fact that each x_i and each rate constant is positive, to obtain the expressions for x_7 and x_9. Our remaining steps proceed similarly: we use $f_6 = 0$ to obtain x_6, then $f_1 = 0$ for x_5, then $f_{10} = 0$ for x_{10}, then $f_8 = 0$ for x_8, then $f_5 = 0$ for x_4, and finally $f_4 = 0$ for x_{12}. □

4. EXISTENCE OF OSCILLATIONS AND BISTABILITY IN A MODEL OF ERK REGULATION*

The material in this chapter is based on the paper "Oscillations and bistability in a model of ERK regulation" [78], which was authored jointly with Anne Shiu, Xiaoxian Tang, and Angélica Torres.

In recent years, significant attention has been devoted to the question of how bistability and oscillations emerge in biological networks involving multisite phosphorylation [26]. Such networks are of great biological importance [19]. The one we consider is the network, depicted in Figure 3.1, comprising extracellular signal-regulated kinase (ERK) regulation by dual-site phosphorylation by the kinase MEK (denoted by E) and dephosphorylation by the phosphatase MKP3 (F) [86]. This network, which we call the ERK network, has an important role in regulating many cellular activities, with dysregulation implicated in many cancers [90]. Accordingly, an important problem is to understand the dynamical properties of the ERK network, with the goal of predicting effects arising from mutations or drug treatments [43].

The ERK network was shown by [86] to be bistable and exhibit oscillations (for some choices of rate constants). Rubinstein *et al.* also observed that the ERK network "limits" to a network without bistability or oscillations. Namely, when the rate constants k_{cat} and ℓ_{cat} are much larger than k_{off} and ℓ_{off}, respectively, this yields the "fully processive" network obtained by deleting all vertical arrows in Figure 3.1, which is globally convergent to a unique steady state [25, 35, 83]. Accordingly, Rubinstein *et al.* asked, How do bistability and oscillations in the ERK network emerge from the processive limit? This question was subsequently articulated as follows by [26]:

Question 4.0.1. *When the processivity levels* $p_k := k_{\text{cat}}/(k_{\text{cat}} + k_{\text{off}})$ *and* $p_\ell := \ell_{\text{cat}}/(\ell_{\text{cat}} + \ell_{\text{off}})$ *are arbitrarily close to 1, is the ERK network still bistable and oscillatory?*

*The material in this chapter is reprinted from [78] by permission from Springer Nature Customer Service Centre GmbH: Springer *Journal of Mathematical Biology* "Oscillations and bistability in a model of ERK regulation", Nida Obatake, Anne Shiu, Xiaoxian Tang, and Angélica Torres, Copyright (2019).

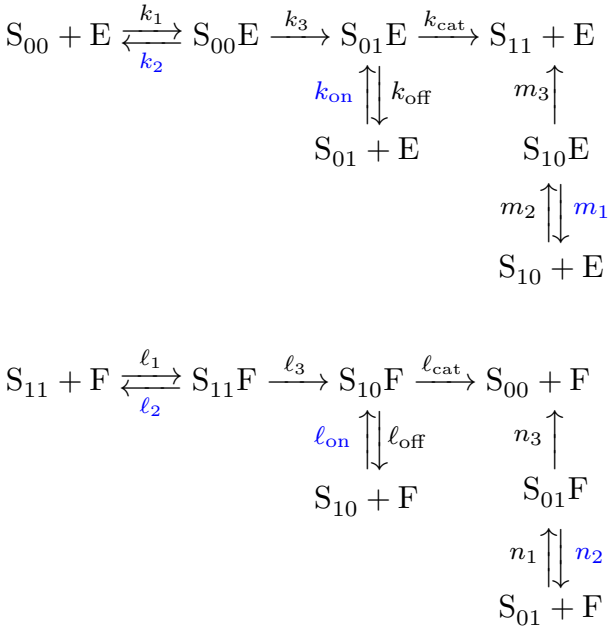

Figure 4.1: The (full) ERK network, from [86], with notation of [33]. Each S_{ij} denotes an ERK phosphoform, with subscripts indicating at which of two sites phosphate groups are attached. The *fully processive* network is obtained by deleting all vertical reactions (those labeled by $k_{on}, k_{off}, m_1, m_2, m_3, \ell_{on}, \ell_{off}, n_1, n_2, n_3$). We also consider irreversible versions of the ERK network obtained by deleting some of the reactions labeled $k_2, k_{on}, m_1, l_2, \ell_{on}, n_2$ (in blue). In particular, deleting all six of those reactions yields the fully irreversible ERK network. Reprinted with permission from [78].

One of our main contributions is to lay foundation toward answering Question 4.0.1. Specifically, we answer a related question, *How do bistability and oscillations emerge from simpler versions of the ERK network?* Our main results, summarized in Table 4.1, are that oscillations are surprisingly robust to operations that simplify the network, while bistability is lost more easily. Specifically, oscillations persist even as reactions are made irreversible and intermediates are removed (see Section 4.2.1), while bistability is lost more quickly, when only a few reactions are made irreversible (Section 4.2.2). Taken together, our results form a case study for the problem of model choice – an investigation into the simplifications of a model that preserve important dynamical properties.

Our focus here – on determining which operations on the ERK network preserve oscillations

ERK network	Oscillations?	Bistability?	Maximum # steady states	Maximum # over $\mathbb{C}$
Full	Yes*	Yes*	Conjecture: 3	7
Irreversible	Yes**	If $k_{\text{on}} > 0$ or $\ell_{\text{on}} > 0$	1	5*
Reduced	Yes	No	1	3

Table 4.1: Summary of results. Yes* indicates results of [86]. Yes** indicates that the fully irreversible ERK network exhibits oscillations (see Figure 4.2), and 5* indicates that 5 is the maximum number of complex-number steady states for the network obtained from the full ERK network by setting $k_{\text{on}} = 0$. For details on results, see Propositions 4.2.1, 4.2.5, and 6.3.4, and Theorem 4.2.6.

and bistability – is similar in spirit to the recent approach proposed by [87]. Indeed, there has been significant interest in understanding which operations on networks preserve oscillations [5], bistability [7, 40, 64], and other properties [49].

A related topic – mentioned earlier – is the question of how dynamical properties arise in phosphorylation systems. Several works have examined this problem at the level of parameters, focusing on the question of which rate constants and/or initial conditions give rise to oscillations [23] or bistability [21, 22]. Our perspective is slightly different; instead of allowing parameter values to change, we modify the network itself. Accordingly, our work is similar in spirit to recent investigations into minimal oscillatory or bistable networks [5, 7, 53, 58, 66].

A key tool we use is a parametrization of the steady states. Such parametrizations have been shown in recent years to be indispensable for analyzing multistationarity (multiple steady states, which are necessary for bistability) and oscillations [45, 63, 100]. Indeed, here we build on previous results [21, 23, 33].

Specifically, following the work of [23], we investigate oscillations by employing a steady-state parametrization together with a criterion proposed by [106] that characterizes Hopf bifurcations in terms of determinants of Hurwitz matrices. Using this approach, [23] showed that the Hopf bifurcations of a mixed-mechanism phosphorylation network lie on a hypersurface defined by the vanishing of a single Hurwitz determinant. For our ERK networks, however, the problem does not reduce to the analysis of a single polynomial, and the size of these polynomials makes the system

difficult to solve. To this end, we introduce an algorithm for analyzing these polynomials, through their Newton polytopes, by using techniques from polyhedral geometry. Using this algorithm, we succeed in finding, for the reduced ERK network, a Hopf bifurcation giving rise to oscillations.

The outline of our work is as follows. Section 4.1 introduces a new result on how to use steady-state parametrizations to detect Hopf bifurcations. Section 4.2 contains our main results on oscillations and bistability. We end with a discussion in Section 4.5.

All supplementary files referenced in this chapter are linked in Appendix A.

4.1 Using parametrizations to detect Hopf bifurcations

Here we prove a new result on how to use steady-state parametrizations to detect Hopf bifurcations (Theorem 4.1.2). The result, which uses Yang's criterion, is a straightforward generalization of the approach used by [23]. We include it here to use later in Section 4.2, and we also expect it to be useful in future work.

Lemma 4.1.1. *Let G be a network with s species, m reactions, and d conservation laws. Denote the ODEs by $\dot{x} = f(x)$, as in* (2.1)*. Assume that the positive steady states of G admit a positive parametrization ϕ with respect to an effective steady-state function for which the reparametrization map* (2.4) *is just the identity map. In other words, the effective parameters $\bar{a}_i$ are the original rate constants κ_i, and so we write $\phi : \mathbb{R}^{\hat{m}}_{>0} \times \mathbb{R}^{s}_{>0} \to \mathbb{R}^{m}_{>0} \times \mathbb{R}^{s}_{>0}$ as $(\hat{\kappa}; x) \mapsto \phi(\hat{\kappa}; x)$. Assume moreover that each coordinate of ϕ_i is a rational function: $\phi_i(\hat{\kappa}; x) \in \mathbb{Q}(\hat{\kappa}; x)$ for $i = 1, 2, \ldots, m + s$. Then the following is a univariate, degree-$(s - d)$ polynomial in λ, with coefficients in $\mathbb{Q}(\hat{\kappa}; x)$:*

$$q(\lambda) \;:=\; \frac{1}{\lambda^d}\, \det\left(\lambda I - \operatorname{Jac} f\right)|_{(\kappa;x)\,=\,\phi(\hat{\kappa};x)}\,. \tag{4.1}$$

Proof. This result is straightforward from the fact that the characteristic polynomial of $\mathrm{Jac}(f)$ is a polynomial of degree s and has zero as a root with multiplicity d (because of the d conservation laws). □

Theorem 4.1.2 (Hopf-bifurcation criterion)**.** *Assume the hypotheses of Lemma 4.1.1. Let $\mathfrak{h}_i$ (for $i = 1, 2, \ldots, s - d$) be the determinant of the i-th Hurwitz matrix of $q(\lambda)$ in* (4.1)*. Let κ_j be one of*

the rate constants in the vector $\hat{\kappa}$. Then the following are equivalent:

(1) there exists a rate-constant vector $\kappa^* \in \mathbb{R}^m_{>0}$ such that the resulting system (2.1) *exhibits a simple Hopf bifurcation with respect to κ_j at some $x^* \in \mathbb{R}^s_{>0}$, and*

(2) there exist $\hat{\kappa}^* \in \mathbb{R}^{\hat{m}}_{>0}$ and $x^* \in \mathbb{R}^s_{>0}$ such that

(i) the constant term of the polynomial $q(\lambda)$, when evaluated at $(\hat{\kappa}; x) = (\hat{\kappa}^*; x^*)$, is positive,

(ii) $\mathfrak{h}_1(\hat{\kappa}^*; x^*) > 0$, $\mathfrak{h}_2(\hat{\kappa}^*; x^*) > 0$, …, $\mathfrak{h}_{s-d-2}(\hat{\kappa}^*; x^*) > 0$, and

(iii) $\mathfrak{h}_{s-d-1}(\hat{\kappa}^*; x^*) = 0$ and $\frac{\partial \mathfrak{h}_{s-d-1}}{\partial \kappa_j}|_{(\hat{\kappa};x)=(\hat{\kappa}^*;x^*)} \neq 0$.

Moreover, given $\hat{\kappa}^*$ and x^* as in (2), a simple Hopf bifurcation with respect to κ_j occurs at x^* when the vector of rate constants is taken to be $\kappa^* := \widetilde{\pi}(\phi(\hat{\kappa}^*; x^*))$. Here, $\widetilde{\pi} : \mathbb{R}^m_{>0} \times \mathbb{R}^s_{>0} \to \mathbb{R}^m_{>0}$ is the natural projection.

Proof. Due to the d conservation laws, we apply Yang's criterion (Proposition 2.2.3) to:

$$\frac{1}{\lambda^d} \det(\lambda I - \operatorname{Jac} f)|_{x=x^*,\ \kappa_i=\kappa_i^*\ \textit{for all}\ i\neq j}\ .$$

Now our result follows directly from Proposition 2.2.3 and Definition 2.2.5. □

Remark 4.1.3. Theorem 4.1.2 easily generalizes beyond parametrizations of the form $\phi(\hat{\kappa}; x)$ to those of the form $\phi(\hat{\kappa}; \hat{x})$ or $\phi(\kappa; \hat{x})$. Indeed, one of the form $\phi(\kappa; \hat{x})$ was used by [23] to establish Hopf bifurcations in a mixed-mechanism phosphorylation system.

4.2 Main results

Each ERK network we investigated admits oscillations via a Hopf bifurcation (Section 4.2.1). Bistability, however, is more subtle (Section 4.2.2).

4.2.1 Oscillations

The full ERK system in Figure 3.1 exhibits oscillations for some values of the rate constants [86]. We now investigate oscillations in the fully irreversible and reduced ERK networks.

4.2.1.1 *Fully irreversible ERK network*

As shown in Figure 4.2, the fully irreversible ERK network admits oscillations. That figure was generated using the following rate constants:

$$\begin{aligned}(k_1, k_3, k_{\text{cat}}, k_{\text{off}}, \ell_1, \ell_3, \ell_{\text{cat}}, \ell_{\text{off}}, m_2, m_3, n_1, n_3) \;=\; (&5241, 5314.5, 1291, 76.203, 64.271, \\ &44.965, 924970, 27238, 2.76250 \times 10^6, \\ &2.0451, 2.1496 \times 10^6, 1.3334)\,.\end{aligned} \tag{4.2}$$

These rate constants (4.2) come from the ones that Rubinstein *et al.* showed generate oscillations for the full ERK network [86, Table 2] (we simply ignore their rate constants for the six deleted reactions). The approximate initial species concentrations used to generate Figure 4.2 are as follows (see supplementary file `ERK-Matcont.txt`):

$$\begin{aligned}(x_1, x_2, \ldots, x_{12}) \;\approx\; (&1.215 \times 10^{-5},\ 4.722 \times 10^{-5},\ 8.777 \times 10^{-4},\ 1.396 \times 10^{-3}, \\ &6.590 \times 10^{-8},\ 2.698 \times 10^{-3},\ 2.873 \times 10^{-4},\ 1.150 \times 10^{-3}, \\ &3.072 \times 10^{-3},\ 2.262 \times 10^{-6},\ 0.042,\quad 0.849)\,.\end{aligned} \tag{4.3}$$

In Figure 4.2, we notice some peculiarities in the graphs $x_i(t)$ of the species concentrations. The species concentrations x_1 and x_2 (corresponding to S_{00} and E, respectively) peak dramatically, while x_3 and x_6 (F and $S_{01}F$) stabilize momentarily at each peak. Also, each of x_1, x_2, x_3, x_4, x_5, x_{10}, x_{11} deplete for some time in each period, whereas x_{12} (S_{11}) never depletes. Finally, the graphs of the pairs x_1 and x_2 are qualitatively similar, and also the pair x_3 and x_6, the pair x_4 and x_5, and the pair x_{10} and x_{11}.

Going beyond the fully irreversible ERK network, all other irreversible ERK networks – those obtained from the full ERK network by deleting one or more the reactions $k_2, k_{\text{on}}, m_1, \ell_2, \ell_{\text{on}}, n_2$ – also admit oscillations. This claim follows from Proposition 4.1 in the article by [5], which "lifts" oscillations when one or more reactions are made reversible.

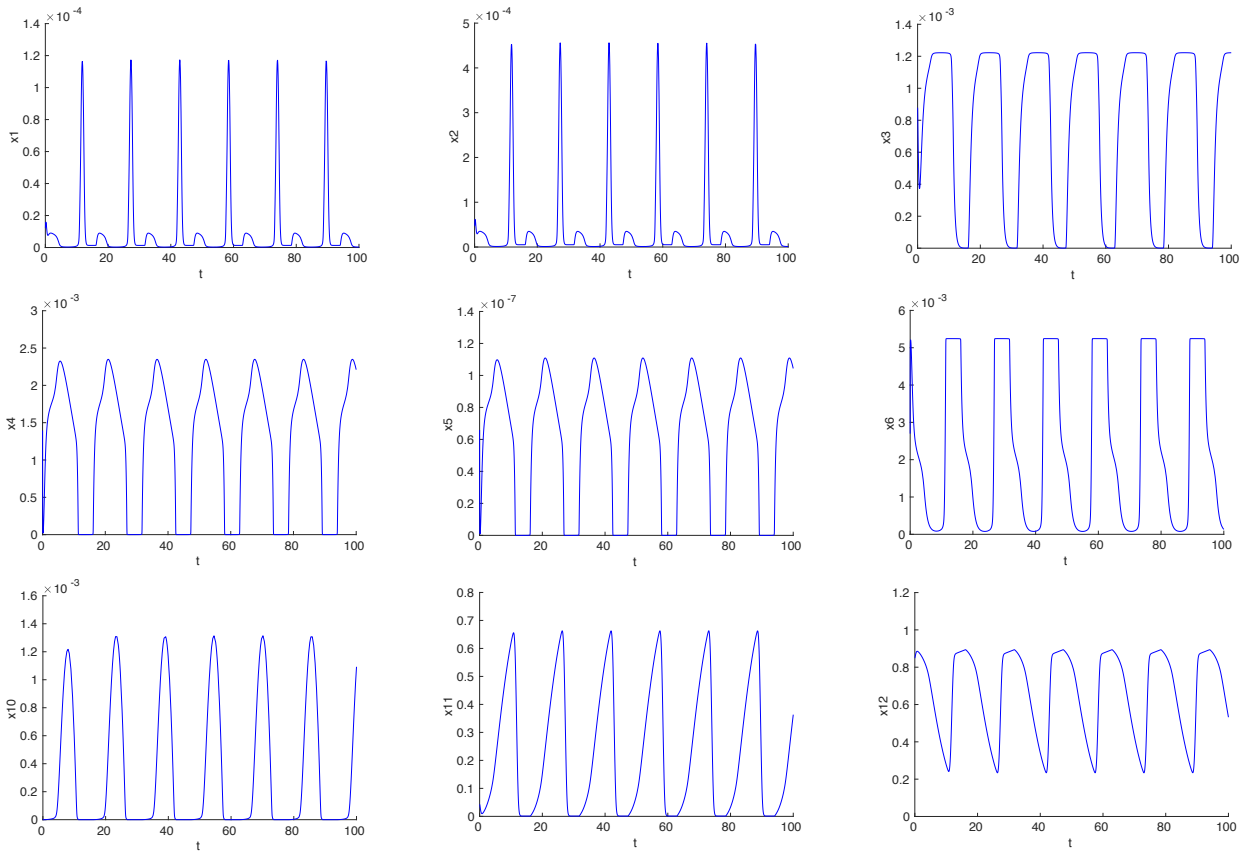

Figure 4.2: The fully irreversible ERK network undergoes oscillations when the rate constants are as in (4.2) and the initial species concentrations are as in (4.3). Displayed in this figure are all species concentrations, except x_7, x_8, and x_9. This figure was generated using `MATCONT`, a numerical bifurcation package [30]. For details, see the supplementary file `ERK-Matcont.txt`. Reprinted with permission from [78].

4.2.1.2 Reduced ERK network

We saw in the previous subsection that the fully irreversible ERK network exhibits oscillations. We now show that a simpler network - the reduced ERK network - also undergoes oscillations via a Hopf bifurcation. These oscillations are shown in Figure 4.3, and the rate constants that yield the corresponding Hopf bifurcation are specified in Theorem 4.2.3.

Compared to the oscillations for the irreversible ERK network (Figure 4.2), the oscillations in the reduced ERK network (Figure 4.3) are more uniform. Also, the period of oscillation is much shorter, and the amplitudes for species x_3, x_8, and x_{10} are small (this may be due to the choice of

rate constants). Finally, three of the six species shown do not deplete completely, whereas nearly all the species of the fully irreversible ERK do deplete in each period.

We discovered oscillations by finding a Hopf bifurcation. How we found this bifurcation – via the Hopf-bifurcation criterion in Section 4.1 – is the focus of the rest of this subsection.

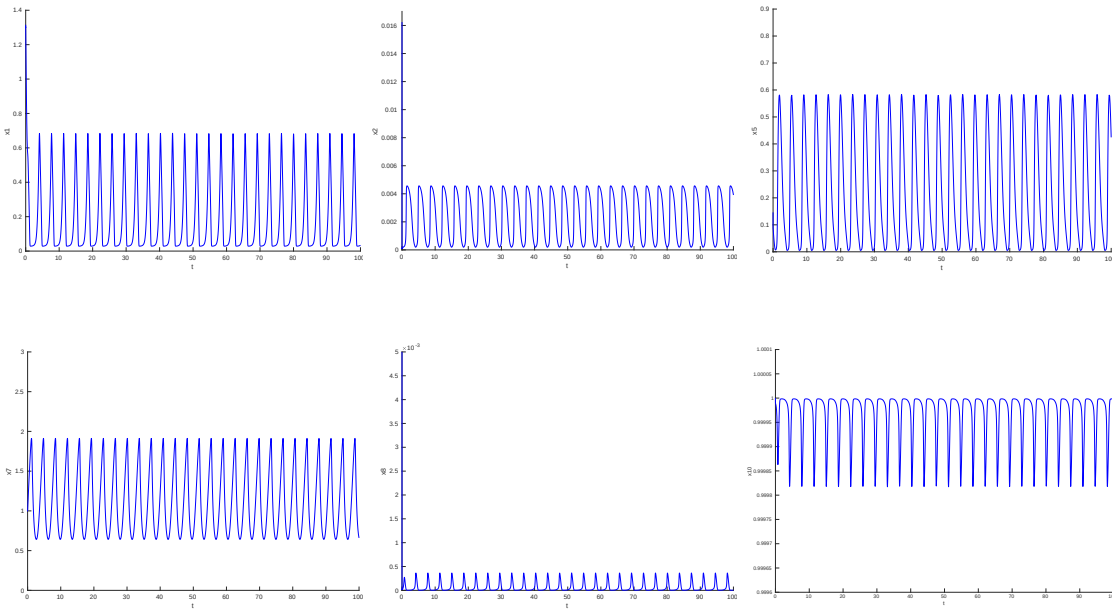

Figure 4.3: The reduced ERK network exhibits oscillations when the rate constants are approximately those in Theorem 4.2.3 and the initial species concentrations are close to the Hopf bifurcation. Details are in the supplementary file `ERK-Matcont.txt`. This figure, generated using `MATCONT`, displays all species concentrations, except x_3, x_4, x_6, and x_9. Reprinted with permission from [78].

Proposition 4.2.1 (Hopf criterion for reduced ERK)**.** *Consider the reduced ERK network, and let the polynomials f_i denote the right-hand sides of the resulting ODEs, as in* (3.7)*. Let $\hat{\kappa} := (k_{\text{cat}}, k_{\text{off}}, \ell_{\text{off}})$ and $x := (x_1, x_2, \ldots, x_{10})$, and let ϕ be the steady-state parametrization* (3.10)*.*

Then the following is a univariate, degree-7 polynomial in λ, with coefficients in $\mathbb{Q}(x)[\hat{\kappa}]$:

$$q(\lambda) \;:=\; \frac{1}{\lambda^3}\,\det\left(\lambda I - \mathrm{Jac}(f)\right)|_{(\kappa;x)=\phi(\hat{\kappa};x)}\,. \tag{4.4}$$

Now let $\mathfrak{h}_i$, for $i = 4, 5, 6$, denote the determinant of the i-th Hurwitz matrix of the polynomial $q(\lambda)$ in (4.4)*. Then the following are equivalent:*

(1) there exists a rate-constant vector $\kappa^* \in \mathbb{R}^{10}_{>0}$ such that the resulting system (3.7) *exhibits a simple Hopf bifurcation, with respect to k_{cat}, at some $x^* \in \mathbb{R}^{10}_{>0}$, and*

(2) there exist $x^* \in \mathbb{R}^{10}_{>0}$ and $\hat{\kappa}^* \in \mathbb{R}^{3}_{>0}$ such that

$$\begin{aligned} &\mathfrak{h}_4(\hat{\kappa}^*;x^*) > 0\,,\ \mathfrak{h}_5(\hat{\kappa}^*;x^*) > 0\,,\ \mathfrak{h}_6(\hat{\kappa}^*;x^*) = 0\,,\ \text{and} \\ &\frac{\partial}{\partial k_{\mathrm{cat}}}\mathfrak{h}_6(\hat{\kappa};x)|_{(\hat{\kappa};x)=(\hat{\kappa}^*;x^*)} \neq 0\,. \end{aligned} \tag{4.5}$$

Moreover, given $\hat{\kappa}^*$ and x^* as in (2), a simple Hopf bifurcation with respect to k_{cat} occurs at x^* when the rate constants are taken to be $\kappa^* := \widetilde{\pi}(\phi(\hat{\kappa}^*;x^*))$. Here, $\widetilde{\pi} : \mathbb{R}^{10}_{>0} \times \mathbb{R}^{10}_{>0} \to \mathbb{R}^{10}_{>0}$ is the natural projection to the first 10 coordinates.

Proof. The fact that $q(\lambda)$ is a degree-7 polynomial follows from Lemma 4.1.1, and the fact that its coefficients are in $\mathbb{Q}(x)[\hat{\kappa}]$ follows from inspecting equations (3.7) and (3.10). The rest of the result will follow immediately from Theorem 4.1.2 and Proposition 3.3.1, once we prove that $\mathfrak{h}_1$, $\mathfrak{h}_2$, $\mathfrak{h}_3$, and the constant term of $q(\lambda)$ are all positive when evaluated at any $(\hat{\kappa};x) \in \mathbb{R}^3_{>0} \times \mathbb{R}^{10}_{>0}$. Indeed, this is shown in the supplementary file `reducedERK-hopf.mw`. (In fact, even before substituting the parametrization $(\kappa;x) = \phi(\hat{\kappa};x)$, the corresponding Hurwitz determinants are already positive polynomials.) □

Remark 4.2.2. Note that k_{cat} is the only free parameter, so it is the natural bifurcation parameter.

We now prove that the reduced ERK network gives rise to a Hopf bifurcation.

Theorem 4.2.3 (Hopf bifurcation in reduced ERK)**.** *The reduced ERK network exhibits a simple Hopf bifurcation with respect to the bifurcation parameter k_{cat} at the following point:*

$$x^* \approx (0.05952457867,\ 0.002204614024,\ 1,\ 1,\ 0.1518056972,\ 1,\ 1,\ 0.00001239529511,\ 1,\ 1)\,,$$

when the rate constants are as follows:

$$(k_1^*, k_3^*, k_{\mathrm{cat}}^*, k_{\mathrm{off}}^*, m^*, \ell_1^*, \ell_3^*, \ell_{\mathrm{cat}}^*, \ell_{\mathrm{off}}^*, n^*) \approx (5.562806640 \times 10^6,\ 730,\ 729,\ 1,\ 453.5941390,\ 3.879519315 \times 10^8,\ 730,\ 729,\ 1,\ 80675.77183)$$

Here, ϕ is the parametrization (3.10)*, and $\widetilde{\pi}$ is the projection to the first 10 coordinates.*

Proof. By Proposition 4.2.1, we need only show that the inequalities and equality in (4.5) are satisfied at $x = x^*$ (with x^* given in the statement of the theorem) and $\hat{\kappa} = \hat{\kappa}^* = (9, 1, 1)$. These are verified in the supplementary file `reducedERK-hopf.mw`. □

Remark 4.2.4. The Hopf bifurcation given in Theorem 4.2.3 was found by analyzing the Newton polytopes of $\mathfrak{h}_4$, $\mathfrak{h}_5$, and $\mathfrak{h}_6$. The theory behind this approach is presented in Section 4.3, and the steps we took to find the Hopf bifurcation are listed in Section 4.4. We include these sections for readers who wish to apply similar approaches to other systems.

4.2.2 Bistability

Although the full ERK network is bistable [86], we now prove that the reduced ERK network is not bistable (Proposition 4.2.5). As for irreversible ERK networks, some of them are bistable, and we show that bistability is controlled by the two reactions k_{on} and ℓ_{on} (Theorem 4.2.6).

Proposition 4.2.5. *The reduced ERK network is not multistationary, and hence not bistable.*

Proof. Let $\mathcal{N}$ denote the reduced ERK network. By definition and Proposition 3.3.1, we obtain the following critical function for $\mathcal{N}$:

$$C(\hat{a}; x) \quad = \quad (\det \mathrm{Jac}\ h_{c,a})\,|_{(a;x)=\phi(\hat{a};x)}\,, \tag{4.6}$$

where $\hat{a} = (k_{\text{cat}}, k_{\text{off}}, \ell_{\text{off}})$, the function $h_{c,a}$ is as in (3.9), and $\phi(\hat{a}; x)$ is as in (3.10).

This critical function $C(\hat{a}; x)$ (see the supplementary file `reducedERK-noMSS.mw`) is a rational function, where the denominator is the following monomial: $x_1x_2x_3x_5x_6x_7x_8x_9$. The numerator of $C(\hat{a}; x)$ is the following polynomial, which is negative when evaluated at any $(\hat{a}; x) \in \mathbb{R}^3_{>0} \times \mathbb{R}^{10}_{>0}$:

$$\begin{aligned} &- k_{\text{cat}}^3(k_{\text{cat}} + k_{\text{off}})^2 x_4^3(k_{\text{cat}}x_4 + \ell_{\text{off}}x_{10})^2 \ell_{\text{off}} k_{\text{off}}(x_1x_2x_8 + x_1x_3x_8 + x_1x_4x_8 + x_{10}x_2x_5 \\ &\quad + x_{10}x_2x_6 + x_{10}x_2x_8 + x_2x_3x_8 + x_2x_4x_8 + x_2x_5x_8 + x_2x_5x_9 + x_2x_6x_8 + x_2x_6x_9 \\ &\quad + x_2x_7x_8 + x_2x_8x_9 + x_3x_7x_8 + x_4x_7x_8) \, . \end{aligned}$$

Thus, the following holds for all $(\hat{a}; x) \in \mathbb{R}^3_{>0} \times \mathbb{R}^{10}_{>0}$:

$$\text{sign}(C(\hat{a}; x)) = -1 = (-1)^{\text{rank}(N)} \, ,$$

where the final equality uses the fact that the stoichiometric matrix N has rank $10 - 3 = 7$.

So, by Proposition 2.2.7 and the fact that $\mathcal{N}$ is conservative with no boundary steady states in any stoichiometric compatibility class (Remark 3.3.4), $\mathcal{N}$ is monostationary. Thus, $\mathcal{N}$ is *not* multistationary and so, by definition, is *not* bistable. □

Although the reduced ERK network is not bistable (Proposition 4.2.5), the next result shows that irreversible versions of the full ERK network are bistable, as long as one of the reactions labeled by k_{on} and ℓ_{on} is present. That is, this result tells us which reactions can be safely deleted (in contrast to standard results concerning reactions that can be added, e.g., the articles of [5] and [7]) while preserving bistability. (In the next section, we investigate the precise number of steady states of ERK networks; see Proposition 6.3.4).

Theorem 4.2.6 (Bistability in irreversible ERK networks)**.** *Consider any network $\mathcal{N}$ obtained from the full ERK network by deleting one or more of the reactions corresponding to rate constants $k_2, k_{\text{on}}, m_1, \ell_2, \ell_{\text{on}}, n_2$ (blue in Figure 3.1). Then the following are equivalent:*

(1) $\mathcal{N}$ is multistationary,

(2) $\mathcal{N}$ is bistable, and

(3) $\mathcal{N}$ contains at least one of the reactions labeled by k_{on} and ℓ_{on}.

Proof. By definition, every bistable network is multistationary, so $(2) \Rightarrow (1)$. We therefore need only show $(1) \Rightarrow (3) \Rightarrow (2)$. (All computations below are found in our supplementary file `irreversibleERK.mw`).

For $(1) \Rightarrow (3)$, we will prove $\neg(3) \Rightarrow \neg(1)$: Assume that $\mathcal{N}$ contains neither the reaction labeled by k_{on} nor the reaction ℓ_{on}. Our proof here is analogous to that of Proposition 4.2.5. By Proposition 3.2.1, we obtain a critical function, $C(\hat{a}; x)$, for $\mathcal{N}$ of the form (4.6), where now $h_{c,a}$ is as in (3.3) (with $\mathbb{1}_{k_{\text{on}}} = \mathbb{1}_{\ell_{\text{on}}} = 0$) and $\phi(\hat{a}; x)$ is as in (3.4) (with $\hat{a} = (a_2, a_4)$).

Here, $\det \text{Jac}(h_{c,a})$ is a rational function with denominator equal to $k_{\text{off}} x_2 (n_2 + n_3) \ell_{\text{cat}} l_3 k_3 m_3$, which is always positive. The numerator is a polynomial of degree 5 in the variables x_2, x_3, and x_9 with coefficients that are always negative (see the supplementary file). The critical function $C(\hat{a}; x)$ is obtained by substituting the positive parametrization into $\det \text{Jac}(h_{c,a})$. Hence, for all $(\hat{a}; x) \in \mathbb{R}^2_{>0} \times \mathbb{R}^{12}_{>0}$, the equality $\text{sign}(C(\hat{a}; x)) = -1 = (-1)^{\text{rank}(N)}$ holds, because the stoichiometric matrix N has rank $12 - 3 = 9$. So, by Proposition 2.2.7 (recall from Remark 3.3.4 that $\mathcal{N}$ is conservative with no boundary steady states in any stoichiometric compatibility class), $\mathcal{N}$ is *not* multistationary.

Now we show $(3) \Rightarrow (2)$, that is, if $\mathcal{N}$ contains at least one of the reactions labeled by k_{on} and ℓ_{on} then $\mathcal{N}$ is bistable. By symmetry (from exchanging in the network E, S_{00}, and S_{01} with, respectively, F, S_{11}, and S_{10}), we may assume that $\mathcal{N}$ contains k_{on}.

Consider the network $\mathcal{N}'$ obtained from the full ERK network by deleting all reactions marked in blue in Figure 3.1, except for k_{on} (equivalently, we set $k_2 = m_1 = \ell_2 = \ell_{\text{on}} = n_2 = 0$). We will

show that the following total constants and rate constants yield bistability:

$$
\begin{gathered}
(c_1,\ c_2,\ c_3)\ =\ (46, 13, 13)\ , \quad \text{and} \\
(k_1, k_3, k_{\text{cat}}, k_{\text{on}}, k_{\text{off}}, \ell_1, \ell_3, \ell_{\text{cat}}, \ell_{\text{off}}, m_2, m_3, n_1, n_3)\ = \\
(2, 1.1, 1, 5, 15, 2, 1.1, 1, 10, 20, 10, 20, 10)\ .
\end{gathered}
\tag{4.7}
$$

Among the resulting three steady states (see the supplementary file), one of them is approximately:

(20.72107755, 0.2956877203, 3.248789181, 7.821850626,
0.7821850626, 1.147175131, 0.7821850626, 0.7821850626,
0.1765542587, 1.322653950, 11.13994215, 1.324191138) .

At the above steady state, the Jacobian matrix (of the system obtained from (3.1) by making the substitutions (4.7) and $k_2 = m_1 = \ell_2 = \ell_{\text{on}} = n_2 = 0$) has three zero eigenvalues (due to the three conservation laws). For the remaining eigenvalues, the real parts are approximately:

-76.0913958200572, -70.7106617930401 , -16.3022723748274,
-10.9324829878475, -10.9324829878475, -8.81318904794782 ,
-4.88866989801728, -4.88866989801728 , -0.0545784672515179 .

Thus, the nonzero eigenvalues have strictly negative real part, so the steady state is exponentially stable.

Another steady state is approximately

(0.1782157709, 8.088440520, 0.2275355904, 11.45336411,
1.145336411, 0.1737638914, 1.145336411, 1.145336411,
0.3818389270, 0.07080081803, 2.620886659, 27.68512059) .

At this steady state, the real part of the eigenvalues of the Jacobian matrix of the system are, in

addition to the three zero eigenvalues, approximately as follows:

-163.308657649675, -68.5596972162577 , -57.0205793889569 ,
-16.4435472947534, -12.1029003142539, -9.27515541335710,
-9.27515541335710, -3.08709626767693 , -0.209550347944487.

This steady state is also exponentially stable. (A third steady state, not shown, is unstable.) Hence, $\mathcal{N}'$ is bistable. Finally, as $\mathcal{N}'$ is a subnetwork obtained from $\mathcal{N}$ by making some reversible reactions irreversible, then by [64, Theorem 3.1], bistability "lifts" from $\mathcal{N}'$ to $\mathcal{N}$. Thus, $\mathcal{N}$ is bistable. □

We obtain the following consequence of Theorem 4.2.6.

Corollary 4.2.7. *The fully irreversible ERK network is monostationary.*

Proof. The fully irreversible ERK network contains neither the reaction labeled by k_{on} nor the one labeled ℓ_{on}, so Theorem 4.2.6 implies that the network is not multistationary. Thus, by a standard application of Brouwer's fixed-point theorem, together with the fact that the network is conservative and has no boundary steady states in any stoichiometric compatibility class (cf. Remark 3.9 in the article by [81]), there is – for every choice of positive rate constants – exactly one positive steady state in every stoichiometric compatibility class. □

4.3 Newton-polytope method

Here we show how analyzing the Newton polytopes of two polynomials can reveal whether there is a positive point at which one polynomial is positive and simultaneously the other is zero (Proposition 4.3.2 and Algorithm 4.3.4). In Section 4.4, we show how we used this approach, which we call the Newton-polytope method, to find a Hopf bifurcation leading to oscillations in the reduced ERK network (in Theorem 4.2.3).

Notation 4.3.1. Consider a polynomial $f = b_1 x^{\sigma_1} + b_2 x^{\sigma_2} + \cdots + b_\ell x^{\sigma_\ell} \in \mathbb{R}[x_1, x_2, \ldots, x_s]$, where the exponent vectors $\sigma_i \in \mathbb{Z}^s_{\geq 0}$ are distinct and $b_i \neq 0$ for all i. A vertex σ_i of $\mathrm{New}(f)$, the Newton

polytope of f, is a positive vertex (respectively, negative vertex) if the corresponding monomial of f is positive, i.e., $b_i > 0$ (respectively, $b_i < 0$). Also, $N_f(\sigma)$ denotes the outer normal cone of the vertex σ of $\mathrm{New}(f)$, i.e., the cone generated by the outer normal vectors to all supporting hyperplanes of $\mathrm{New}(f)$ containing the vertex σ. Finally, for a cone C, let $\mathrm{int}(C)$ denote the relative interior of the cone.

For an extensive discussion on polytopes and normal cones, see the book of [107].

Proposition 4.3.2. *Let $f, g \in \mathbb{R}[x_1, x_2, \ldots x_s]$. Assume that α is a positive vertex of $\mathrm{New}(f)$, β_+ is a positive vertex of $\mathrm{New}(g)$, and β_- is a negative vertex of $\mathrm{New}(g)$. Then, if $\mathrm{int}(N_f(\alpha)) \cap \mathrm{int}(N_g(\beta_+))$ and $\mathrm{int}(N_f(\alpha)) \cap \mathrm{int}(N_g(\beta_-))$ are both nonempty, then there exists $x^* \in \mathbb{R}^s_{>0}$ such that $f(x^*) > 0$ and $g(x^*) = 0$.*

To prove Proposition 4.3.2 we use the following well-known lemma and its proof.

Lemma 4.3.3. *Let $f = b_1 x^{\sigma_1} + b_2 x^{\sigma_2} + \cdots + b_\ell x^{\sigma_\ell} \in \mathbb{R}[x_1, x_2, \ldots, x_s]$ be a real, multivariate polynomial. If σ_i is a positive vertex (respectively, negative vertex) of $\mathrm{New}(f)$, then there exists $x^* \in \mathbb{R}^s_{>0}$ such that $f(x^*) > 0$ (respectively, $f(x^*) < 0$).*

Proof. Let σ_i be a vertex of $\mathrm{New}(f)$. Pick $w = (w_1, w_2, \ldots, w_s)$ in the relative interior of the outer normal cone $N_f(\sigma_i)$, which exists because σ_i is a vertex. Then, by construction, the linear functional $\langle w, - \rangle$ is maximized over the exponent-vectors $\sigma_1, \sigma_2, \ldots, \sigma_\ell$ at σ_i. Thus, we have the following univariate "polynomial with real exponents" in t:

$$f(t^{w_1}, t^{w_2}, \ldots, t^{w_s}) \;=\; b_1 t^{\langle w, \sigma_1 \rangle} + b_2 t^{\langle w, \sigma_1 \rangle} + \cdots + b_\ell t^{\langle w, \sigma_\ell \rangle} \;=\; b_i t^{\langle w, \sigma_i \rangle} + \text{lower-order terms}\,.$$

So, for t large, $\mathrm{sign}(f(t^{w_1}, t^{w_2}, \ldots, t^{w_s})) = \mathrm{sign}(b_i)$. Note that $(t^{w_1}, t^{w_2}, \ldots, t^{w_s}) \in \mathbb{R}^s_{>0}$. □

Our proof of Proposition 4.3.2 is constructive, through the following algorithm, where we use the notation $f_w(t) := f(t^{w_1}, t^{w_2}, \ldots, t^{w_s})$, for $t \in \mathbb{R}$ and $w = (w_1, w_2, \ldots, w_s) \in \mathbb{R}^s$.

Algorithm 4.3.4: Newton-polytope method

input : polynomials f, g, and vertices α, β_+, β_-, as in Proposition 4.3.2

output: a point $x^* \in \mathbb{R}^s_{>0}$ s.t. $f(x^*) > 0$ and $g(x^*) = 0$

1 define $C_0 := \operatorname{int}(N_f(\alpha)) \cap \operatorname{int}(N_g(\beta_+))$ and $C_1 := \operatorname{int}(N_f(\alpha)) \cap \operatorname{int}(N_g(\beta_-))$;

2 pick $\ell = (\ell_1, \ell_2, \ldots, \ell_s) \in C_0$ and $m = (m_1, m_2, \ldots, m_s) \in C_1$;

3 define $f_\ell(t) := f(t^{\ell_1}, t^{\ell_2}, \ldots, t^{\ell_s})$; define $f_m(t)$; define $g_\ell(t)$; define $g_m(t)$;

4 define $\tau_\ell := \inf\{t^* \in \mathbb{R}_{>0} \mid f_\ell(t) > 0 \text{ and } g_\ell(t) > 0 \text{ for all } t > t^*\}$;

5 define $\tau_m := \inf\{t^* \in \mathbb{R}_{>0} \mid f_m(t) > 0 \text{ and } g_m(t) < 0 \text{ for all } t > t^*\}$;

6 define $T := \max\{\tau_\ell, \tau_m\} + 1$;

7 define $h(r) := f_{r\ell+(1-r)m}(T)$;

8 **while** $\min\{h(r) \mid r \in [0,1]\} \le 0$ **do**

9 $\quad T := 2T$;

10 $\quad h(r) := f_{r\ell+(1-r)m}(T)$;

11 define $r^* := \operatorname{argmin}\{\big(g_{r\cdot\ell+(1-r)m}(T)\big)^2 \mid r \in [0,1]\}$ (pick one r^* if there are multiple);

return: $T^{r^*\ell+(1-r^*)m} := \big(T^{r^*\ell_1+(1-r^*)m_1}, T^{r^*\ell_2+(1-r^*)m_2}, \ldots, T^{r^*\ell_s+(1-r^*)m_s}\big)$

Proof of Proposition 4.3.2. Let a_+x^α be the term of f corresponding to the vertex α of $\operatorname{New}(f)$, and similarly let $b_+x^{\beta_+}$ (respectively, $b_-x^{\beta_-}$) be the term of g corresponding to the vertex β_+ (respectively, β_-) of $\operatorname{New}(g)$. Thus, $a_+ > 0$, $b_+ > 0$, and $b_- < 0$. Let $\{a_1, a_2, \ldots, a_d\} \subseteq \mathbb{R}$ denote the remaining set of coefficients of f, so that $f = a_+x^\alpha + (a_1x^{\sigma_1} + a_2x^{\sigma_2} + \cdots + a_dx^{\sigma_d})$, for some exponent vectors $\sigma_i \in \mathbb{Z}^s_{\ge 0}$.

Algorithm 4.3.4 terminates: First, ℓ and m in line 2 exist by hypothesis. Also, τ_ℓ and τ_m in lines 4–5 exist by the proof of Lemma 4.3.3 and by construction. Next, $\min h(r)$ in line 8 exists because h is a continuous univariate function defined on a compact interval.

By construction and because cones are convex, the vector $r\ell + (1-r)m$, which is a convex combination of ℓ and m, is in the relative interior of $N_f(\alpha)$ for all $r \in [0,1]$. Thus, $\langle r\ell + (1 -$

$r)m,\ \alpha - \sigma_i\rangle > 0$ for all $i = 1, 2, \ldots, d$ and for all $r \in [0, 1]$. This (together with a straightforward argument using continuity and compactness) implies the following:

$$\delta \ := \ \inf_{r\in[0,1]} \min_{i=1,2,\ldots,d} \langle r\ell + (1-r)m,\ \alpha - \sigma_i\rangle \ > \ 0.$$

Next, let $\beta := \inf_{r\in[0,1]}\langle r\ell + (1-r)m,\ \alpha\rangle$. Then, for all $r \in [0, 1]$ and $t > 0$,

$$\begin{aligned} f_{r\ell+(1-r)m}(t) \ &= \ a_+ t^{\langle r\ell+(1-r)m),\alpha\rangle} + \left(a_1 t^{\langle r\ell+(1-r)m),\sigma_1\rangle} + \cdots + a_d t^{\langle r\ell+(1-r)m),\sigma_d\rangle}\right) \\ &> \ a_+ t^{\beta} - (|a_1| + |a_2| + \cdots + |a_d|)t^{\beta-\delta} \ =: \ \widetilde{f}(t)\ . \end{aligned} \tag{4.8}$$

In $\widetilde{f}(t)$, the term a_+t^β dominates the other term, for t large, so there exists $T^* > 0$ such that $\widetilde{f}(t) \geq 0$ when $t \geq T^*$. So, by (4.8), the while loop in line 8 ends when $T \geq T^*$ (or earlier).

Algorithm 4.3.4 is correct: For T fixed, the minimum of $\psi(r) := \left(g(T^{r\ell+(1-r)m})\right)^2$ over the compact set $[0, 1]$ is attained, because ψ is continuous. Next we show that this minimum value is 0, or equivalently that for $\chi(r) := g(T^{r\ell+(1-r)m})$ there exists some $r^* \in (0, 1)$ such that $\chi(r^*) = 0$. Indeed, this follows from the Intermediate Value Theorem, because χ is continuous, $\chi(0) = g(T^m) < 0$ (because $T > \tau_m$), and $\chi(1) = g(T^\ell) > 0$ (because $T > \tau_\ell$).

Finally, the inequality $f(T^{r^*\ell+(1-r^*)m}) > 0$ holds by construction of T, so defining $x^* := T^{r^*\ell+(1-r^*)m} \in \mathbb{R}^s_{>0}$ yields the desired vector satisfying $f(x^*) > 0$ and $g(x^*) = 0$. □

Remark 4.3.5. As we showed in the proof above, Algorithm 4.3.4 terminates since the while loop in Lines 8–10 ends because the minimum values we are looking for exist because the functions h are continuous functions defined on compact sets. However, in practical terms, finding the `argmin` in Step 11 requires numerical methods, and these methods finish after achieving certain precision or a maximum number of iterations. In practice, then, the algorithm terminates with an approximation, and after a certain precision is reached.

4.4 Using the Newton-polytope method

Here we show how we used Algorithm 4.3.4 to find the Hopf bifurcation in Theorem 4.2.3. (For details, see the supplementary files `reducedERK-hopf.mw` and `reducedERK-cones.sws`). Recall from the proof of that theorem, that our goal was to find some $x^* \in \mathbb{R}^{10}_{>0}$ and $\hat{\kappa}^* = (k^*_{\text{cat}}, k^*_{\text{off}}, \ell^*_{\text{off}}) \in \mathbb{R}^3_{>0}$ satisfying the following conditions from Proposition 4.2.1:

$$\mathfrak{h}_4(\hat{\kappa}^*; x^*) > 0 \ , \ \mathfrak{h}_5(\hat{\kappa}^*; x^*) > 0 \ , \ \mathfrak{h}_6(\hat{\kappa}^*; x^*) = 0 \ , \text{ and } \frac{\partial}{\partial k_{\text{cat}}} \quad \mathfrak{h}_6(\hat{\kappa}; x)|_{(\hat{\kappa};x)=(\hat{\kappa}^*;x^*)} \neq 0 \ . \quad (4.9)$$

Step One. Specialize some of the parameters: set $k_{\text{off}} = \ell_{\text{off}} = 1$ and $x_3 = x_4 = x_6 = x_7 = x_9 = x_{10} = 1$. (Otherwise, $\mathfrak{h}_5$ and $\mathfrak{h}_6$ are too large to be computed.)

Step Two. Do a change of variables: let $y_i = 1/x_i$ for $i = 1, 2, 5, 8$. These variables x_i were in the denominator, so switching to the variables y_i yield polynomials.

Let $\mathcal{H}_4$, $\mathcal{H}_5$, and $\mathcal{H}_6$ denote the resulting polynomials in $\mathbb{Q}[k_{\text{cat}}, y_1, y_2, y_5, y_8]$ after performing Steps One and Two. Accordingly, our updated goal is to find $(k^*_{\text{cat}}, y^*_1, y^*_2, y^*_5, y^*_8) \in \mathbb{R}^5_{>0}$ at which $\mathcal{H}_4$ and $\mathcal{H}_5$ are positive and $\mathcal{H}_6$ is zero. (In a later step, we must also check the partial-derivative condition in (4.9).)

Step Three. Apply (a straightforward generalization of) Algorithm 4.3.4 as follows.

(i) Find a positive vertex of $\mathcal{H}_4$ and a positive vertex of $\mathcal{H}_5$ whose outer normal cones intersect (denote the intersection by C), and a positive vertex and a negative vertex of $\mathcal{H}_6$ (denote their outer normal cones by D_+ and D_-, respectively) for which:

   (a) the intersection $D_+ \cap D_-$ is 4-dimensional, and

   (b) the intersections $C \cap D_+$ and $C \cap D_-$ are both 5-dimensional.

(ii) By Proposition 4.3.2, a vector $(k^*_{\text{cat}}, y^*_1, y^*_2, y^*_5, y^*_8)$ that accomplishes our updated goal, is guaranteed. To find such a point, we follow Algorithm 4.3.4 to obtain $k^*_{\text{cat}} = 729, y^*_1 \approx 16.79978292, y^*_2 \approx 453.5941389, y^*_5 \approx 6.587368051$, and $y^*_8 \approx 80675.77181$.

Recall the specializations in Step One and change of variables in Step Two, to obtain $\hat{\kappa} = (729, 1, 1)$ and

$$x^* \approx (0.05952457867,\ 0.002204614024,\ 1,\ 1,\ 0.1518056972,\ 1,\ 1,\ 0.00001239529511,\ 1,\ 1)\,.$$

Step Four. Verify that the conditions in (4.9) hold.

4.5 Discussion

Phosphorylation plays a key role in cellular signaling networks, such as *mitogen-activated protein kinase (MAPK) cascades*, which enable cells to make decisions (to differentiate, proliferate, die, and so on) [17]. This decision-making role of MAPK cascades suggests that they exhibit switch-like behavior, i.e., bistability. Indeed, bistability in such cascades has been seen in experiments [3, 9]. Oscillations also have been observed [59, 62], hinting at a role in timekeeping. Indeed, multisite phosphorylation is the main mechanism for establishing the 24-hour period in eukaryotic circadian clocks [79, 103].

These experimental findings motivated the questions we pursued. Specifically, we investigated robustness of oscillations and bistability in models of ERK regulation by dual-site phosphorylation. Bistability, we found, is quickly lost when reactions are made irreversible. Indeed, bistability is characterized by the presence of two specific reactions. Oscillations, in contrast, persist even as the network is greatly simplified. Indeed, we discovered oscillations in the reduced ERK network. Moreover, this network has the same number of reactions (ten) as the mixed-mechanism network which Suwanmajo and Krishnan surmised "could be the simplest enzymatic modification scheme that can intrinsically exhibit oscillation" [98, §3.1]. Our reduced ERK network, therefore, may also be such a minimal oscillatory network.

Returning to our bistability criterion (Theorem 4.2.6), recall that this result elucidates which reactions can be safely *deleted* while preserving bistability – in contrast to standard results concerning reactions that can be *added* [7, 40, 64]. We desire more results of this type, so we comment on how we proved our result. The key was the special form of the steady-state parametrization. In par-

ticular, following [33], our parametrizations allow both species concentrations and rate constants to be solved (at steady state) in terms of other variables. Additionally, a single parametrizations specialized (by setting rates to zero for deleted reactions) to obtain parametrizations for a whole family of networks. Together, these properties gave us access to new information on how bistability is controlled. We are interested, therefore, in the following question: *Which networks admit a steady-state parametrization that specializes for irreversible versions of the network?*

Our results on oscillations were enabled by new mathematical approaches to find Hopf bifurcations. Specifically, building on the article by [23], we gave a Hopf-bifurcation criterion for networks admitting a steady-state parametrization. Additionally, we successfully applied this criterion to the reduced ERK network by analyzing the Newton polytopes of certain Hurwitz determinants. We expect these techniques to apply to more networks.

Finally, our work generated a number of open questions. First, what are the mixed volumes of irreversible versions of the ERK network (beyond those shown in Table 6.1)? In particular, is there a mixed-volume analogue of our bistability criterion, which is in terms of the reactions k_{on} and ℓ_{on}? And, what is the maximum number of (stable) steady states in the full ERK network (Conjecture 6.3.5)? Progress toward these questions will yield further insight into robustness of bistability and oscillations in biological signaling networks.

5. ROBUSTNESS OF OSCILLATIONS AND BISTABILITY IN A MODEL OF ERK REGULATION*

The material in this chapter is based on the paper "Dynamics of ERK regulation in the processive limit" [24], which was authored jointly with Carsten Conradi, Anne Shiu, and Xiaoxian Tang.

We focus on the following question, posed by [86], pertaining to a model of extracellular signal-regulated kinase (ERK) regulation (Figure 5.1):

Question 5.0.1. *For all processivity levels*[2] $p_k := k_{\text{cat}}/(k_{\text{cat}} + k_{\text{off}})$ *and* $p_\ell := \ell_{\text{cat}}/(\ell_{\text{cat}} + \ell_{\text{off}})$ *close to 1, is the ERK network in Figure 5.1, bistable and oscillatory?*

The motivation behind this question was given earlier [43, 78, 86], which we summarize here. Briefly, as both p_k and p_ℓ approach 1, the ERK network "limits" to a (fully processive) network that is globally convergent to a unique steady state, and thus lacks bistability and oscillations [25]. As bistability and oscillations may allow networks to act as a biological switch or clock [102], we want to know how far "along the way" to the limit, the network maintains the capacity for these important dynamical properties.

A partial result toward resolving Question 5.0.1 was given by [86], who exhibited, in simulations, oscillations for $p_k, p_\ell \approx 0.97$. This left open the question of oscillations for $0.97 < p_k, p_\ell < 1$. Our result in this direction is given in Theorem 5.2.1 (described below).

Additional prior results aimed at answering Question 5.0.1 appeared in Chapter 4. We showed that bistability is preserved when reactions in the ERK network are made irreversible, as long at least one of the reactions labeled by k_{on} and ℓ_{on} is preserved. We therefore give the name "minimally bistable ERK subnetwork" to the network obtained by making all reaction irreversible

*The material in this chapter is reprinted from [24] by permission from Springer Nature Customer Service Centre GmbH: Springer *Journal of Mathematical Biology* "Dynamics of ERK regulation in the processive limit", Carsten Conradi, Nida Obatake, Anne Shiu, and Xiaoxiang Tang, Copyright (2020).

[2]This level is the probability that the enzyme acts processively, that is, adds a second phosphate group after adding the first [89]. A somewhat similar idea, from [97], is the "degree of processivity".

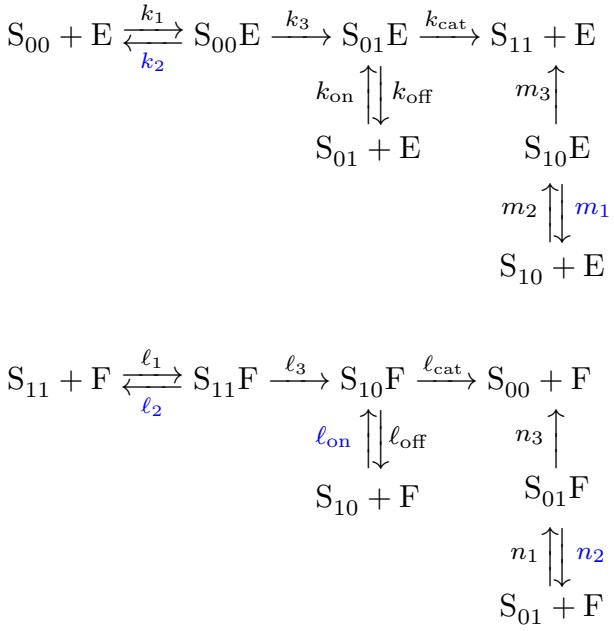

Figure 5.1: The ERK network consists of ERK regulation through dual-site phosphorylation by the kinase MEK (denoted by E) and dephosphorylation by the phosphatase MKP3 (F). Each S_{ij} denotes an ERK phosphoform, with subscripts indicating at which of two sites phosphate groups are attached. Deleting from this network the reactions labeled $k_2, m_1, l_2, \ell_{\text{on}}, n_2$ (in blue) yields the minimally bistable ERK subnetwork (the explanation for this name is given before Question 5.0.2). Reprinted with permission from [24].

except the reversible-reaction pair k_{on} and k_{off} (Figure 5.1). (By symmetry, the network preserving ℓ_{on} and ℓ_{off}, rather than k_{on} and k_{off}, is equivalent.) We therefore state the following version of Question 5.0.1 for bistability:

Question 5.0.2. *For p_k and p_ℓ close to 1, is the minimally bistable ERK subnetwork, bistable?*

If yes, then by results lifting bistability from subnetworks to larger networks [64], this also answers in the affirmative the part of Question 5.0.1 pertaining to bistability.

Similarly, for oscillations, we showed that when reactions are made irreversible and also two "intermediates" (namely, $S_{10}E$ and $S_{01}F$) are removed, oscillations are preserved (Chapter 4).For this network, called the "reduced ERK network" (Figure 3.3), we now ask a variant of Question 5.0.1 for oscillations (an affirmative answer to Question 5.0.3 likely "lifts" to an affirmative answer to Question 5.0.1; see Remark 5.2.3):

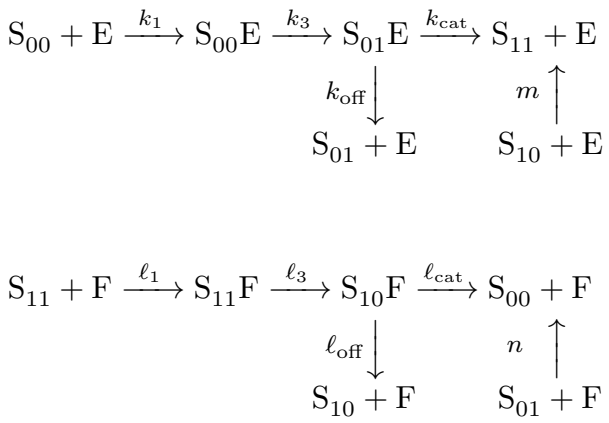

Figure 5.2: Reduced ERK network (see Section 3.3). Reprinted with permission from [24].

Question 5.0.3. *For p_k and p_ℓ close to 1, is the reduced ERK network, oscillatory?*

Our answers to Questions 5.0.2 and 5.0.3 are as follows. For the first question, at *all* processivity levels – not just near 1 – the minimally bistable ERK subnetwork admits multiple steady states, a necessary condition for bistability (Theorem 5.1.1). Furthermore, computational evidence suggests that indeed we have bistability. We also investigate how varying processivity levels affects the range of parameter values that yield multistationarity and also *how* multistationarity (and thus bistability) is lost as the ERK network limits to a (fully processive) network without bistability. Our numerical observations suggest that as the processivity levels approach 1, the classical S-shaped curve often associated with multistationarity deforms to a steep Hill function (see Figure 5.5 in Section 5.1.3).

Similarly, for Question 5.0.3, again at (nearly) all processivity levels, the reduced ERK network admits a Hopf bifurcation (Theorem 5.2.1), a precursor to oscillations. We also numerically investigate such oscillations (see Figure 5.6).

Finally, we pursue several more questions pertaining to ERK networks. We investigate in the ERK network whether – for some choice of rate constants – bistability and Hopf bifurcations can coexist (see Theorem 5.3.1). We also pursue Conjecture 5.3.2 on the maximum number of steady

states in the minimally bistable ERK network.

Our results fit into related literature as follows. First, as other authors have done for their models of interest [20, 46, 88], we analyze simplified versions of the ERK network obtained by removing intermediate species and/or reactions (in some cases, bistability and oscillations can be "lifted" from smaller networks to larger ones [5, 7, 15, 41, 64]). Also, our proofs harness two results from previous work: a Hopf-bifurcation criterion for the reduced ERK network (Proposition 4.2.1) and a criterion for multistationarity arising from degree theory [21, 33].

This work primarily concerns two networks, the minimally bistable ERK subnetwork and the reduced ERK network. We refer the reader to Sections 3.4 and 3.3 of Chapter 3 respectively for details about these networks. We present our main results on multistationarity and bistability (Section 5.1), Hopf bifurcations and oscillations (Section 5.2), and coexistence of bistability and oscillations (Section 5.3). In Section 5.4, we prove results on the maximum number of steady states in the minimally bistable ERK network. We conclude with a discussion in Section 5.5.

All supplementary files referenced in this chapter are linked in Appendix B.

5.1 Bistability

In this section, we show that, for *every* choice of processivity levels, the minimally bistable ERK network is multistationary (Theorem 5.1.1). We also give evidence suggesting that in fact, when we have multistationarity, we always have bistability (Section 5.1.2). Finally, we investigate multistationarity numerically for processivity levels close to 1 (Section 5.1.3).

5.1.1 Multistationarity at all processivity levels

Theorem 5.1.1 (Multistationarity at all processivity levels)**.** *Consider the minimally bistable ERK subnetwork. For every choice of processivity levels $p_k \in (0,1)$ and $p_\ell \in (0,1)$, there is a rate-constant vector $(k_1^*, k_3^*, k_{\text{cat}}^*, k_{\text{on}}^*, k_{\text{off}}^*, \ell_1^*, \ell_3^*, \ell_{\text{cat}}^*, \ell_{\text{off}}^*, m_2^*, m_3^*, n_1^*, n_3^*) \in \mathbb{R}^{13}_{>0}$ such that*

1. *$p_k = k_{\text{cat}}^*/(k_{\text{cat}}^* + k_{\text{off}}^*)$ and $p_\ell = \ell_{\text{cat}}^*/(\ell_{\text{cat}}^* + \ell_{\text{off}}^*)$, and*

2. *the resulting system admits multiple positive steady states (in some compatibility class).*

Proof. Let $C(\kappa; \hat{x})$ (where $\hat{x} = (x_1, x_2, x_3)$) denote the critical function of the steady-state

parametrization (3.16) in Proposition 3.4.1.

By setting $k^*_{\text{off}} = \ell^*_{\text{off}} = 1$ and allowing k^*_{cat} and ℓ^*_{cat} to be arbitrary positive values, we obtain all processivity levels $p_k = k^*_{\text{cat}}/(k^*_{\text{cat}} + k^*_{\text{off}})$ and $p_\ell = \ell^*_{\text{cat}}/(\ell^*_{\text{cat}} + \ell^*_{\text{off}})$ in $(0, 1)$. Also, the rank of stoichiometric matrix N for this network is 9; hence, $(-1)^{\text{rank}(N)+1} = 1$. So, by Proposition 2.2.7, it suffices to show that for all $k^*_{\text{cat}} > 0$ and $\ell^*_{\text{cat}} > 0$, the following specialization of the critical function is positive when we further specialize at some choice of $(k_1, k_3, k_{\text{on}}, \ell_1, \ell_3, m_2, m_3, n_1, n_3) \in \mathbb{R}^9_{>0}$, and $\hat{x} \in \mathbb{R}^3_{>0}$:

$$C(\kappa; \hat{x})|_{k_{\text{off}}=\ell_{\text{off}}=1,\ k_{\text{cat}}=k^*_{\text{cat}},\ \ell_{\text{cat}}=\ell^*_{\text{cat}}} \tag{5.1}$$

To see that the function (5.1) can be positive, note that the denominator of $C(\kappa; \hat{x})|_{k_{\text{off}}=\ell_{\text{off}}=1}$, shown here, is always positive (all rate constants and x_i's are positive):

$$(k_{\text{cat}}k_{\text{on}}x_2 + k_{\text{cat}}n_1x_3 + n_1x_3)^2\ell_{\text{cat}}x_3\ .$$

(See the supplementary file `minERK-mss-bistab.mw`.) Thus, it suffices to analyze the numerator of $C(\kappa; \hat{x})|_{k_{\text{off}}=\ell_{\text{off}}=1}$. We denote this numerator by $\widetilde{C}$, and specialize as follows to obtain (see the supplementary file):

$$\widetilde{C}|_{k_1=t^{-1},k_3=t^{-1},k_{\text{on}}=1,\ell_1=t,\ell_3=t^{-1},m_2=1,m_3=1,n_1=1,n_3=1,x_1=t,x_2=t,x_3=1} \tag{5.2}$$

$$\begin{aligned} &= (2k^2_{\text{cat}}\ell^2_{\text{cat}} + 2k^2_{\text{cat}}\ell_{\text{cat}})t^5 \qquad (5.3)\\ &\quad + (-4k^3_{\text{cat}}\ell^2_{\text{cat}} - 3k^3_{\text{cat}}\ell_{\text{cat}} + 3k^2_{\text{cat}}\ell^2_{\text{cat}} - k^3_{\text{cat}} + 9k^2_{\text{cat}}\ell_{\text{cat}} + 3k_{\text{cat}}\ell^2_{\text{cat}} + 2k^2_{\text{cat}} + 3k_{\text{cat}}\ell_{\text{cat}})t^4\\ &\quad + \text{lower-order terms in } t. \end{aligned}$$

Therefore, for all $k_{\text{cat}} > 0$ and $\ell_{\text{cat}} > 0$, the leading coefficient with respect to t in (5.3) is positive and so the specialization of $\widetilde{C}$ is positive for sufficiently large t, which yields the desired values for the rate constants shown in (5.2). □

Remark 5.1.2. In the proof of Theorem 5.1.1, the specialization (5.2) was obtained by viewing $\widetilde{C}$

as a polynomial in which each coefficient is a polynomial in k_{on}, k_{cat} and ℓ_{cat}, and then analyzing the resulting Newton polytope in a standard way (cf. Lemma 4.3.3), as follows. We first found a vertex of the polytope whose corresponding coefficient is a positive polynomial (namely, the leading coefficient in (5.3)). Next, we chose a vector v in the interior of the corresponding cone in the polytope's outer normal fan (specifically, $v = [1, 1, 0, -1, -1, 1, -1, 0, 0, 0, 0]$). So, by substituting $k_{\text{on}} = 1$ and $t^{v_1}, t^{v_2}, \ldots$ for the variables $x_1, x_2, x_3, k_1, k_3, \ell_1, \ell_3, m_2, m_3, n_1, n_3$, the resulting polynomial is positive for large t.

5.1.2 Evidence for bistability

Theorem 5.1.1 states that the minimally bistable ERK network is multistationary at all processivity levels. Multistationarity is a necessary condition for bistability, which is the focus of the original Question 5.0.2 from the Introduction. Accordingly, we show bistability at many processivity levels with $p_k = p_\ell$ (Proposition 5.1.4). Furthermore, we give additional evidence for bistability at *all* processivity levels (Remark 5.1.5), which we state as Conjecture 5.1.6.

Remark 5.1.3 (Assessing bistability is difficult)**.** Although there are many criteria for checking whether a network is multistationary, there are relatively few for checking bistability [101]. Moreover, here we consider a more difficult question: does our network exhibit bistability for an infinite family of parameters (rather than a single parameter vector), encompassing all processivity levels? Thus, it is perhaps unsurprising that we obtain only partial results in this direction. Another "infinite" analysis of bistability was performed recently by [99], who proved that an infinite family of sequestration networks all are bistable.

Proposition 5.1.4 (Bistability at many processivity levels)**.** *Consider the minimally bistable ERK subnetwork. For each of the following processivity levels:*

$$p_k \;=\; p_\ell \;\in\; \{0.1, 0.2, \ldots, 0.9,\; 0.91, 0.92, \ldots, 0.99\}\,, \tag{5.4}$$

there is a rate-constant vector $(k_1^*, k_3^*, k_{\text{cat}}^*, k_{\text{on}}^*, k_{\text{off}}^*, \ell_1^*, \ell_3^*, \ell_{\text{cat}}^*, \ell_{\text{off}}^*, m_2^*, m_3^*, n_1^*, n_3^*) \in \mathbb{R}^{13}_{>0}$ *such that* $p_k = k_{\text{cat}}^*/(k_{\text{cat}}^* + k_{\text{off}}^*)$ *and* $p_\ell = \ell_{\text{cat}}^*/(\ell_{\text{cat}}^* + \ell_{\text{off}}^*)$*, and the resulting system admits multiple*

exponentially stable positive steady states (in some compatibility class).

Proof. As in the proof of Theorem 5.1.1, we achieve each value of $p_k^* = p_\ell^*$, as in (5.4), by setting $k_{\text{off}}^* = \ell_{\text{off}}^* = 1$ and $k_{\text{cat}}^* = \ell_{\text{cat}}^* = p_k^*/(1 - p_k^*)$.

Next, we follow the proof of Theorem 5.1.1 to find a witness to multistationarity. Recall that the specialized numerator of the critical function given in (5.2), which is a polynomial in k_{cat}, ℓ_{cat}, and t, is positive (indicating multistationarity) for sufficiently large t. That is, there exists a $T \in \mathbb{R}_{>0}$, which depends on the value of $p_k^* = p_\ell^*$, at which the specialized critical function is positive for all $t \geq T$. For each value of $p_k^* = p_\ell^*$, we pick such a positive number T, as follows:

$p_k^* = p_\ell^*$	0.1	0.2	0.3	0.4	0.5	0.6	0.7	0.8	0.9
T	3	3	3	3	4	5	7	10	20
$p_k^* = p_\ell^*$	0.91	0.92	0.93	0.94	0.95	0.96	0.97	0.98	0.99
T	22	25	28	33	40	50	66	100	200

It follows, from (5.2) and Proposition 2.2.7(B), that with the following rate-constant vector:

$$\begin{aligned}\kappa^* &:= (k_1^*, k_3^*, k_{\text{cat}}^*, k_{\text{on}}^*, k_{\text{off}}^*, \ell_1^*, \ell_3^*, \ell_{\text{cat}}^*, \ell_{\text{off}}^*, m_2^*, m_3^*, n_1^*, n_3^*) \\ &= (T^{-1},\ T^{-1},\ p_k^*/(1-p_k^*),\ 1,\ 1,\ T,\ T^{-1},\ p_k^*/(1-p_k^*),\ 1,\ 1,\ 1,\ 1,\ 1)\,, \end{aligned} \tag{5.5}$$

there are multiple steady states in the compatibility class containing $x^* := \pi(\phi(\kappa^*; 1, T, 1))$, where $\phi : \mathbb{R}_{>0}^{13} \times \mathbb{R}_{>0}^{3} \to \mathbb{R}_{>0}^{13} \times \mathbb{R}_{>0}^{12}$ is the steady-state parametrization in Proposition 3.4.1 and $\pi : \mathbb{R}_{>0}^{13} \times \mathbb{R}_{>0}^{12} \to \mathbb{R}_{>0}^{12}$ denotes the canonical projection to the last 12 coordinates.

Finally, for each such x^* (one for each choice of $p_k^* = p_\ell^*$), the stoichiometric compatibility class of x^* contains exactly three positive steady states (arising from the rate-constant vector κ^*); see `minERK-mss-bistab.mw`. Moreover, two of the steady states each have three zero eigenvalues and the remaining eigenvalues having strictly negative real parts (indicating that these two steady states are exponentially stable), and one steady state has a (single) non-zero eigenvalue with positive real part (indicating it is unstable); see the supplementary file. Therefore, we have bistability for each of the processivity levels in (5.4). □

Proposition 5.1.4 showed bistability for certain processivity levels with $p_k = p_\ell$. Even when $p_k \neq p_\ell$ (see Remark 5.1.5), we found – in every instance we examined – bistability.

Remark 5.1.5 (Bistability at random processivity levels)**.** For the minimally bistable ERK subnetwork, we generated random pairs of processivity levels p_k and p_ℓ between 0 and 1 (Table 5.1). For all such pairs, following the procedure described in the proof of Proposition 5.1.4, we found bistability. For details, see the supplementary file `minERK-MSS-bistab.mw`.

p_k	0.01570	0.02229	0.06748	0.2203	0.2268	0.2576	0.2897	0.4613	0.5378
p_ℓ	0.05004	0.3476	0.6011	0.6076	0.9461	0.2263	0.9883	0.4217	0.3770
p_k	0.5893	0.6613	0.6968	0.9076	0.9307	0.9598	0.9771	0.9845	
p_ℓ	0.5289	0.04355	0.1351	0.2668	0.9010	0.6118	0.07128	0.9809	

Table 5.1: Randomly generated pairs of processivity levels, rounded to four significant digits. At every such pair, the minimally bistable ERK network exhibits bistability (in some compatibility class). Computations are in the supplementary file `minERK-MSS-bistab.mw`.

In light of Proposition 5.1.4 and Remark 5.1.5, we conjecture that, in Theorem 5.1.1, multistationarity can be strengthened to bistability. In other words, we conjecture that the answer to Question 5.0.2 is "yes":

Conjecture 5.1.6 (Bistability at all processivity levels)**.** *Consider the minimally bistable ERK subnetwork. For every choice of processivity levels $p_k \in (0,1)$ and $p_\ell \in (0,1)$, there is a rate-constant vector $(k_1^*, k_3^*, k_{\text{cat}}^*, k_{\text{on}}^*, k_{\text{off}}^*, \ell_1^*, \ell_3^*, \ell_{\text{cat}}^*, \ell_{\text{off}}^*, m_2^*, m_3^*, n_1^*, n_3^*) \in \mathbb{R}^{13}_{>0}$ such that $p_k = k_{\text{cat}}^*/(k_{\text{cat}}^* + k_{\text{off}}^*)$ and $p_\ell = \ell_{\text{cat}}^*/(\ell_{\text{cat}}^* + \ell_{\text{off}}^*)$, and the resulting system admits multiple exponentially <u>stable</u> positive steady states (in some compatibility class).*

If Conjecture 5.1.6 holds, then [64, Theorem 3.1] implies that bistability "lifts" to the original ERK network. In other words, this would answer in the affirmative the original Question 5.0.1, for bistability.

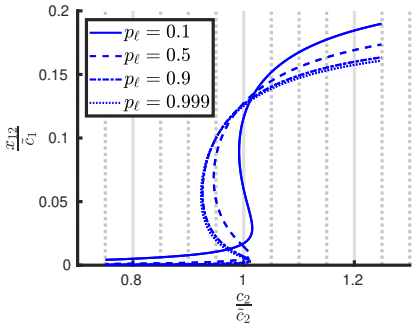

(a) $0.75 \leq \frac{c_2}{\tilde{c}_2} \leq 1.25$

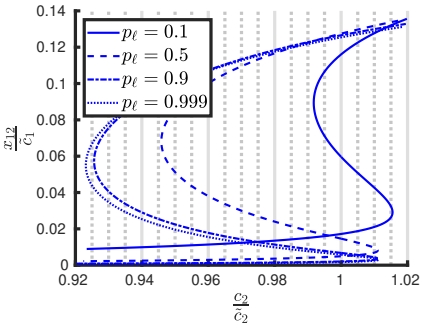

(b) $0.9 \leq \frac{c_2}{\tilde{c}_2} \leq 1.05$

Figure 5.3: Numerical investigation of multistationarity as $p_\ell \to 1$ (for $p_k = 0.1$; see Section 5.1.3.1 and Appendix B.1 for figure setup and generation). An increase of p_ℓ leads to a (small) decrease of $\frac{x_{12}}{\tilde{c}_1}$ at $\frac{c_2}{\tilde{c}_2} \approx 1.25$ (display a) and to a larger multistationarity interval (from approximately $0.99 \leq \frac{c_2}{\tilde{c}_2} \leq 1.01$ to $0.92 \leq \frac{c_2}{\tilde{c}_2} \leq 1.02$) (display b). Reprinted with permission from [24].

5.1.3 Numerical investigation for processivity levels near 1

In this subsection, we numerically investigate multistationarity of the minimally bistable ERK network, for processivity levels close to 1. Specifically, we examine how processivity levels near 1 affect the S-shaped steady-state curves (as in [34, Figure 9.6]) usually associated with multistationarity. We focus in particular on the concentration of the fully phosphorylated substrate (x_{12}), as this species is arguably the most interesting in our signaling network. Indeed, this substrate is generally further processed by other signaling modules.

5.1.3.1 Setup for Figures 5.3–5.5

Figures 5.3–5.5 were generated by numerical continuation using `Matlab` and `Matcont`. Further details on how we obtained these figures are in Appendix B.1. In particular, parameter values, total concentrations, and initial conditions were obtained by equation (5.5) and also (in the appendix) (B.1)–(B.2) and the values in Tables B.2–B.3. In all figures, the x-axis is the relative total amount of kinase ($c_2/\tilde{c}_2$ obtained in step (iii) of the procedure described in the appendix), and the y-axis is the relative amount of fully phosphorylated substrate ($x_{12}/\tilde{c}_1$), also obtained in step (iii)). The reason for examining relative (rather than actual) amounts is that, as p_k and/or p_ℓ approach

1, certain total amounts differ by orders of magnitude, and so it is more meaningful to compare values relative to a reference point.

5.1.3.2 Results

Figure 5.3 shows that, for $p_k = 0.1$ and various values of p_ℓ, we obtain classical S-shaped curves often associated with multistationarity. We also see that increasing p_ℓ alone has only a modest effect on the curve: at the relative total concentration $\frac{c_2}{\tilde{c}_2} \approx 1.25$, the fraction of fully phosphorylated substrate $\frac{x_{12}}{\tilde{c}_1}$ (at steady state) decreases but only by a small amount (see Figure 5.3a).

Next, we investigate the interval of values of $c_2/\tilde{c}_2$ at which multistationarity occurs, which we call the multistationarity interval. We see in Figure 5.3b (which is a "zoomed in" version of Figure 5.3a) that as p_ℓ increases (with $p_k = 0.1$), the multistationarity interval enlarges (see the caption of Figure 5.3b). We can view the size of this interval as a measure of the robustness of multistationarity with respect to fluctuations of the total amount of kinase. Hence, Figure 5.3 motivates us to conjecture that increasing only one processivity level leads to increased robustness of multistationarity, as follows: *When one processivity level is fixed and close to 0, increasing the other processivity level leads to a larger multistationarity interval.*

Next, we fix p_ℓ at a high value (namely, $p_\ell = 0.9$) and increase p_k (see Figure 5.4). Again, increasing p_k reduces the fraction of fully phosphorylated substrate $\frac{x_{12}}{\tilde{c}_1}$ at $\frac{c_2}{\tilde{c}_2} \approx 1.25$, now substantially. Moreover, the multistationarity interval shrinks (see Figures 5.4b and 5.4c). This motivates the following conjecture: *When one processivity level is fixed and close to 1, increasing the other processivity level leads to a smaller multistationarity interval.*

Finally, in Figure 5.5, we investigate values of $p_k = p_\ell$ close to 1. Now the multistationarity interval becomes vanishingly small (see, in particular, Figure 5.5c), leading to a steady-state function that approaches a steep Hill function. We conjecture that this phenomenon is the norm: *As both processivity levels approach 1, the length of the multistationarity interval approaches 0.*

Remark 5.1.7. In the limiting case of $p_k \to 1$ and $p_\ell \to 1$, multistationarity deforms to monostationarity. It would be interesting to investigate what happens to the steady states; for instance, do two of them merge to form one? One setup for studying this in a controlled way is to fix k_{cat} and

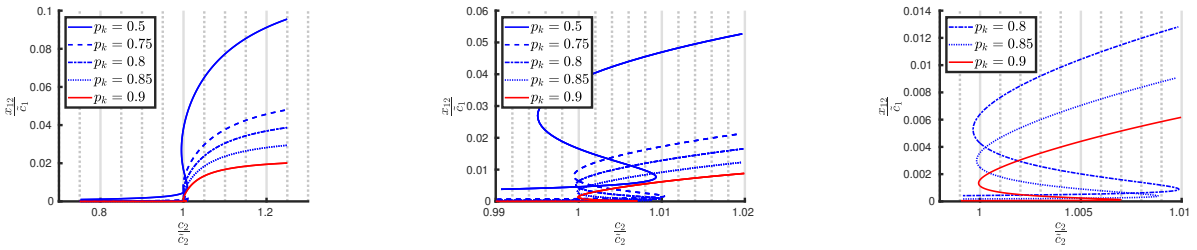

(a) $0.75 \leq \frac{c_2}{\tilde{c}_2} \leq 1.25$ (b) $0.99 \leq \frac{c_2}{\tilde{c}_2} \leq 1.05$ (c) $0.99 \leq \frac{c_2}{\tilde{c}_2} \leq 1.01$

Figure 5.4: Numerical investigation of multistationarity as $p_k \to 1$ (for $p_\ell = 0.9$). An increase in p_k leads to a substantial decrease in $\frac{x_{12}}{\tilde{c}_1}$ at $\frac{c_2}{\tilde{c}_2} \approx 1.25$ (display a) and a smaller multistationarity interval (from $0.992 \leq \frac{c_2}{\tilde{c}_2} \leq 1.01$ to $1 \leq \frac{c_2}{\tilde{c}_2} \leq 1.007$) (displays b–c). Reprinted with permission from [24].

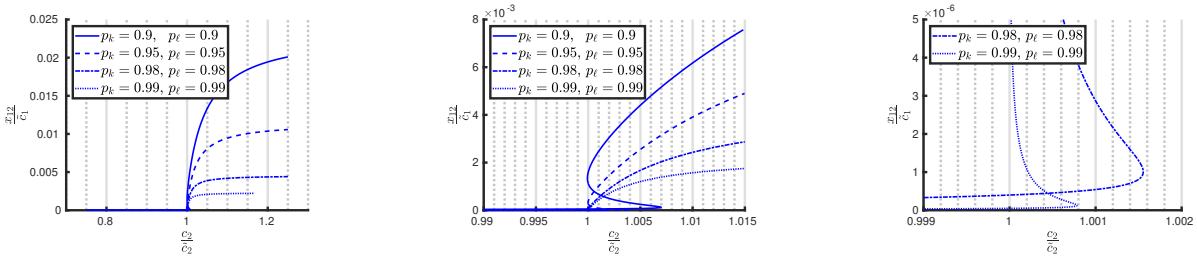

(a) $0.75 \leq \frac{c_2}{\tilde{c}_2} \leq 1.25$ (b) $0.99 \leq \frac{c_2}{\tilde{c}_2} \leq 1.05$ (c) $0.99 \leq \frac{c_2}{\tilde{c}_2} \leq 1.01$

Figure 5.5: Numerical investigation of multistationarity for $p_k = p_\ell$ close to 1. An increase in p_k and p_ℓ leads to a decrease in $\frac{x_{12}}{\tilde{c}_1}$ at $\frac{c_2}{\tilde{c}_2} \approx 1.25$ (display a). Also, when there is multistationarity, the values of $\frac{x_{12}}{\tilde{c}_1}$ (at all three steady states) decrease (possibly approaching 0) as p_k and p_ℓ approach 1. (display b). Finally, as p_k and p_ℓ approach 1, the multistationarity interval becomes so small that the curve approaches a step function (displays a–c). Reprinted with permission from [24].

ℓ_{cat}, and then let k_{off} and ℓ_{off} go to 0.

5.2 Hopf bifurcations and oscillations

In this section, we investigate Hopf bifurcations and oscillations in the reduced ERK network. First, we answer Question 5.0.3 in the affirmative: Theorem 5.2.1 asserts that a Hopf bifurcation exists at all processivity levels p_k and p_ℓ arbitrarily close to 1 – and in fact for all levels greater than 0.003. Subsequently, we perform a numerical investigation into oscillations.

Theorem 5.2.1 (Hopf bifurcations at all processivity levels)**.** *Consider the reduced ERK network.*

For all $0.002295 < \epsilon < 1$*, there exists a rate-constant vector* $\kappa^* = (k_1^*, k_3^*, k_{\text{cat}}^*, k_{\text{off}}^*, m^*, \ell_1^*, \ell_3^*, \ell_{\text{cat}}^*, \ell_{\text{off}}^*, n^*)$ *such that*

1. $p_k = k_{\text{cat}}^*/(k_{\text{cat}}^* + k_{\text{off}}^*) > \epsilon$ *and* $p_\ell = \ell_{\text{cat}}^*/(\ell_{\text{cat}}^* + \ell_{\text{off}}^*) > \epsilon$*, and*

2. *the resulting system* (3.7) *admits a simple Hopf bifurcation (with respect to* k_{cat}*).*

Proof. Fix $0.002295 < \epsilon < 1$. Observe that, for every choice of rate constants for which (a) $k_{\text{cat}}^* > \epsilon/(1-\epsilon) > 0.002295/(1-0.002295) \approx 0.0023$, (b) $\ell_{\text{cat}}^* := t^2 k_{\text{cat}}^*$ (for any choice of $t > 1$), and (c) $k_{\text{off}}^* = \ell_{\text{off}}^* := 1$, we obtain the desired inequalities for p_k and p_ℓ:

$$\epsilon \;<\; \frac{k_{\text{cat}}^*}{k_{\text{cat}}^* + 1} \;=\; p_k \;<\; \frac{t^2 k_{\text{cat}}^*}{t^2 k_{\text{cat}}^* + 1} \;=\; p_\ell \,. \tag{5.6}$$

Next, we show that a Hopf bifurcation exists, by verifying the conditions on $\mathfrak{h}_4$, $\mathfrak{h}_5$, and $\mathfrak{h}_6$ (as in Proposition 4.2.1). First, we show in the supplementary file `redERK-Hopf.mw` that $\mathfrak{h}_4(\hat{\kappa};\, x)$ is a sum of positive terms, and thus $\mathfrak{h}_4(\hat{\kappa};\, x) > 0$ for all $\hat{\kappa} = (k_{\text{cat}}, k_{\text{off}}, \ell_{\text{off}}) \in \mathbb{R}^3_{>0}$ and $x \in \mathbb{R}^{10}_{>0}$.

Next, let $(\widehat{\kappa};\, x) := (k_{\text{cat}}^*, 1, 1;\; 1, 1, 1, t^2, 1, t^2, 1/t, 1, t^2, 1)$. We verify (using `Mathematica`) that if $k_{\text{cat}}^* > 0.0023$, then $\mathfrak{h}_5(\hat{\kappa}^*; x) > 0$ for all $t > 0$; see the supplementary file `h5pos.nb`. Fix $k_{\text{cat}}^* > 0.0023$. Substituting $t^* = 1$ into $\mathfrak{h}_6(\widehat{\kappa}^*; x^*)$ yields a positive polynomial (in k_{cat}^*):

$$\begin{aligned}\mathfrak{h}_6(\widehat{\kappa}^*; x^*)|_{t^*=1} = (k_{\text{cat}}^*+1)^2\Big(&31824000{k_{\text{cat}}^*}^{18} + 713988320{k_{\text{cat}}^*}^{17} + 7660517072{k_{\text{cat}}^*}^{16} + 52115784592{k_{\text{cat}}^*}^{15}\\ &+ 251452795392{k_{\text{cat}}^*}^{14} + 912214161728{k_{\text{cat}}^*}^{13} + 2574990720896{k_{\text{cat}}^*}^{12} + 5775757031984{k_{\text{cat}}^*}^{11}\\ &+ 10424374721840{k_{\text{cat}}^*}^{10} + 15237491111424{k_{\text{cat}}^*}^{9} + 18065664178000{k_{\text{cat}}^*}^{8}\\ &+ 17318286301088{k_{\text{cat}}^*}^{7} + 13314668410544{k_{\text{cat}}^*}^{6} + 8093460125184{k_{\text{cat}}^*}^{5} + 3802097816832{k_{\text{cat}}^*}^{4}\\ &+ 1331324403072{k_{\text{cat}}^*}^{3} + 327072356352{k_{\text{cat}}^*}^{2} + 50292006912k_{\text{cat}}^* + 3641573376\Big)\,.\end{aligned}$$

Also, as $t \to \infty$, the limit of $\mathfrak{h}_6(\hat{\kappa}^*; x^*)$ is $-\infty$. Hence, there exists $t^* > 1$ such that $\mathfrak{h}_6(\widehat{\kappa}^*; x^*) = 0$ (where $x^* = \big(1, 1, 1, {t^*}^2, 1, {t^*}^2, 1/t^*, 1, {t^*}^2, 1\big)$); see the supplementary file `redERK-Hopf.mw`. Finally, we check that $\frac{\partial \mathfrak{h}_6}{\partial k_{\text{cat}}}(\widehat{\kappa}^*; x^*) \neq 0$ whenever $\mathfrak{h}_6(\widehat{\kappa}^*; x^*) = 0$ – we verified this using the `Julia` package `HomotopyContinuation.jl` [12] (see the supplementary file `nondegen-close-to-1.txt`).

Thus, the reduced ERK system admits a Hopf bifurcation at

$$x^* \;:=\; (x_1^*, x_2^*, \ldots, x_{10}^*) \;=\; \left(1, 1, 1, t^{*2}, 1, t^{*2}, 1/t^*, 1, t^{*2}, 1\right) \;, \tag{5.7}$$

when the rate-constant vector is

$$\begin{aligned} \kappa^* \;&:=\; (k_1^*, k_3^*, k_{\text{cat}}^*, k_{\text{off}}^*, m^*, \ell_1^*, \ell_3^*, \ell_{\text{cat}}^*, \ell_{\text{off}}^*, n^*) \\ &= \left((k_{\text{cat}}^* + 1)t^{*2}, (k_{\text{cat}}^* + 1)t^{*2}, k_{\text{cat}}^*, 1, t^*, k_{\text{cat}}^* t^{*2} + 1, (k_{\text{cat}}^* t^{*2} + 1)/t^{*2}, k_{\text{cat}}^* t^{*2}, 1, 1\right) \;. \end{aligned} \tag{5.8}$$

By construction, these rate constants satisfy the conditions (a), (b) (with $t = t^* > 1$), and (c) listed at the beginning of the proof. So, the inequalities (5.6) hold. □

Remark 5.2.2. Following the proof of Theorem 5.2.1, we provide witnesses for the Hopf bifurcation for several values of p_k and p_ℓ in the supplementary file `redERK-Hopf.mw` (under the "First Vertex Analysis" section) for the interested reader. For instance, when $\epsilon = 0.89$, then then the choices $k_{\text{cat}}^* = 9$ and $t^* \approx 124.02$ satisfy the conditions imposed in the proof, and so we obtain, as in (5.6), the processivity levels $p_k = 0.9$ and $p_\ell \approx 0.999993$. Thus, from (5.7), there is a Hopf bifurcation at $x^* \approx (1, 1, 1, 15380.68, 1, 15380.68, 0.008, 1, 15380.68, 1)$ when the rate-constant vector is as in (5.8):

$$\kappa^* \;\approx (153806.78, 153806.78, 9, 1, 124.02, 138427.1, 9.00, 138426.11, 1, 1) \;.$$

Remark 5.2.3 (Relation to Question 5.0.1)**.** As noted earlier, Theorem 5.2.1 addresses Question 5.0.3, the reduced-ERK version of the original Question 5.0.1. We focused on the reduced ERK network rather than the original ERK network, because analyzing the original one is computationally challenging.

Nevertheless, we conjecture that Theorem 5.2.1 "lifts" to the original ERK network. Indeed, to go from the reduced ERK network to the original ERK network, we make some reactions reversible (which is known to preserve oscillations [5]) and add some intermediate complexes (which is

conjectured to preserve oscillations [5]). More precisely, we hope for a future result that states that adding intermediates preserves oscillations and Hopf bifurcations, while the "old" rate constants are only slightly perturbed. Such a result would help us to elevate Theorem 5.2.1 to an answer to Question 5.0.1 for the original ERK network. An approach to achieving such a result is to use the results of [39] to write the reduced system as a limiting case of the original system, where some parameter goes to zero, and then give an argument like that in [57, §3].

Remark 5.2.4. The bounds $p_k, p_\ell > 0.002295$ in Theorem 5.2.1 arose from our choice of specialization in the proof, namely, $(\widehat{\kappa};\ x) := (k^*_{\text{cat}}, 1, 1;\ 1, 1, 1, t^2, 1, t^2, 1/t, 1, t^2, 1)$. Another specialization (that admits a Hopf bifurcation) would give rise to other bounds on p_k and p_ℓ. Nevertheless, as our interest is in p_k and p_ℓ close to 1, our bounds are not restrictive.

Next, we relax the hypothesis $p_k > 0.002295$ in Theorem 5.2.1 to allow for all values of $p_k > 0$. However, we cannot also simultaneously control p_ℓ.

Proposition 5.2.5 (Hopf bifurcations at all p_k)**.** *Consider the reduced ERK network. For every choice of processivity level $p_k \in (0, 1)$, there exists a rate-constant vector $\kappa^* = (k^*_1, k^*_3, k^*_{\text{cat}}, k^*_{\text{off}}, m^*, \ell^*_1, \ell^*_3, \ell^*_{\text{cat}}, \ell^*_{\text{off}}, n^*)$ such that*

1. *$p_k = k^*_{\text{cat}}/(k^*_{\text{cat}} + k^*_{\text{off}})$, and*
2. *the resulting system admits a Hopf bifurcation.*

Moreover, by symmetry of k_{cat} and ℓ_{cat} in the reduced ERK network, we have the analogous result for all choices of p_ℓ.

Proof. As in the proof of Theorem 5.2.1, we achieve any desired value of $p_k \in (0, 1)$ by setting $k^*_{\text{off}} = 1$ and $k^*_{\text{cat}} = p_k/(1 - p_k)$. Accordingly, consider any $k^*_{\text{cat}} \in \mathbb{R}_{>0}$. We will show, using Proposition 4.2.1, that there exists $t^* > 0$ such that the reduced ERK network admits a Hopf bifurcation at

$$x^* := (x^*_1, x^*_2, \ldots, x^*_{10}) = \left(1, 1, 1, 1/{t^*}^2, 1, 1, t^*, 1, 1/{t^*}^2, 1\right),$$

when the rate-constant vector is

$$(k_1^*, k_3^*, k_{\text{cat}}^*, k_{\text{off}}^*, m^*, \ell_1^*, \ell_3^*, \ell_{\text{cat}}^*, \ell_{\text{off}}^*, n^*)$$
$$= \Big((k_{\text{cat}}^* + 1)/t^{*2},\ (k_{\text{cat}}^* + 1)/t^{*2},\ k_{\text{cat}}^*,\ 1,\ 1/t^*,$$
$$(t^{*2} + k_{\text{cat}}^*)/t^{*2},\ (t^{*2} + k_{\text{cat}}^*)/t^{*4},\ k_{\text{cat}}^*/t^{*2},\ 1,\ 1/t^{*2} \Big).$$

Indeed, we verify that $\mathfrak{h}_4(\widehat{\kappa};\ x) > 0$ and $\mathfrak{h}_5(\widehat{\kappa};\ x) > 0$ for all $\hat{\kappa} = (k_{\text{cat}}, 1, 1) \in \mathbb{R}^3_{>0}$ and $x = (1, 1, 1, x_4, 1, 1, x_7, 1, x_9, 1) \in \mathbb{R}^{10}_{>0}$, and that $\mathfrak{h}_6(\widehat{\kappa}^*;\ x^*) = 0$ for some $t^* > 0$ (see the supplementary file `redERK-Hopf-all-pk-values.mw`). Finally, in the supplementary file `nondegen-all-process.txt`, we show that $\frac{\partial \mathfrak{h}_6}{\partial k_{\text{cat}}}(\widehat{\kappa}^*; x^*) \neq 0$ whenever $\mathfrak{h}_6(\widehat{\kappa}^*; x^*) = 0$. $\square$

We end this section with a numerical investigation into the effect of processivity levels on oscillations arising from the Hopf bifurcations analyzed above. Again we focus on the concentration of the fully phosphorylated substrate, in this case x_5. We see in Figure 5.6 that indeed processivity levels have a large effect on the dynamics: as p_k and p_ℓ approach 1, the amplitude decreases while the period increases – at least for the rate-constant vectors κ^* and initial conditions we investigated (see the caption of Figure 5.6). It is an interesting question whether or not this phenomenon arises at other regions of parameter space. We conjecture that indeed oscillations always dampen as as p_k and p_ℓ approach 1.

k_{cat}^*	t^*	p_k	p_ℓ
1	11.3685	0.5	0.992322
3	28.7451	0.75	0.999597
9	130.22	0.9	0.999993

Table 5.2: Values of k_{cat}^* and t^* used for Figure 5.6, and resulting processivity levels, as in (5.6).

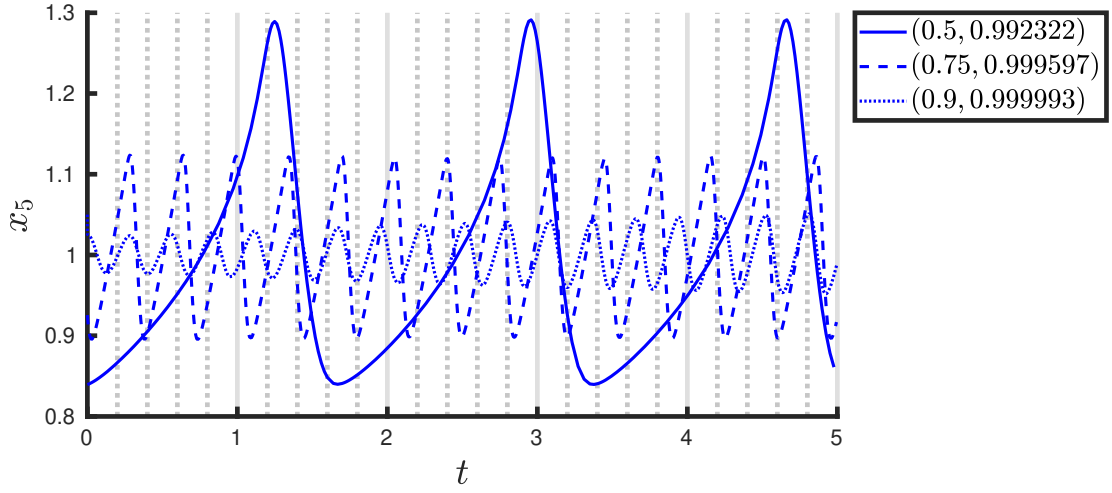

Figure 5.6: For the reduced ERK network, oscillations in x_5 arising from three pairs of processivity levels (p_k, p_ℓ). The rate-constant vectors κ^* were obtained from (5.8), using the values in Table 5.2. The initial conditions were chosen to be close to – and in the same compatibility class as – the corresponding Hopf bifurcation x^* from (5.7) (using the values in Table 5.2); specifically, we perturbed x^* by adding 0.05 to x_5^* and subtracting 0.05 from x_6^*. Reprinted with permission from [24].

5.3 Coexistence of bistability and oscillations

Having shown that multistationarity and Hopf bifurcations exist in certain ERK systems for (nearly) all possible processivity levels, we now investigate whether these two dynamical phenomena can occur together. The first question is whether bistability and oscillations can coexist in the same compatibility class (Section 5.3.1), and then we consider coexistence in distinct compatibility classes (Section 5.3.2).

5.3.1 Precluding coexistence in a compatibility class

The next result, which applies to general networks, forbids bistability and Hopf bifurcations from occurring in the same compatibility class, when there are up to 3 steady states and certain other conditions are satisfied. These conditions allow us to apply (in the proof) results from degree theory.

Theorem 5.3.1. *Consider a reaction system (G, κ). Let $\mathcal{S}_c$ be a compatibility class such that (1)*

the system is dissipative[3] *with respect to $\mathcal{S}_c$, and (2) $\mathcal{S}_c$ contains at most 3 steady states and no boundary steady states. Then $\mathcal{S}_c$ does not contain both a simple Hopf bifurcation and two stable steady states.*

Proof. Let W be a $d \times s$ (row-reduced) conservation-law matrix, where d is the number of conservation laws and s is the number of species. Let $f_{c,\kappa}$ be the resulting augmented system.

We examine, for certain x^* in $\mathcal{S}_c$, the coefficient of λ^d in $\det(\lambda I - \operatorname{Jac} f)|_{x=x^*}$. If x^* is a Hopf bifurcation, then (by a criterion of [106], restated in [23, Proposition 2.3]) the coefficient is positive. Similarly, if x^* is a stable steady state, then (by the Routh-Hurwitz criterion) the coefficient is positive. Finally, by a straightforward generalization of [105, Proposition 5.3], the coefficient equals $(-1)^{s-d} \det \operatorname{Jac} f_{c,\kappa}|_{x=x^*}$.

Assume for contradiction that $\mathcal{S}_c$ contains a simple Hopf bifurcation $x^{(1)}$ and two stable steady states $x^{(2)}$ and $x^{(3)}$ (and hence no more steady states by hypothesis). Then (by definition [21] and by above) the Brouwer degree of $f_{c,\kappa}$ with respect to $\mathcal{S}_c$ is as follows:

$$\begin{aligned}\operatorname{sign} \det \operatorname{Jac} f_{c,\kappa}|_{x=x^{(1)}} + \operatorname{sign} \det \operatorname{Jac} f_{c,\kappa}|_{x=x^{(2)}} + \operatorname{sign} \det \operatorname{Jac} f_{c,\kappa}|_{x=x^{(3)}} \\ = (-1)^{s-d} + (-1)^{s-d} + (-1)^{s-d},\end{aligned}$$

which yields a contradiction, as the degree must be ± 1 (see [21]). □

For the minimally bistable ERK subnetwork, Theorem 5.3.1 implies that, *if the following conjecture holds, Hopf bifurcations and bistability do not coexist in compatibility classes*:

Conjecture 5.3.2. *For the minimally bistable ERK subnetwork, the maximum number of positive steady states (in any compatibility class, for any choice of rate constants) is 3.*

Later in this dissertation, namely in Section 6.3, we will see that the maximum number of positive steady states is at most 5 (see Proposition 6.3.4). There we also will pursue a version of the above conjecture (see also, Conjecture 6.3.5).

[3] *Dissipative* means that there is a compact subset of $\mathcal{S}_c$ that every trajectory eventually enters; being dissipative is automatic when the network is conservative [21].

5.3.2 Coexistence in distinct compatibility classes

Theorem 5.3.1 precludes, for certain reaction systems, the coexistence of bistability and a simple Hopf bifurcation in a single compatibility class. Next, for ERK systems, we ask about coexistence in *distinct* compatibility classes.

Question 5.3.3. *Is it possible in one of the ERK networks (the original one or the minimally bistable ERK subnetwork*[4]*) to have – for some choice of positive rate constants – 2 stable steady states in one compatibility class and a simple Hopf bifurcation in another?*

As an initial investigation we examine the minimally bistable ERK network (see the supplementary file `min-bistab-ERK-Hopf-and-Bistability.mw`). This network yields a Hopf bifurcation when $k_{\text{on}} = 4.0205$ and the other rate constants are as in [78, Equation (23)] (these non-k_{on} rate constants yield oscillations in the fully irreversible ERK network). However, for this choice of rate constants, there is no bistability (in any compatibility class), which we determined by computing the critical function, much like in the proof of [78, Proposition 4.5].

5.4 Maximum number of steady states

In this section, we pursue Conjecture 5.3.2, which states that the maximum number of positive steady states of the minimally bistable ERK subnetwork is 3. The idea is first to reduce to a system of 3 equations in 3 variables (Proposition 5.4.1) and then, using resultants, to further reduce to a single univariate polynomial (Proposition 5.4.3).

Our methods are similar to the approach that [104] took to analyze the fully distributive, dual-site phosphorylation system. Namely, we substitute a steady-state parametrization from for the minimally bistable ERK subnetwork (see Proposition 3.2.1) into the conservation laws, which yields a polynomial system in only 3 variables. We then show that the maximum number of positive roots of this family of polynomial systems is equal to the maximum number of steady states (as in Conjecture 5.3.2).

[4]The reduced ERK network is not in this list, as it does not admit bistability (see Proposition 4.2.5).

Proposition 5.4.1. *Consider the family of polynomial systems in x_1, x_2, x_3 given by:*

$$\begin{aligned} c_1 - c_2 - c_3 &= x_1 - x_2 - x_3 + \frac{a_5 a_9 a_{10} x_1 x_2}{a_8 x_2 + a_{13} x_3 + a_4 a_9 a_{13} x_3} + \frac{a_5 a_7 a_{10} x_1 (a_8 x_2 + a_{13} x_3)}{a_1 a_{11} (a_8 x_2 + a_{13} x_3 + a_4 a_9 a_{13} x_3)} \\ &\quad + \frac{a_5 a_{10} x_1 x_2 (a_8 x_2 + a_2 a_7 a_8 x_2 + a_{13} x_3 + a_2 a_7 a_{13} x_3)}{a_1 a_3 a_{12} x_3 (a_8 x_2 + a_{13} x_3 + a_4 a_9 a_{13} x_3)}\,, \qquad (5.9) \\ c_2 &= x_2 + \frac{a_5 a_{10} x_1 x_2 (a_8 x_2 + a_{13} x_3)}{a_8 x_2 + a_{13} x_3 + a_4 a_9 a_{13} x_3} + \frac{a_5 a_7 a_{10} x_1 x_2 (a_8 x_2 + a_{13} x_3)}{a_1 (a_8 x_2 + a_{13} x_3 + a_4 a_9 a_{13} x_3)} + a_{10} x_1 x_2\,, \qquad (5.10) \\ c_3 &= x_3 + \frac{a_5 a_{10} x_1 x_2 (a_8 x_2 + a_2 a_7 a_8 x_2 + a_{13} x_3 + a_2 a_7 a_{13} x_3)}{a_1 a_3 (a_8 x_2 + a_{13} x_3 + a_4 a_9 a_{13} x_3)} \\ &\quad + \frac{a_5 a_{10} x_1 x_2 (a_8 x_2 + a_{13} x_3)}{a_1 (a_8 x_2 + a_{13} x_3 + a_4 a_9 a_{13} x_3)} + \frac{a_5 a_9 a_{10} a_{13} x_1 x_2 x_3}{a_8 x_2 + a_{13} x_3 + a_4 a_9 a_{13} x_3}\,, \qquad (5.11) \end{aligned}$$

where the coefficients a_i and c_i are arbitrary positive real numbers. Then the maximum number of positive roots $x^* \in \mathbb{R}^3_{>0}$, among all such systems, equals the maximum number of positive steady states of the minimally bistable ERK network.

Proof. The equations (5.9)–(5.11) are obtained as follows. Using the "effective steady-state function" $h_{c,a}$ from [78, Proposition 3.1], we solve for $x_4, x_5, \ldots, x_{12}$ in terms of x_1, x_2, x_3 (and the a_i's), and then substitute the resulting expressions into the conservation equations (3.15), except we replace the first conservation equation by the first one minus the sum of the second and third. Now the result follows from the definition of "effective steady-state function" (Definition 2.2.4). □

Next, we go from the 3 equations (in x_1, x_2, x_3) in (5.9)–(5.11) to 2 equations (in x_2 and x_3), as follows. All 3 equations in (5.9)–(5.11) are linear in x_1, so we solve each for x_1, obtaining equations of the form $x_1 = \gamma_1(x_2, x_3)$, $x_1 = \gamma_2(x_2, x_3)$, and $x_1 = \gamma_3(x_2, x_3)$, respectively. Now, let $g_1 := \gamma_3 - \gamma_2$ and $g_2 := \gamma_1 - \gamma_2$. These g_i's are polynomials in x_2 and x_3 (with coefficients which are polynomials in the a_i's and c_i's). By construction, and by Proposition 5.4.1, we immediately obtain the following result:

Proposition 5.4.2. *Let g_1, g_2, and γ_1 be as above. Then for the system $g_1 = g_2 = 0$ (where the coefficients a_i and c_i are arbitrary positive real numbers), the maximum number of positive roots $(x_2^*, x_3^*) \in \mathbb{R}^2_{>0}$ with $\gamma_1(x_2^*, x_3^*) > 0$, is equal to the maximum number of (positive) steady states of the minimally bistable ERK network.*

Let R be the resultant [27] of g_1 and g_2, with respect to x_2 (this resultant is shown in the supplementary files `maxNUMss.mw` and `resultant.txt`). We apply a standard argument using resultants to obtain the following result:

Proposition 5.4.3. *Let $(a^*; c^*) = (a_1^*, \ldots, a_{13}^*, c_1^*, c_2^*, c_3^*) \in \mathbb{R}_{>0}^{16}$. Let R be as above. If the univariate polynomial $R|_{(a^*;c^*)}$ has at most 3 roots in the interval $(0, \min\{c_1, c_3\})$, and if for every $x_3^* \in \mathbb{R}_{>0}$, the equation $g_1(x_2, x_3^*)|_{(a^*;c^*)} = 0$ has at most one positive solution for x_2, then system* (5.9)–(5.11)*, when specialized at $(a^*; c^*)$, has at most 3 positive roots $x^* \in \mathbb{R}_{>0}^3$.*

Proof. By [27, Page 163, Chapter 3, Sec. 6, Proposition 1(i)],

$$R \ \in \ \langle g_1, g_2 \rangle \cap \mathbb{Q}[a_1, a_2, \ldots, a_{13}, c_1, c_2, c_3, x_3] \ . \tag{5.12}$$

By [27, Page 125, Chapter 3, Sec. 2, Theorem 3(i)],

$$\overline{\pi\left(\mathcal{V}\left(g_1, g_2\right)\right)} \ = \ \mathcal{V}\left(\ \langle g_1, g_2 \rangle \cap \mathbb{Q}[a_1, a_2, \ldots, a_{13}, c_1, c_2, c_3, x_3] \ \right) \ , \tag{5.13}$$

where $\pi : \mathbb{C}^{18} \to \mathbb{C}^{17}$ denotes the standard projection given by $(a; c; x_3, x_2) \mapsto (a; c; x_3)$, $\mathcal{V}(\cdot)$ denotes zero set over $\mathbb{C}$ of a set of polynomials, and $\overline{S}$ denotes the Zariski closure in $\mathbb{C}^n$ [27, Chapter 4] of a subset $S \subseteq \mathbb{C}^n$. So, by (5.12) and (5.13),

$$\overline{\pi\left(\mathcal{V}\left(g_1, g_2\right)\right)} \ \subseteq \ \mathcal{V}\left(R\right) \ .$$

Thus, for a given $(a^*; c^*) \in \mathbb{R}_{>0}^{16}$, because $R|_{(a^*;c^*)}$ has at most 3 positive roots x_3 in the interval $(0, \min\{c_1, c_3\})$, it follows that the solutions of the system $g_1|_{(a^*;c^*)} = g_2|_{(a^*;c^*)} = 0$ have up to 3 possibilities for x_3-coordinates in the interval $(0, \min\{c_1, c_3\})$. Next, we use the hypothesis that (for every $x_3^* \in \mathbb{R}_{>0}$) the equation $g_1(x_2, x_3^*)|_{(a^*;c^*)} = 0$ has at most 1 positive solution for x_2, to conclude that $g_1|_{(a^*;c^*)} = g_2|_{(a^*;c^*)} = 0$ has at most 3 positive solutions $(x_2, x_3) \in \mathbb{R}_{>0}^2$ with $x_3 < \min\{c_1, c_3\}$. Thus, by construction of g_1 and g_2 (see the paragraph before Proposition 5.4.2), the original system (5.9)–(5.11), when specialized at $(a^*; c^*)$, has at most 3 positive roots $x^* \in$

$\mathbb{R}^3_{>0}$. $\square$

As an example of how we can use Proposition 5.4.3 to tackle Conjecture 5.3.2, we next give two corollaries. We hope to pursue this direction more in future work.

Corollary 5.4.4. *For every choice of $c_1^*, c_2^*, c_3^*, a_9^* \in \mathbb{R}_{>0}$, if all other a_i^*'s are equal to 1, then the (specialized at $(a^*; c^*)$) original system* (5.9) *has at most 3 positive roots $x^* \in \mathbb{R}^3_{>0}$.*

Proof. To apply Proposition 5.4.3, we first show that the univariate polynomial $R|_{(a^*;c^*)}$ has at most 3 positive roots x_3. When all a_i^*'s except a_9^* are equal to 1, then this specialized resultant (see the supplementary file `maxNUMss.mw`) is as follows:

$$R|_{(a^*;c^*)} \;=\; a_9^* x_3^2 (a_9^* x_3 + 3c_2^* + 3x_3)(C_4 x_3^4 + C_3 x_3^3 + C_2 x_3^2 + C_1 x_3 + C_0)\;, \tag{5.14}$$

where

$$C_4 \;=\; 2{a_9^*}^2 + 12a_9^*\;, \qquad C_0 \;=\; -2c_3^*(c_2^* - c_3^*)^2,$$

and $C_1, C_2, C_3 \in \mathbb{Q}[a_9^*; c^*]$. By inspection, $C_4 > 0$ and $C_0 \leq 0$, for all $c_1^*, c_2^*, c_3^*, a_9^* \in \mathbb{R}_{>0}$. We consider two cases. If $C_0 = 0$, then $x_3 = 0$ is solution of $R|_{(a^*;c^*)} = 0$, and so (because the "relevant" factor of $R|_{(a^*;c^*)} = 0$ in (5.14) has degree four) $R|_{(a^*;c^*)} = 0$ has at most 3 positive roots x_3. If $C_0 < 0$, then the sequence C_4, C_3, C_2, C_1, C_0 has at most 3 sign changes, and so, by Descartes' rule of signs, $R|_{(a^*;c^*)} = 0$ has at most 3 positive roots x_3.

Second, we show that for every $x_3^* \in \mathbb{R}_{>0}$, the equation $g_1(x_2, x_3^*)|_{(a^*;c^*)} = 0$ has at most one positive solution for x_2. When all a_i^*'s except a_9^* are equal to 1, we have (see the supplementary file `maxNUMss.mw`):

$$g_1(x_2, x_3^*)|_{(a^*;c^*)} = 3x_2^2 + (a_9^* x_3^* - 3c_2^* + 3c_3^*)x_2 - x_3^*(x_3^* + c_2^* - c_3^*)(a_9^* + 3)\;.$$

Viewing $g_1(x_2, x_3^*)|_{(a^*;c^*)}$ as a polynomial in x_2, the leading coefficient is 3, which is positive. So, by Descartes' rule of signs, it suffices to show that either the constant term is non-positive or the coefficient of x_2 is positive. In other words, we must show that if the constant term is positive, then

the coefficient of x_2 is positive. Indeed, if $-x_3(x_3+c_2^*-c_3^*)(a_9^*+3)>0$, then $c_3^*>c_2^*$, and so the coefficient of x_2 is $a_9^*x_3^*-3c_2^*+3c_3^*=a_9^*x_3^*+3(c_3^*-c_2^*)>0$.

By the above two steps and Proposition 5.4.3, we conclude that the system (5.9) – when specialized at $(a^*;c^*)$ – has at most 3 positive roots $x^*\in\mathbb{R}^3_{>0}$. □

Corollary 5.4.5. *For every choice of $c_1^*, c_3^*\in\mathbb{R}_{>0}$, if*

(i) a_9^* and c_2^* are sufficiently large,

(ii) all other a_i^*'s are equal to the same value b and are sufficiently large, and also

(iii) $b>c_2^*/c_3^*>1$ and $c_2^*>c_3^*+1$,

then the (specialized at $(a^*;c^*)$) original system (5.9)–(5.11) *has at most 3 positive roots $x^*\in\mathbb{R}^3_{>0}$.*

Proof. First, we show that the univariate polynomial $R|_{(a^*;c^*)}$ has at most 3 positive roots x_3. When all a_i^*'s except a_9^* are equal to b, then (see `maxNUMss.mw`) we have:

$$R|_{(a^*;c^*)} \;=\; -\Sigma\cdot(C_5x_3^5+C_4x_3^4+C_3x_3^3+C_2x_3^2+C_1x_3+C_0)\;, \tag{5.15}$$

where $\Sigma=b^{17}a_9^*x_3^2(2bc_2^*+c_2^*+a_9^*bx_3+2bx_3+x_3)$ (which is positive), and

$$C_5 \;=\; 2a_9^*b^5(b-1)(b+1)(a_9^*b+2b+1)\;,$$

$$\begin{aligned} C_1 \;&=\; c_3^*(-a_9^*c_2^{*2}-c_2^{*2}-3a_9^*c_2^*c_3^*+2a_9^*c_1^*c_2^*-2a_9^*c_1^*c_3^*+4a_9^*c_3^{*2}+c_1^*c_2^*-2c_1^*c_3^*+c_2^*c_3^*+2c_3^{*2})b^7\\ &\quad+\;\text{lower-order terms in } b\;,\\ &=\; c_3^*(-a_9^*c_2^{*2}+\;[\text{lower-order terms in } a_9^* \text{ and } c_2^*])b^7\;+\;\text{lower-order terms in } b\;, \end{aligned}$$

$$
\begin{aligned}
C_0 \;=\; & -c_3^*(b^2+1)(c_2^*-c_3^*)\Big(a_9^*b^4c_3^* - a_9^*b^3c_2^* + a_9^*b^3c_3^* - a_9^*b^2c_3^* \\
& \qquad\qquad - b^3c_2^* + 2b^3c_3^* - b^2c_3^* - bc_3^* + c_2^*\Big) \\
=\; & -b^9c_3^*(b^2+1)(c_2^*-c_3^*)\left(a_9^*b^3(bc_3^*-c_2^*) + \text{ [lower-order terms in } a_9^*,\, b,\, c_2^*]\right) ,
\end{aligned}
$$

and $C_2, C_3, C_4 \in \mathbb{Q}[a_9^*; c^*]$. Assume that a_9^*, b, and c_2^* are sufficiently large positive numbers. Assume also that $b > c_2^*/c_3^* > 1$. Then, by inspection, $C_5 > 0$, $C_1 < 0$, and $C_0 < 0$. So the sequence $C_5, C_4, C_3, C_2, C_1, C_0$ has at most 3 sign changes. Hence, Descartes' rule of signs implies that $R|_{(a^*;c^*)} = 0$ has at most 3 positive roots x_3.

Second, we show that for every $x_3^* \in \mathbb{R}_{>0}$, $g_1(x_2, x_3^*)|_{(a^*;c^*)} = 0$ has at most 1 positive solution for x_2. When all a_i^*'s except a_9^* are equal to b, then (see `maxNUMss.mw`)

$$
\begin{aligned}
g_1(x_2, x_3^*)|_{(a^*;c^*)} \;=\; & (b^4+b^3+b^2)x_2^2 \\
& + (a_9^*b^4x_3^* - b^4c_2^* + 2b^4c_3^* - b^4x_3^* - b^3c_2^* + b^3c_3^* - b^2c_2^* + b^2x_3^*)x_2 \\
& - b^2x_3^*\Big(a_9^*b^2c_2^* - a_9^*b^2c_3^* + a_9^*b^2x_3^* + b^2c_2^* - 2b^2c_3^* \\
& \qquad + 2b^2x_3^* + bc_2^* - bc_3^* + bx_3^* + c_2^*\Big)
\end{aligned}
$$

In particular, the constant term can be rewritten and bounded above as follows, where we use the assumption that $c_2^* > c_3^* + 1$:

$$
\begin{aligned}
& -b^2x_3^*\left([a_9^*b^2][c_2^* - c_3^* + x_3^* + c_2^*/a_9^*] - 2b^2c_3^* + 2b^2x_3^* + bc_2^* - bc_3^* + bx_3^* + c_2^*\right) \\
< \;\; & -b^2x_3^*\left([a_9^*b^2] + \text{ [lower-order terms in } a_9^*,\, b,\, c_2^*]\right) .
\end{aligned}
$$

So, if a_9^*, b, and c_2^* are sufficiently large (and $c_2^* > c_3^* + 1$), then the constant term of $g_1(x_2, x_3^*)|_{(a^*;c^*)}$ is negative. Also, the leading coefficient, $b^4+b^3+b^2$, is positive. So, there is exactly 1 sign change in the sequence of coefficients, and hence, by Descartes' rule of signs, $g_1(x_2, x_3^*)|_{(a^*;c^*)}$ has at most 1 positive solution.

The above two steps and Proposition 5.4.3 together imply that the (specialized at $(a^*; c^*)$) system (5.9) has at most 3 positive roots $x^* \in \mathbb{R}^3_{>0}$. □

Remark 5.4.6. In the two above proofs, we saw the (specialized) resultants (5.14) and (5.15) have some "irrelevant" factors (those that are always positive) and one "relevant" factor, such that the sign of the resultant equals the sign of the relevant factor. This is true for the resultant, even before specialization; see the supplementary file `maxNUMss.mw`.

5.5 Discussion

The motivating question for this work is Question 5.0.1, which pertains to the important problem of how bistability and oscillations emerge in ERK networks. We essentially answered this question. What "essentially" means here is that we answered the question for some closely related ERK networks, and only two conjectures (Conjecture 5.1.6 and see also Remark 5.2.3) – which we believe to be true – stand in the way of complete answers.

We also pursued two related topics, the coexistence of oscillations and bistability, and the maximum number of positive steady states. We showed that if another conjecture we believe to be true (Conjecture 5.3.2) holds, then Hopf bifurcations and bistability do not coexist in compatibility classes in the minimally bistable ERK subnetwork. We then pursued Conjecture 5.3.2 using resultants, achieving partial results and laying the groundwork for future progress on this conjecture. This question of the maximum number of positive steady states is important – it is one way to measure a network's capacity for processing information – and we would like in the future some easy criterion for computing this number for phosphorylation and other signaling networks.

Finally, our interest in phosphorylation networks is due to their role in mitogen-activated protein kinase (MAPK) cascades, which enable cells to make decisions (to differentiate, proliferate, die, and so on) [82]. We therefore want to understand which types of dynamics MAPK cascades and phosphorylation networks are capable of, as bistability and oscillations may be used by cells to make decisions and process information [102]. For MAPK cascades, to quote from [97], "By adjusting the degree of processivity in our model, we find that the MAPK cascade is able to switch among the ultrasensitivity, bistability, and oscillatory dynamical states". Our results here

are complementary – even while keeping the processivity levels constant (at any amount), the ERK network can switch between a range of dynamical behaviors, from bistability to oscillations via a Hopf bifurcation.

6. MIXED VOLUME OF REACTION NETWORKS*

This chapter contains both published and unpublished work. Section 6.3 of this chapter is based on the paper "Oscillations and bistability in a model of ERK regulation" [78], which is jointly authored with Anne Shiu, Xiaoxian Tang, and Angélica Torres. Section 6.4 is based on the paper "Mixed volume of small reaction networks" [77], which is jointly authored with Anne Shiu and Dilruba Sofia. Section 6.6 contains new, unpublished material.

6.1 Introduction

For chemical reaction networks, information about steady states – both their number and their nature (stability, etc.) – yields insight into a network's capacity for processing information. Therefore, there have been numerous investigations into the capacity for multiple steady states, especially for networks arising from biology (see, e.g., [6, 21, 29, 33, 65, 101]).

The next step, determining the maximum number of steady states of a given network, is more difficult. Indeed, this question, mathematically, asks us to compute the maximum number of positive roots of a family of parametrized polynomial systems. Therefore, we are interested in upper bounds on this maximum number that are easy to compute.

This chapter proceeds as follows. Section 6.2 introduces the mixed volume of a reaction network. In general, the mixed volume is an upper bound on the number of complex-number steady states, and we show that this bound is surprisingly good for certain biological signaling networks, specifically, ERK networks (Section 6.3). Indeed, we show that the "mixed-volume overcount" – the difference between the mixed volume and the maximum number of (positive) steady states – is no more than 2 or 4 for ERK networks.

Section 6.4 further investigates the mixed volume and the mixed-volume overcount, with a

*Part of this chapter is reprinted from [78] by permission from Springer Nature Customer Service Centre GmbH: Springer *Journal of Mathematical Biology* "Oscillations and bistability in a model of ERK regulation", Nida Obatake, Anne Shiu, Xiaoxian Tang, and Angélica Torres, Copyright (2019). Part of this chapter is reprinted from [77], first published in *Involve, a Journal of Mathematics* in Vol. 13 (2020), No. 5, published by Mathematical Sciences Publishers.

focus on small networks, those with just a few species or reactions. Our results here are as follows. First, for networks with only one species, we show how to read off the mixed volume (and mixed-volume overcount) directly from the network (Theorems 6.4.6 and 6.4.8), and we conclude that the mixed-volume overcount can be arbitrarily large (Corollary 6.4.7). Next, we investigate networks with two species and two reactions, and show that among those that are at-most-bimolecular, nearly all have mixed-volume overcount 0 (Theorem 6.4.17). Thus, the mixed volume is an excellent bound for such networks.

Section 6.5 lists all genuine 2-species, 2-reaction networks with nonzero mixed volume. In Section 6.6, we compare related definitions of mixed volume from [50, 51], and we introduce a new definition for use in future investigations. We conclude with a summary of our contributions in Section 6.7.

6.2 Mixed volume of reaction networks

6.2.1 Background

We recall, the concept of mixed volume from convex geometry, which we will apply to reaction networks. For background on convex and polyhedral geometry (such as polytopes and Minkowski sums), we direct the reader to texts [36, 107]. In particular, for a polynomial $f = b_1x^{\sigma_1} + b_2x^{\sigma_2} + \cdots + b_\ell x^{\sigma_\ell} \in \mathbb{R}[x_1, x_2, \ldots, x_s]$, where the exponent vectors $\sigma_i \in \mathbb{Z}^s$ are distinct and $b_i \neq 0$ for all i, the Newton polytope of f is the convex hull of its exponent vectors: $\text{Newt}(f) \coloneqq \text{conv}\{\sigma_1,\ \sigma_2,\ \ldots\ ,\ \sigma_\ell\} \subseteq \mathbb{R}^s$.

Definition 6.2.1. Let $P_1, P_2, \ldots, P_s \subseteq \mathbb{R}^s$ be polytopes. The volume of the Minkowski sum $\lambda_1P_1 + \lambda_2P_2 + \cdots + \lambda_sP_s$ is a homogeneous polynomial of degree s in nonnegative variables $\lambda_1, \lambda_2, \ldots, \lambda_s$. In this polynomial, the coefficient of $\lambda_1\lambda_2\cdots\lambda_s$, denoted by $\text{mv}(P_1, P_2, \ldots, P_s)$, is the mixed volume of $P_1, P_2, ..., P_s$.

An equivalent formulation of the mixed volume of $P_1, P_2, ..., P_s$ is given by the following

inclusion-exclusion formula:

$$\mathrm{mv}(P_1, P_2, \ldots, P_s) \;:=\; \sum_{J \subset \{1,2,\ldots,s\}} (-1)^{s-\#J} \cdot \text{volume}\left(\sum_{j \in J} P_j\right) . \tag{6.1}$$

where volume(Q) denotes the s-dimensional Euclidean volume of Q in $\mathbb{R}^s$.

The Bernstein-Khovanskii-Kushnirenko (BKK) theorem connects convex geometry with algebraic geometry: the mixed volume counts the number of solutions in $(\mathbb{C}^*)^s$ of a generic polynomial system.

Proposition 6.2.2 ([8])**.** *Consider s real polynomials $g_1, g_2, \ldots, g_s \in \mathbb{R}[x_1, x_2, \ldots, x_s]$. Then the number of isolated solutions in $(\mathbb{C}^*)^s$, counted with multiplicity, of the system $g_1(x) = g_2(x) = \cdots = g_s(x) = 0$ is at most* $\mathrm{mv}(\mathrm{New}(g_1), \ldots, \mathrm{New}(g_s))$.

Recall that it is our interest to compute the maximum number of steady states of a chemical reaction network, which corresponds to counting the maximum possible number of positive real roots of its defining parametrized polynomial system. In the next subsection, then, we will interpret the mixed volume in the context of chemical reaction networks.

6.2.2 New definitions and bounds

We now introduce the definition of the mixed volume of a chemical reaction network.

Definition 6.2.3. Let G be a network with s species, m reactions, and a $d \times s$ conservation-law matrix W, which results in the system augmented by conservation laws $f_{c,\kappa}$, as in (2.3). Let $c^* \in \mathbb{R}^d_{\neq 0}$, and let $\kappa^* \in \mathbb{R}^m_{>0}$ be generic. Let $P_1, P_2, \ldots, P_s \subset \mathbb{R}^s$ be the Newton polytopes of $f_{c^*,\kappa^*,1}, f_{c^*,\kappa^*,2}, \ldots, f_{c^*,\kappa^*,s}$, respectively. The mixed volume of G (with respect to W) is the mixed volume of $P_1, P_2, \ldots, P_s$. We will later refer to this mixed volume as the augMV of G (see Section 6.6).

Remark 6.2.4. The mixed volume (Definition 6.2.3) is well defined. Indeed, it is straightforward to check that the exponents appearing in f_{c^*,κ^*} are the same as long as $c^* \in \mathbb{R}^d_{\neq 0}$ and κ^* is chosen

generically (so that no coefficients of f_{c^*,κ^*} vanish, or equivalently certain linear combinations of the κ_j's do not vanish).

Every positive steady state is a steady state over $\mathbb{C}^*$. Also, the mixed volume pertains to polynomial systems with the same supports (i.e., the exponents that appear in each polynomial) as the augmented system $f_{c,\kappa} = 0$ (but without constraining the coefficients to come from a reaction network). We obtain, therefore, the bounds in the following result:

Proposition 6.2.5. *For every network, the following inequalities hold among the maximum number of positive steady states, the maximum number of steady states over $\mathbb{C}^*$, and the mixed volume of the network (with respect to any conservation-law matrix):*

$$\max \#\text{ of positive steady states} \;\leq\; \max \#\text{ of steady states over } \mathbb{C}^* \;\leq\; \text{mixed volume}\,.$$

Proof. This result follows from Proposition 6.2.2 and Definitions 6.3.1–6.3.3. □

The *mixed-volume overcount* measures how tight the bound on the maximum number of steady states is. Of particular interest are networks with 0 mixed-volume overcount, because for these networks, the mixed volume precisely and efficiently calculates the maximum number of positive steady states.

Definition 6.2.6. The mixed-volume overcount of a reaction network G is

$$(\text{mixed volume of } G) \;-\; (\text{maximum number of positive steady states of } G)\,.$$

We illustrate the definitions introduced here in an example.

Example 6.2.7. Consider the following network G:

$$\begin{aligned} \mathrm{A} &\xrightarrow{k_1} \mathrm{B} \\ \mathrm{A}+\mathrm{B} &\xrightarrow{k_2} 2\,\mathrm{A}\,. \end{aligned}$$

Its corresponding mass-action system (2.1) is

$$\begin{cases} \dot{a} = -k_1 a + k_2 ab \\ \dot{b} = k_1 a - k_2 ab \, , \end{cases}$$

and it has one conservation law $a + b - c_1 = 0$ for some $c_1 \in \mathbb{R}_{\geq 0}$. The corresponding augmented system (2.3) is

$$\begin{cases} a + b - c_1 =: f_1 \\ k_1 a - k_2 ab =: f_2 \, . \end{cases}$$

By a straightforward computation, the system $f_1 = f_2 = 0$ has at most one positive steady state $(a, b) = \left(c_1 - \dfrac{k_1}{k_2} \, , \, \dfrac{k_1}{k_2} \right)$. This positive steady state is achieved for every choice of rate constants, provided that $c_1 > \dfrac{k_1}{k_2}$.

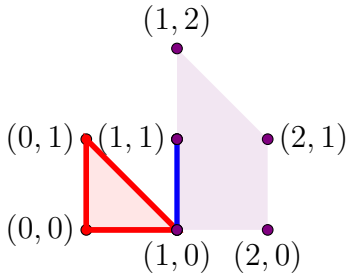

Figure 6.1: The Newton polytopes of f_1 (in red) and f_2 (in blue) from Example 6.2.7 and the Minkowski sum of these polytopes (in purple).

Figure 6.1 shows the Newton polytopes of f_1 (in red) and f_2 (in blue) and the Minkowski sum of these polytopes (in purple). Next we compute its mixed volume using the inclusion-exclusion

formula (6.1) and Figure 6.1:

$$\begin{aligned}\text{mixed volume of } G &= \operatorname{vol}(\operatorname{New}(f_1) + \operatorname{New}(f_2)) - \operatorname{vol}(\operatorname{New}(f_1)) - \operatorname{vol}(\operatorname{New}(f_2)) \\ &= \frac{3}{2} - \frac{1}{2} - 0 \\ &= 1 = \text{maximum number of positive steady states.}\end{aligned}$$

So, the network G has mixed-volume overcount 0, since its maximum number of steady states is equal to its mixed volume.

Example 6.2.7 illustrates how the mixed volume effectively calculates the maximum number of steady states of network G. An open problem is when this is true for arbitrary networks. The remainder of this chapter pursues this problem for ERK networks (Section 6.3) and networks with few species and few reactions (Section 6.4).

6.3 Maximum number of steady states for ERK networks

In Chapter 4 (Section 4.2.2), we saw that the full ERK network and some irreversible ERK networks (those with k_{on} or ℓ_{on}) are bistable, admitting two stable steady states in a stoichiometric compatibility class. The question arises, Do these networks admit three or more such steady states? We suspect not (Conjecture 6.3.5).

As a step toward resolving this problem, here we investigate the maximum number of positive steady states in ERK networks, together with the mixed volume defined in Section 6.2 we introduce, the maximum number of (non-boundary) complex-number steady states. The mixed volume is always an upper bound on the number of complex steady states (Proposition 6.2.5), but we show these numbers are equal for ERK networks (Proposition 6.3.4).

6.3.1 Background definitions

Here we recall a network's maximum number of positive steady states [66], and then extend the definition to allow for complex-number steady states.

Definition 6.3.1. A network admits k positive steady states (for some $k \in \mathbb{Z}_{\geq 0}$) if there exists

a choice of positive rate constants so that the resulting mass-action system (2.1) has exactly k positive steady states in some stoichiometric compatibility class (2.2).

[66] allowed $k = \infty$ when there are infinitely many steady states in a stoichiometric compatibility class. Here, however, we do not allow $k = \infty$ so that we consider isolated roots only (as in Proposition 6.2.2).

Definition 6.3.2. Let G be a network with s species, m reactions, and a $d \times s$ conservation-law matrix W, which results in the system augmented by conservation laws $f_{c,\kappa}$, as in (2.3). The network G admits k steady states over $\mathbb{C}^*$ if there exists a choice of positive rate constants $\kappa \in \mathbb{R}^m_{>0}$ and a total-constant vector $c \in \mathbb{R}^d$ such that the system $f_{c,\kappa} = 0$ has exactly k solutions in $(\mathbb{C}^*)^s = (\mathbb{C} \setminus \{0\})^s$.

It is straightforward to check that Definition 6.3.2 does not depend on the choice of W.

Definition 6.3.3. The maximum number of positive steady states (respectively, maximum number of steady states over $\mathbb{C}^*$) of a network G is the maximum value of k for which G admits k positive steady states (respectively, k steady states over $\mathbb{C}^*$).

6.3.2 Results

We investigate the numbers in Proposition 6.2.5 for ERK networks in the following result. All supplementary files referenced in this subsection are linked in Appendix A.

Proposition 6.3.4. *Consider four ERK networks: the full ERK network, the full ERK network with the reaction k_{on} removed, the fully irreversible network, and the reduced network. For these networks, the following numbers (or bounds on them) are given in Table 6.1: the maximum number of positive steady states, the maximum number of steady states over $\mathbb{C}^*$, and the mixed volume of the network (with respect to the conservation laws* (3.2) *or* (3.8)*).*

Proof. The results on the mixed volume were computed using the `PHCpack` [52] package[2] in `Macaulay2` [48]. See the supplementary file `ERK-mixedVol.m2`.

[2]The `mixedVolume` method in `PHCpack` efficiently computes the mixed volume for networks of the size we consider in this dissertation. Indeed, we will utilize `PHCpack` again to compute the mixed volume for small networks in Procedure 6.4.12.

ERK network	Max # positive steady states	Max # over $\mathbb{C}^*$	Mixed volume
Full	≥ 3	7	7
Full with $k_{\text{on}} = 0$	≥ 3	5	5
Fully irreversible	1	3	3
Reduced	1	3	3

Table 6.1: Results on ERK networks.

The mixed volume is an upper bound on the maximum number of steady states over $\mathbb{C}^*$ (Proposition 6.2.5), so we need only show that each network admits the number shown in Table 6.1 for steady states over $\mathbb{C}^*$.

The full ERK network admits 7 steady states over $\mathbb{C}^*$ (including 3 positive steady states) [33, Example 3.18]. Next, we consider the remaining three networks (see the supplementary file `ERK-MaxComplexNumber.nb`.

For the full ERK network with $k_{on} = 0$, when $(c_1, c_2, c_3) = (1, 2, 3)$ and

$$\begin{aligned}&(k_1, k_2, k_3, k_{\text{cat}}, k_{\text{on}}, k_{\text{off}}, \ell_1, \ell_2, \ell_3, \ell_{\text{cat}}, \ell_{\text{on}}, \ell_{\text{off}}, m_1, m_2, m_3, n_1, n_2, n_3)\\ =\ &(3, 25, 1, 5, 0, 6, 5, 23, 11, 13, 43, 41, 12, 7, 8, 12, 31, 21),\end{aligned}$$

we obtain 5 steady states over $\mathbb{C}^*$, three real and one complex-conjugate pair, which are approximately as follows:

(21.7475, 1.97705, 2.40601, 2.64849, 0.760404, 0.564871, -24.1306, -0.973762, -2.51373, -0.28488, -7.81077, -18.495),

(5.4105 + 14.8132 i, 0.491864 + 1.34665 i, 1.97942 - 3.45492 i, 1.66315 - 1.90055 i, 0.189178 + 0.517943 i, 0.140532 + 0.384758 i, -5.88178 - 12.7049 i, 1.00714 + 0.997852 i, 1.13283 + 0.533085 i, 0.470121 + 0.662785 i, -9.72843 - 0.81303 i, -0.749157 - 12.0899 i),

(5.4105 - 14.8132 i, 0.491864 - 1.34665 i, 1.97942 + 3.45492 i, 1.66315 + 1.90055 i, 0.189178 - 0.517943 i, 0.140532 - 0.384758 i, -5.88178 + 12.7049 i, 1.00714 - 0.997852 i, 1.13283 - 0.533085 i, 0.470121 - 0.662785 i, -9.72843 + 0.81303 i, -0.749157 + 12.0899 i)

(9.63546, 0.875951, -0.488295, 0.0430355, 0.336904, 0.250272, -8.02311, 2.36979, 0.45764, 0.173889, -10.4083, 0.123488),

and

(0.163415, 0.0148559, 0.00111949, 0.00756688, 0.00571382, 0.00424455, 1.82061, 2.98247, 0.00616705, 0.00175686, 0.777908, 0.0172524).

For the fully irreversible ERK network, when $(c_1, c_2, c_3) = (1, 2, 3)$ and

$$(k_1, k_3, k_{\text{cat}}, k_{\text{off}}, \ell_1, \ell_3, \ell_{\text{cat}}, \ell_{\text{off}}, m_2, m_3, n_1, n_3) = (3, 1, 5, 6, 5, 11, 13, 41, 7, 8, 12, 21),$$

there are 3 steady states over $\mathbb{C}^*$, all real, with approximate values:

(14.199,	1.29082,	2.5444,	2.43721,	0.496468,	0.368805,	-16.0342,	-0.302478,
-2.13373,	-0.181355,	-0.295181,	-17.7264),				
(0.490202,	0.0445638,	0.0878422,	0.0841415,	0.0171399,	0.0127325,	1.37739,	2.88599,
0.00772073,	0.0728849,	0.118631,	0.0641415),	and			
(1.9419,	0.176536,	0.34798,	0.33332,	0.0678986,	0.050439,	-0.466416,	2.54834,
0.0346375,	-0.852654,	-1.38782,	0.287758).				

For the reduced ERK network, let $(c_1, c_2, c_3) = (1, 2, 3)$ and

$$(k_1, k_3, k_{\text{cat}}, k_{\text{off}}, m, n, \ell_1, \ell_3, \ell_{\text{cat}}, \ell_{\text{off}}) = (3, 4, 1, 5, 6, 8, 7, 11, 12, 5).$$

We obtain 3 steady states over $\mathbb{C}^*$, all real, which are approximately:

(-0.843105,	-37.1185,	23.4711,	15.6474,	-9.92245,	-30.6429,	-0.0292745,	-0.319149,
2.0152,	1.30395),						
(0.314129,	1.4361,	0.338341,	0.22556,	0.015463,	0.0477534,	0.0109073,	2.95215,
0.0290494,	0.0187967),	and					
(-2.47545,	-0.954967,	1.77298,	1.18199,	0.087009,	0.268704,	-0.0859532,	2.74928,
0.152226,	0.0984989).						

Finally, we examine the maximum number of positive steady states. We already saw that the fully irreversible and reduced networks are monostationary (Corollary 4.2.7 and Proposition 4.2.5, respectively). For the "partially irreversible" network, we saw in the proof of Theorem 4.2.6 that it admits 3 positive steady states. As for the full network, as noted above, 3 positive steady states were shown in [33, Example 3.18]. □

Table 6.1 suggests that the mixed volume is a measure of the complexity of a network. The full ERK network is multistationary, and its mixed volume is 7. The mixed volume drops to 5 when $k_{\text{on}} = 0$. When the network is further simplified to the fully irreversible, or even to the reduced ERK network, the mixed volume becomes 3, and bistability is lost as well.

Finally, we conjecture that the bounds in Table 6.1 are strict, and ask about stability.

Conjecture 6.3.5. *For the full ERK network and the full ERK network with $k_{\text{on}} = 0$, the maximum number of positive (respectively, positive stable) steady states is 3 (respectively, 2).*

6.3.3 Summary

For the ERK network and several simplified versions of the network, the mixed-volume overcount is 2 – for the fully irreversible and reduced subnetworks – or (conjectured to be) 4 - for the full network and the subnetwork obtained by removing one reaction (specifically, the reaction k_{on}). The ERK network case-study exemplifies the good bounds achieved by mixed volume. We wish for a systematic theory to identify mixed-volume overcount without specifying a network's parameters. In the next section, we will develop a related procedure for computing the mixed-volume overcount for small networks (Procedure 6.4.12).

6.4 Mixed volume of small reaction networks

Next, we analyze the mixed-volume overcount for small networks. We view this work as a tool for future work studying multistationarity in larger networks (e.g., the ERK network and the network in Example 6.4.19). In Section 6.4.1, we characterize the mixed volume and mixed-volume overcount of networks with only one reaction or one species. As a consequence, we show that the mixed-volume overcount can be arbitrarily large (Corollary 6.4.7). Subsequently, in Section 6.4.2, we show that nearly all (genuine) networks with two species and two reactions have mixed-volume overcount 0 (Theorem 6.4.17).

6.4.1 Networks with only one reaction or one species

First, we recall some definitions for one-species networks from [66].

Definition 6.4.1. Let G be a reaction network containing only one species A and at least one reaction. Each reaction of G therefore has the form $aA \to bA$, where $a, b \geq 0$ and $a \neq b$. Let m be the number of (distinct) reactant complexes, and let $a_1 < a_2 < \cdots < a_m$ be the stoichiometric coefficients. The arrow diagram of G, denoted by $\underline{\rho} = (\rho_1, \ldots, \rho_m)$, is the element of $\{\to, \leftarrow, \leftarrow\!\bullet\!\to\}^m$ with:

$$\underline{\rho_i} := \begin{cases} \to & \text{if for all reactions } a_iA \to bA \text{ in } G, \text{ we have } b > a_i \\ \leftarrow & \text{if for all reactions } a_iA \to bA \text{ in } G, \text{ we have } b < a_i \\ \leftarrow\!\bullet\!\to & \text{otherwise.} \end{cases}$$

Definition 6.4.2. For nonnegative integers $T \geq 0$, a T-alternating network is a 1-species network with exactly $T+1$ reactions and with arrow diagram $\rho \in \{\to, \leftarrow\}^{T+1}$ such that, if $T \geq 1$, we have $\rho_i = \to$ if and only if $\rho_{i+1} = \leftarrow$ for all $i \in \{1, 2, \ldots, T\}$.

Example 6.4.3. Consider the following network:

$$G \;=\; \{0 \leftarrow A \to 2A \rightleftharpoons 3A\}\,.$$

Two 1-alternating subnetworks of G have arrow diagram $(\to, \leftarrow)$: $\{A \to 2A,\ 2A \leftarrow 3A\}$ and $\{2A \to 3A,\ 2A \leftarrow 3A\}$. On the other hand, $\{0 \leftarrow A,\ A \to 2A\}$ is *not* a 1-alternating subnetwork of G: its arrow diagram is $(\leftarrow\!\bullet\!\to)$. Finally, $\{0 \leftarrow A,\ 2A \to 3A,\ 2A \leftarrow 3A\}$ is a 2-alternating subnetwork of G with arrow diagram $(\leftarrow, \to, \leftarrow)$.

The following result follows directly from [66, Theorem 3.6] and its proof:

Proposition 6.4.4 (Number of steady states for one-species networks)**.** *Let G be a reaction network with only one species (and at least one reaction). Then, the maximum number of positive steady states of G equals the maximum value of $T \in \mathbb{Z}_{\geq 0}$ for which G has a T-alternating subnetwork.*

We now characterize the mixed volume and mixed-volume overcount of networks with only one reaction or one species.

Proposition 6.4.5 (Mixed volume of one-reaction networks)**.** *For a network with only a single reaction, the mixed volume is 0 and the mixed-volume overcount is 0.*

Proof. Let G be a network with only one reaction. The right-hand side of the ODE consists of a single monomial, so the Newton polytope is just a point (the exponent vector of the monomial). Hence, the mixed volume of G is 0, and so the mixed-volume overcount is 0, by Proposition 6.2.5. □

Theorem 6.4.6 (Mixed volume of one-species networks)**.** *Let G be a reaction network that contains only one species A. Let m be the number of (distinct) reactant complexes, and let $a_1 < a_2 < \cdots < a_m$ be their stoichiometric coefficients. Then*

$$\text{mixed volume of } G \;=\; a_m - a_1 \;.$$

Proof. As G has only one species, there are no conservation laws and only one differential equation. In this equation, the leading monomial is $x_1^{a_m}$, and the lowest-degree monomial is $x_1^{a_1}$. The Newton polytope of this single polynomial is therefore the line segment between a_1 and a_m. Thus, by definition, the mixed volume of G is $a_m - a_1$. □

Corollary 6.4.7. *The mixed-volume overcount can be arbitrarily large.*

Proof. Consider the network $0 \underset{k_2}{\overset{k_1}{\rightleftharpoons}} n\,\mathrm{A}$, where $n \in \mathbb{N}$. The right-hand side of the mass-action ODEs (2.1) is the polynomial $-k_2 a^n + k_1$, which has precisely one positive real root (namely, $a = \sqrt[n]{k_1/k_2}$). However, by Theorem 6.4.6, the mixed volume is n. So, the mixed-volume overcount is $(n-1)$. □

Theorem 6.4.8 (One-species networks with mixed-volume overcount 0)**.** *Let G be a reaction network that contains only one species A. Let m be the number of (distinct) reactant complexes, and let $a_1 < a_2 < \cdots < a_m$ be their stoichiometric coefficients. Then G has mixed-volume overcount 0 if and only if G has an $(m-1)$-alternating subnetwork and $a_i = a_1 + i - 1$ for all $i \in \{2, 3, \ldots, m\}$.*

Proof. This result follows directly from Proposition 6.4.4 and Theorem 6.4.6. □

Example 6.4.9 (Example 6.4.3 continued)**.** By Theorem 6.4.8, the network from Example 6.4.3 has mixed-volume overcount 0. Indeed, it is a one-species network with 3 distinct reactant complexes (note that 0 is not a reactant complex in this network) satisfying $a_i = a_1 + i - 1$ for $i \in \{2, 3\}$ (here the notation is as in Theorem 6.4.8 with $a_1 = 1$), and it has a 2-alternating subnetwork.

6.4.2 Networks with two species and two reactions

Recall that a reaction network is genuine if every species takes part in at least one reaction. Up to relabeling species, there are 210 genuine, at-most-bimolecular networks with two species and two reactions [4]. These networks, which were enumerated by Banaji, were originally available at `https://reaction-networks.net/networks/`. A file containing the list of these networks is also in the repository `https://github.com/neeedz/mixedvolume`. Here we determine that 92% of these networks have mixed-volume overcount 0 (Theorem 6.4.17); the 16 exceptional networks are listed in Table 6.2.

The following result, which follows directly from [66, Lemma 2.7, Lemma 4.1, and Theorem 4.8] (also cf. [66, Corollary 4.12 and the preceding paragraph]), implies that the 210 networks we consider in this subsection are *not* multistationary.

Proposition 6.4.10. *If G is an at-most-bimolecular reaction network with exactly two species and two reactions, then the maximum number of positive steady states of G is at most 1. Moreover, this maximum number is 1 if the two reaction vectors of G are negative scalar multiples of each other, and 0 otherwise.*

Proposition 6.4.10 and the definition of mixed-volume overcount directly yield the following:

Corollary 6.4.11. *Let G be an at-most-bimolecular reaction network with exactly two species and two reactions. If the mixed volume of G is at least 2, then the mixed-volume overcount is at least 1.*

We use the following procedure to compute (by using `PHCpack` [52], as in the proof of Proposition 6.3.4) the mixed-volume overcount of a 2-species, 2-reaction network:

Procedure 6.4.12. *Input*: A 2-species, 2-reaction network G.

Output: The mixed-volume overcount of G.

0. Compute the system augmented by conservation laws (2.3), denoted by $f_{c,\kappa}$, for some choice of conservation-law matrix W.

1. Compute the mixed volume of G, as follows. Viewing the two polynomials in $f_{c,\kappa}$ as polynomials in x_1 and x_2, substitute 1 for all coefficients; let `poly1` and `poly2` be the resulting polynomials. Next, run the following `Macaulay2` code:

```
loadPackage "PHCpack"
S = CC[x1,x2];
F = {poly1 , poly2};
mixedVolume(F)
```

2. Compute the maximum number of positive steady states:

   (a) If G has no linear conservation laws, the maximum number of positive steady states is 0.

   (b) If G has a linear conservation law, determine the maximum number of positive steady states of G by analyzing the possible numbers of positive roots of $f_{c,\kappa} = 0$ (or by other means, e.g., if applicable, Proposition 6.4.10).

3. Output the difference between the mixed volume (from Step 1) and the maximum number of positive steady states (from Step 2).

Proof of correctness of Procedure 6.4.12. The correctness of Step 1 is due to the fact that mixed volume considers only the supports of polynomials. The correctness of Step 2(a) follows from [66, Lemma 4.1]. Step 2(b) is correct by construction of $f_{c,\kappa}$. Finally, the correctness of Step 3 follows directly from the definition of mixed-volume overcount (Definition 6.2.6). □

Example 6.4.13. Consider $G = \{\mathrm{A} + \mathrm{B} \xrightarrow{k_1} 2\,\mathrm{B} \xleftarrow{k_2} 2\,\mathrm{A}\}$.

0. The system augmented by conservation laws is

$$\begin{cases} f_1(x_1, x_2) = x_1 + x_2 - c_1 \\ f_2(x_1, x_2) = 2k_2x_1^2 + k_1x_1x_2 \quad . \end{cases} \tag{6.2}$$

1. Take $k_1 = 2k_2 = -c_1 = 1$ in (6.2), and compute the mixed volume of the resulting polynomial system. The mixed volume of the network is 1.

2. We compute the maximum number of steady states:

   (a) There is a linear conservation law (namely, f_1), so continue to Step 2(b).

   (b) The reaction vectors, $(-1, 1)$ and $(-2, 2)$, are *not* negative scalar multiples of each other. So, by Proposition 6.4.10, the maximum number of positive steady states is 0. Alternatively, notice that $f_2(x_1^*, x_2^*) > 0$ when $x_1^*, x_2^* > 0$, and so $f_{c,\kappa} = 0$ never has positive roots.

3. The mixed-volume overcount is $1 - 0 = 1$.

Next we provide two more examples of genuine 2-species, 2-reaction networks. These examples show that determining the maximum number of positive steady states by analyzing the roots of $f_{c,\kappa} = 0$ (Step 2(b) of Procedure 6.4.12) is not straightforward in general.

Example 6.4.14 (Example 2.2.1 continued)**.** Recall the genuine 2-species, 2-reaction network $\{2\,\mathrm{A} \xrightarrow{k_1} 2\,\mathrm{B},\ \mathrm{B} \xrightarrow{k_2} \mathrm{A}\}$. Using Procedure 6.4.12, we show below that the mixed-volume overcount of the network is 1.

0. The system augmented by conservation laws is

$$\begin{cases} f_1(x_1, x_2) = x_1 + x_2 - c_1 \\ f_2(x_1, x_2) = 2k_1x_1^2 - k_2x_2 \quad . \end{cases} \tag{6.3}$$

1. Take $2k_1 = -k_2 = -c_1 = 1$ in (6.3), and compute the mixed volume of the resulting polynomial system. The mixed volume of the network is 2.

2. We compute the maximum number of steady states:

   (a) There is a linear conservation law (namely, f_1), so continue to Step 2(b).

   (b) The reaction vectors are $(-2, 2)$ and $(1, -1)$, which are negative scalar multiples of each other. So, by Proposition 6.4.10, the maximum number of positive steady states is 1. Alternatively, we analyze the roots of $f_{c,\kappa} = 0$, as follows. First, $f_1 = 0$ yields $x_2 = c_1 - x_1$, which we substitute into $f_2 = 0$ to get

$$g(x_1) \;=\; 2k_1x_1^2 - k_2(c_1 - x_1) \;=\; 2k_1x_1^2 + k_2x_1 - k_2c_1 \;.$$

   This is a quadratic in x_1 with positive leading coefficient and negative vertical intercept (since $k_1, k_2, c_1 > 0$). Thus, for every choice of $k_1, k_2, c_1 > 0$, the quadratic has a unique positive real root in x_1, namely, $x_1^* = \left(-k_2 + \sqrt{k_2^2 + 8c_1k_1k_2}\right)/(4k_1)$. Therefore, the maximum number of steady states is at most 1. In fact, this number is 1: when $k_1 = 1/2$, $k_2 = 1$ and $c_1 = 2$, there is a unique positive steady state, namely, $(x_1^*, x_2^*) = (1, 1)$.

3. The mixed-volume overcount is $2 - 1 = 1$.

Example 6.4.15. Let $G = \{2\,\mathrm{A} \xrightarrow{k_1} 2\,\mathrm{B} \xrightarrow{k_2} \mathrm{A} + \mathrm{B}\}$.

0. The system augmented by conservation laws is

$$\begin{cases} f_1(x_1, x_2) = x_1 + x_2 - c_1 \\ f_2(x_1, x_2) = 2k_1x_1^2 - k_2x_2^2 \quad . \end{cases} \tag{6.4}$$

1. Take $2k_1 = -k_2 = -c_1 = 1$ in (6.3), and compute the mixed volume of the resulting polynomial system. The mixed volume of the network is 2.

2. We compute the maximum number of steady states:

   (a) There is a linear conservation law (namely, f_1), so continue to Step 2(b).

   (b) The reaction vectors, $(-2, 2)$ and $(1, -1)$, are negative scalar multiples of each other. So, Proposition 6.4.10 implies that the maximum number of positive steady states is 1. An alternate approach is as follows. We solve $f_2 = 0$ for x_2 (and use the fact that we are interested in only positive x_1, x_2), which yields $x_2^* = (\sqrt{2k_1/k_2})x_1^*$. Next, we substitute this expression into $f_1 = 0$ and then solve to obtain $x_1^* = c_1/(1 + \sqrt{2k_1/k_2})$. Thus, the network always admits a unique positive steady state (x_1^*, x_2^*).

3. The mixed-volume overcount is $2 - 1 = 1$.

Remark 6.4.16. The approaches that we present in this section for computing the maximum number of steady states of a network (Steps 2(a) and 2(b) of Procedure 6.4.12) rely on the fact that the networks are at-most-bimolecular and have only two reactions and two species. In general, however, completing Step 2 is not straightforward: as mentioned in the Introduction to this chapter, it requires counting the number of positive real roots of a parametrized polynomial system. This complication further motivates the need for graphical, algebraic, and geometric tools for counting positive steady states, in order to bypass a direct analysis of the polynomial system $f_{c,\kappa} = 0$.

By applying Procedure 6.4.12, we obtain a classification of genuine, at-most-bimolecular networks with two species and two reactions (Theorem 6.4.17).

Theorem 6.4.17 (Mixed volume of two-species, two-reaction networks)**.** *Let G be a genuine, at-most-bimolecular network with 2 species and 2 reactions. Then G has mixed-volume overcount 0 if and only if G is (up to relabeling species)* not *one of the 16 networks listed in Table 6.2. Moreover, each network in Table 6.2 has mixed-volume overcount 1.*

Proof. Using Procedure 6.4.12, we computed the mixed-volume overcount for all genuine 2-species, 2-reaction networks; see the file `MV-overcount-2s-2r-networks.csv` in the repository `https://github.com/neeedz/mixedvolume`. More details are as follows.

	Network	Mixed volume
(1)	$2\,\mathrm{A} \longrightarrow 2\,\mathrm{B} \longrightarrow \mathrm{A}+\mathrm{B}$	2
(2)	$2\,\mathrm{A} \longrightarrow 2\,\mathrm{B}\,,\ \mathrm{B} \longrightarrow \mathrm{A}$	2
(3)	$2\,\mathrm{A} \longrightarrow \mathrm{A}\,,\ \mathrm{B} \longrightarrow \mathrm{A}+\mathrm{B}$	2
(4)	$\mathrm{B} \longrightarrow \mathrm{A}\,,\ 2\,\mathrm{A} \longrightarrow \mathrm{A}+\mathrm{B}$	2
(5)	$\mathrm{B} \longrightarrow \mathrm{A}\,,\ 2\,\mathrm{B} \longrightarrow \mathrm{A}+\mathrm{B}$	1
(6)	$2\,\mathrm{A} \rightleftharpoons 2\,\mathrm{B}$	2
(7)	$2\,\mathrm{A} \longrightarrow \mathrm{A}+\mathrm{B} \longleftarrow 2\,\mathrm{B}$	2
(8)	$\mathrm{B} \longrightarrow \mathrm{A}\,,\ 2\,\mathrm{B} \longrightarrow 2\,\mathrm{A}$	1
(9)	$\mathrm{B} \longrightarrow 2\,\mathrm{B}\,,\ \mathrm{A} \longrightarrow \mathrm{A}+\mathrm{B}$	1
(10)	$2\,\mathrm{B} \longrightarrow 0\,,\ \mathrm{A} \longrightarrow \mathrm{A}+\mathrm{B}$	2
(11)	$\mathrm{A} \rightleftharpoons 2\,\mathrm{B}$	2
(12)	$\mathrm{A}+\mathrm{B} \longrightarrow 2\,\mathrm{B} \longleftarrow 2\,\mathrm{A}$	1
(13)	$2\,\mathrm{A} \longrightarrow \mathrm{A}+\mathrm{B} \longrightarrow 2\,\mathrm{B}$	1
(14)	$2\,\mathrm{A} \longrightarrow \mathrm{A}\,,\ \mathrm{A}+\mathrm{B} \longrightarrow \mathrm{B}$	1
(15)	$\mathrm{A}+\mathrm{B} \rightleftharpoons 0$	2
(16)	$\mathrm{B} \longrightarrow \mathrm{A}\,,\ \mathrm{A}+\mathrm{B} \longrightarrow 2\,\mathrm{A}$	1

Table 6.2: Genuine, at-most-bimolecular networks with two species and two reactions for which the mixed-volume overcount is nonzero. Each network has mixed-volume overcount 1.

Among the 210 networks, 185 of them have mixed volume 0 and thus have mixed-volume overcount 0. For the remaining 25 networks (see Section 6.5), it is straightforward to compute the maximum number of positive steady states using Proposition 6.4.10 or by directly analyzing the system $f_{c,\kappa} = 0$ as in Examples 6.4.13–6.4.15. □

We end this section by investigating why the networks in Table 6.2 have nonzero mixed-volume overcount. These 16 networks fall into four classes:

1. Networks (3), (9), (10), and (14) are essentially one-species networks (for each network, one of the two ODEs is 0), and so can be analyzed using the results in Section 6.4.1.

2. Networks (6), (11), and (15) consist of a single pair of reversible reactions, so (e.g., by Proposition 6.4.10) the maximum number of positive steady states is 1.

3. Networks (5), (8), (12), (13), and (16) have one species that is consumed in every reaction (while the other species is produced). Thus, the maximum number of positive steady states

is 0.

4. Networks (1), (2), (4), and (7) (and also networks (3), (6), (10), (11), and (15)) have mixed volume 2, so, by Corollary 6.4.11, the mixed-volume overcount is at least 1.

Remark 6.4.18. In Examples 6.4.14 and 6.4.15, we computed the maximum number of positive steady states (Step 2 of Procedure 6.4.12) by reducing the system $f_{c,\kappa} = 0$ to a single univariate polynomial, and then checking that the positive roots (which can be viewed as "partial solutions") can be extended to positive roots of the original system. Doing this for general networks, however, is difficult. Indeed, for readers with knowledge of algebraic geometry, we note that the Extension Theorem [27, pp. 118-120] requires an algebraically closed field and polynomials with a certain shape.

Example 6.4.19. Consider the following network with 3 species and 10 reactions:

$$0 \rightleftharpoons \mathrm{A}\ ,\ 0 \rightleftharpoons \mathrm{B}\ ,\ 0 \rightleftharpoons \mathrm{C}$$
$$2\,\mathrm{A} \rightleftharpoons \mathrm{A}+\mathrm{B} \rightleftharpoons \mathrm{B}+\mathrm{C}\ .$$

This network has no conservation laws, and its augmented system is

$$\begin{cases} f_1 = k_1 - k_2x_1 - k_7x_1^2 + (k_8 - k_9)x_1x_2 + k_{10}x_2x_3 \\ f_2 = k_3 - k_4x_2 + k_7x_1^2 - k_8x_1x_2 \\ f_3 = k_5 - k_6x_3 + k_9x_1x_2 - k_{10}x_2x_3\ . \end{cases}$$

Analyzing this augmented system is challenging, and determining the maximum number of steady states of the network is not straightforward. This number is at least 2 [65], and we compute that its mixed volume is 6. What is the mixed-volume overcount? Our wish is to answer this question in the future through a generalized version of Procedure 6.4.12. Such a procedure would then give us a way to study multistationarity in this and other large networks.

6.5 Networks with nonzero mixed volume

Below, we list the 25 genuine 2-species, 2-reaction networks with nonzero mixed volume, together with their maximum number of positive steady states and their augmented systems. The first 16 networks here coincide with those listed in Table 6.2.

	Network	Mixed volume	Max #	System
(1)	$2\,\mathrm{A} \longrightarrow 2\,\mathrm{B} \longrightarrow \mathrm{A}+\mathrm{B}$	2	1	$a+b-c_1$ $2k_1a^2-k_2b^2$
(2)	$2\,\mathrm{A} \longrightarrow 2\,\mathrm{B}\ ,\ \mathrm{B} \longrightarrow \mathrm{A}$	2	1	$a+b-c_1$ $2k_1a^2-k_2b$
(3)	$2\,\mathrm{A} \longrightarrow \mathrm{A}\ ,\ \mathrm{B} \longrightarrow \mathrm{A}+\mathrm{B}$	2	1	$-k_1a^2+k_2b$ 0
(4)	$\mathrm{B} \longrightarrow \mathrm{A}\ ,\ 2\,\mathrm{A} \longrightarrow \mathrm{A}+\mathrm{B}$	2	1	$a+b-c_1$ $k_2a^2-k_1b$
(5)	$\mathrm{B} \longrightarrow \mathrm{A}\ ,\ 2\,\mathrm{B} \longrightarrow \mathrm{A}+\mathrm{B}$	1	0	$a+b-c_1$ $-k_2b^2-k_1b$
(6)	$2\,\mathrm{A} \rightleftharpoons 2\,\mathrm{B}$	2	1	$a+b-c_1$ $2k_1a^2-2k_2b^2$
(7)	$2\,\mathrm{A} \longrightarrow \mathrm{A}+\mathrm{B} \longleftarrow 2\,\mathrm{B}$	2	1	$a+b-c_1$ $k_1a^2-k_2b^2$
(8)	$\mathrm{B} \longrightarrow \mathrm{A}\ ,\ 2\,\mathrm{B} \longrightarrow 2\,\mathrm{A}$	1	0	$a+b-c_1$ $-k_1b-2k_2b^2$
(9)	$\mathrm{B} \longrightarrow 2\,\mathrm{B}\ ,\ \mathrm{A} \longrightarrow \mathrm{A}+\mathrm{B}$	1	0	0 k_1b+k_2a

	Network	Mixed volume	Max #	System
(10)	$2\,\mathrm{B} \longrightarrow 0\ ,\ \mathrm{A} \longrightarrow \mathrm{A} + \mathrm{B}$	2	1	$\begin{cases} 0 \\ -2k_1b^2 + k_2a \end{cases}$
(11)	$\mathrm{A} \rightleftharpoons 2\,\mathrm{B}$	2	1	$\begin{cases} a + b - c_1 \\ -k_2b^2 + k_1a \end{cases}$
(12)	$\mathrm{A} + \mathrm{B} \longrightarrow 2\,\mathrm{B} \longleftarrow 2\,\mathrm{A}$	1	0	$\begin{cases} a + b - c_1 \\ 2k_2a^2 + k_1ab \end{cases}$
(13)	$2\,\mathrm{A} \longrightarrow \mathrm{A} + \mathrm{B} \longrightarrow 2\,\mathrm{B}$	1	0	$\begin{cases} a + b - c_1 \\ k_1a^2 + k_2ab \end{cases}$
(14)	$2\,\mathrm{A} \longrightarrow \mathrm{A}\ ,\ \mathrm{A} + \mathrm{B} \longrightarrow \mathrm{B}$	1	0	$\begin{cases} -k_2a^2 - k_1ab \\ 0 \end{cases}$
(15)	$\mathrm{A} + \mathrm{B} \rightleftharpoons 0$	2	1	$\begin{cases} -k_1ab + k_2 \\ a - b \end{cases}$
(16)	$\mathrm{B} \longrightarrow \mathrm{A}\ ,\ \mathrm{A} + \mathrm{B} \longrightarrow 2\,\mathrm{A}$	1	0	$\begin{cases} a + b - c_1 \\ -k_1b - k_2ab \end{cases}$
(17)	$0 \longrightarrow 2\,\mathrm{B}\ ,\ \mathrm{A} + \mathrm{B} \longrightarrow \mathrm{A}$	1	1	$\begin{cases} 0 \\ -k_2ab + 2k_1 \end{cases}$
(18)	$2\,\mathrm{B} \longrightarrow 0\ ,\ \mathrm{A} + \mathrm{B} \longrightarrow \mathrm{A}$	1	1	$\begin{cases} 0 \\ -2k_1b^2 - k_2ab \end{cases}$
(19)	$\mathrm{A} + \mathrm{B} \longrightarrow 2\,\mathrm{A} \longrightarrow 2\,\mathrm{B}$	1	1	$\begin{cases} a + b - c_1 \\ 2k_2a^2 - k_1ab \end{cases}$

	Network	Mixed volume	Max #	System
(20)	$\mathrm{A}+\mathrm{B}\longrightarrow 2\,\mathrm{B}\longrightarrow \mathrm{A}+\mathrm{B}$	1	1	$\begin{cases} a+b-c_1 \\ k_1ab-k_2b^2 \end{cases}$
(21)	$\mathrm{A}+\mathrm{B}\longrightarrow 2\,\mathrm{B}\ ,\ \mathrm{B}\longrightarrow \mathrm{A}$	1	1	$\begin{cases} a+b-c_1 \\ k_1ab-k_2b \end{cases}$
(22)	$\mathrm{A}\longrightarrow 0\ ,\ \mathrm{B}\longrightarrow \mathrm{A}+\mathrm{B}$	1	1	$\begin{cases} -k_1a+k_2b \\ 0 \end{cases}$
(23)	$\mathrm{A}\rightleftharpoons \mathrm{B}$	1	1	$\begin{cases} a+b-c_1 \\ k_1a-k_2b \end{cases}$
(24)	$\mathrm{A}+\mathrm{B}\longrightarrow \mathrm{A}\ ,\ 0\longrightarrow \mathrm{B}$	1	1	$\begin{cases} 0 \\ -k_1ab+k_2 \end{cases}$
(25)	$\mathrm{A}+\mathrm{B}\rightleftharpoons \mathrm{A}$	1	1	$\begin{cases} 0 \\ -k_1ab+k_2a \end{cases}$

6.6 Comparing related definitions of mixed volume

Related notions of mixed volume for chemical reaction networks were studied by Gross et al. [50] and later by Gross and Hill [51]. While the overarching goal of each definition of mixed volume is to bound the maximum number of steady states, the motivations were different. For example, Gross and Hill approached from the viewpoint of numerical algebraic geometry: when there are no boundary steady states, their mixed volume counts the number of paths that need to be tracked when using a parameter-homotopy to solve the steady-state system. As for Gross et al., their definition was motivated by model rejection: the authors used algebraic geometry to compute the maximum number of complex-number steady states and subsequently used mixed volume to select from thousands of parametrizations of the steady state variety that give rise to the predicted number of complex-number steady states. Complementary to the case-study approach of [51]

and [50], we take a systematic approach. Our motivation is a general definition for *any* chemical reaction network that is easy to compute using existing software.

In the next subsection, we formalize the related definitions of mixed volume and compare them to our definition from Section 6.2. We introduce a fourth notion of mixed volume, which is related to that of [50] (see Procedure 6.6.4). We suspect that by incorporating steady-state parametrizations, this new notion will improve our mixed-volume bound from Section 6.2.

6.6.1 Four notions of a chemical reaction network's mixed volume

The authors of [50] and [51] describe the mixed volume for chemical reaction networks by way of case studies. Since a computational approach is taken – in contrast to a theoretical approach – no formal definition of mixed volume was developed in these works. Accordingly, here, we formalize their definitions of mixed volume of reaction networks.

Recall from Definition 6.2.3 that our mixed volume – which we will now call augMV – is the mixed volume of the augmented system (2.3), where conservation laws are substituted for the linearly redundant ordinary differential equations obtained from mass-action kinetics.

6.6.2 The 'unmixed' mixed volume

Gross and Hill [51] computed the mixed volume of three infinite families of networks. For the first family (the *Cell death model*), the mixed volume that they compute is identical to the augMV: the augmented system is obtained, and the mixed volume of the network is defined to be the mixed volume of the augmented system. In their second and third examples (the *Edelstein model* and *multisite distributive phosphorylation systems* [51, Sections 3.2 and 3.3]), the authors deduced a formula for the mixed volume of the chemical reaction network as the volume of the convex hull of the union of the Newton polytopes of the augmented systems. Their method bypasses an explicit computation of the mixed volume of the Newton polytopes of an augmented system and instead deduces the mixed volume by analyzing the volume of a related polytope with a nice combinatorial structure. The upshot of this method is a formula for computing mixed volume of infinite families of models that depends only on an indexing parameter (e.g. [51, Theorem 3.12])

(see Remark 6.6.1). Next, we formalize their definition for arbitrary chemical reaction networks.

Remark 6.6.1. In contrast to the approach of [51], getting a single formula to compute the mixed volume associated to an infinite family of networks using augMV is not immediately straightforward. The augMV favors explicit computation of the mixed volume bypassing the explicit computation of the Minkowski sum. Our procedure for computing the augMV uses `PHCpack` as a black box, so the mixed volume would need to be recomputed for each member of an infinite family of networks producing a new augmented system. The strength of the [51] approach is to give a combinatorial formula – in terms of an indexing parameter for an infinite family of reaction networks – for the volume of an associated polytope. This volume gives an upper bound on the number of steady states. However, it is not clear if a combinatorially nice polytope exists for arbitrary reaction networks. Indeed, [51] only consider 3 infinite families of reaction networks whose resulting polytopes have a desirable combinatorial structure.

Let G be a reaction network with augmented system (2.3), denoted by $\widetilde{F_s}$. Every solution of $\widetilde{F_s}$ is also a solution of a randomized system $F_s := M \cdot \widetilde{F_s}$, for a generic matrix $M \in \mathbb{C}^{s\times s}$. By construction, the system F_s is a square system where each polynomial is a linear combination of the polynomials $f_{c,\kappa,i}$, and each polynomial of F_s has Newton polytope $P := \bigcup_i^s \mathrm{New}(f_{c,\kappa,i})$. The [51] mixed volume – umxMV – of a G is $s!\mathrm{vol}(P)$, the mixed volume of its corresponding randomized system F_s.

By increasing the support set, umxMV can increase the bound on the number of steady states.

Proposition 6.6.2. *augMV $\leq$ umxMV.*

Proof. Let G be a chemical reaction network with augmented system (2.3), given by polynomials $f_1, \ldots, f_s$. The polynomials of the augmented system have Newton polytopes $\mathrm{New}(f_i)$. By definition, the augMV of G is the mixed volume of the Newton polytopes $\mathrm{New}(f_i)$. The polynomials of the corresponding unmixed system have Newton polytopes $\mathrm{New}(F)$, where $\mathrm{New}(F)$ is the convex hull of the stoichiometric coefficients of all the network's reactant complexes. In particular, $\mathrm{New}(f_i) \subseteq \mathrm{New}(F)$. By definition, the umxMV of G is the mixed volume of the Newton poly-

topes $\underbrace{\mathrm{New}(F), \ldots, \mathrm{New}(F)}_{s \text{ times}}$. By the monotonicity of mixed volume, if $K_1, \ldots, K_s$ and $L_1, \ldots, L_s$ are convex bodies such that $K_i \subseteq L_i$ for $1 \leq i \leq s$, then $\mathrm{mv}(K_1, \ldots, K_s) \leq \mathrm{mv}(L_1, \ldots, L_s)$. And so, augMV is bounded above by umxMV. □

6.6.3 The matroidal mixed volume

Mixed volume of the Wnt shuttle model was defined in the context of algebraic matroids associated with the steady-state system. Here we give an overview of the procedure, and we refer the reader to [50, Sections 2 and 5] for details.

The [50] mixed volume – matMV – computes the mixed volume of different bases of an algebraic matroid that arises from the steady state variety. First, the authors compute a primary decomposition of the ideal generated by (2.1), viewing it as an ideal in $\mathbb{Q}(\kappa)[x]$. The variety of the steady-state ideal is then the union of two irreducible components, given by the varieties of each of the prime ideals in the primary decomposition. Positive steady states are in the variety of what the authors call the *main component* of the prime ideal, denoted by $\widetilde{I_m}$. The prime ideal $\widetilde{I_m}$ defines an *algebraic matroid* M. Degree-1 bases of the matroid give rise to rational parametrizations of $V(\widetilde{I_m})$. Each parametrization subsequently produces a representation of the steady-state variety: the parametrization is substituted into the conservation equations, denominators are cleared, and then a saturation of the resulting ideal is obtained. The saturation ideal represents the preimage of the steady state variety under the rational parametrization. In summary, each degree 1-basis Y of the algebraic matroid M defined by $\widetilde{I_m}$ produces a saturation ideal J_Y. The mixed volume of Y is defined to be the minimum mixed volume of the Newton polytopes of any subset of $\mathrm{rank}(M)$ generators of J_Y.

However, an associated "matMV" is not well defined. In the Wnt-pathway case study, the authors show that this mixed volume of the resulting choice of basis varied widely depending on the choice of steady-state parametrization (see [50, Table 6]): the possible mixed volumes ranged from 5 to 45. For this model, the authors used other techniques to establish the maximum number of complex-number steady states, and used the mixed volume to match this number. Without

the foresight of the maximum number of complex-number of steady states, however, computing matMV is impractical for general networks.

However, we suspect that the inequality matMV $\leq$ augMV holds for the "right" choice of basis. Indeed, augMV for the Wnt-pathway is 56. Gross et al. determined that there are at most 9 complex-number steady states ([50, Theorem 1.1]) and conjectured that the maximum number of positive steady states is 3 ([50, Remark 4.2]). There exists a choice of basis for the associated algebraic matroid whose corresponding mixed volume is 9.

We end our comparison of matMV and augMV with the following question.

Question 6.6.3. *For an arbitrary chemical reaction network, can we a priori choose an appropriate basis for the associated algebraic matroid (and thus an appropriate rational parametrization of the steady-state variety) so that matMV gives a sharp bound on the number of (positive) steady states, without knowing the maximum number of complex-number steady states?*

6.6.4 The steady-state parametrization mixed volume

One unique aspect of matMV is the use of a steady-state parametrization to build a simpler polynomial system without losing the steady states of the original system. Guided by the idea of incorporating steady-state parametrizations before computing the mixed volume, as for matMV, we ask the following question. What if we take a (positive) parametrization and use it to build an equivalent polynomial system, and then compute the mixed volume of this "smaller" system? We propose the following procedure for computing the *steady-state parametrization mixed volume*, sspMV:

Procedure 6.6.4.

Input: A network G on s species with d linear conservation laws.

Output: the sspMV of G.

0. Choose d species in the support of the d conservation laws. A parametrization will be obtained in terms of these d species.

1. Solve the $s - d$ non-conservation-law equations for the remaining $s - d$ variables to obtain a steady-state parameterization. (This can be done, e.g., using `Mathematica` or `Maple`.)

2. Check whether this is a *positive* parametrization. If not, go back to Step 1 and choose a different set of d variables.

3. Substitute this parametrization into the d conservation laws. Get a system of d rational equations on the d chosen variables, with coefficients k_i, c_i.

4. Clear denominators to get a square $d \times d$ polynomial system whose positive roots are the same as the original ODE system. (Recall from Step 2 that we chose a positive parametrization, so denominators in the parametrization have no positive roots. Then, clearing denominators does not affect the positive roots.)

5. Compute the mixed volume of the resulting square system in Step 5 using `PHCpack`[3].

6. Output the mixed volume from Step 5. This is the sspMV of G.

Proposition 6.6.5. *The maximum number of positive steady states of a given network is at most its sspMV.*

Proof. By construction, a positive parametrization is surjective, so all positive steady states are preserved under the parametrization (see Definition 2.2.5). Specifically, within a compatibility class defined by a total-constant vector c, positive solutions x^* to (2.3) are in one-to-one correspondence with positive solutions $(a^*;\ x^*) = \phi(\hat{a}^*;\ x^*)$ to (2.7), for steady-state parametrization ϕ. So, sspMV gives an upper bound on the maximum number of positive steady states of the network. □

The sspMV combines ideas from the defining principles of both the augMV and the matMV. By constructing a smaller (with respect to number of variables) polynomial system with the same positive roots as the original system, we hope that we can improve the bound on the maximum

[3]This step is analogous to Step 1 of Procedure 6.4.12.

number of steady states. However, the sspMV still depends on the choice of parametrization, as we will see in Example 6.6.8. In future work, we wish for criteria on a network to get the sharpest bound possible from the sspMV. More explicitly, we hope to answer the following question: Under which conditions can we choose a steady-state parametrization such that strictly non-real steady states are lost, so that sspMV is strictly less than augMV?

Remark 6.6.6. Step 2 requires a positive steady-state parametrization; such a parametrization does not always exist. However, there are criteria for determining its existence for certain classes of networks (e.g., [33, 63, 81]).

Question 6.6.7. *Procedure 6.6.4 leads to the following questions, for future work. Here, in contrast to the positive parametrization from Definition 2.2.5, we use* non-positive parametrization *to describe a rational parameterization* $\phi : \mathbb{R}^{\hat{m}}_{>0} \times \mathbb{R}^{s}_{>0} \to \mathbb{R}^{\bar{m}} \times \mathbb{R}^{s}$ *of a network's steady states whose image intersects the positive orthant in the set of positive steady states.*

1. *In Step 2 of Procedure 6.6.4, does it matter if we choose a positive parametrization, especially since only the roots in* $\mathbb{C}^*$ *are considered anyway? Does taking a non-positive parametrization increase the mixed volume?*

2. *In Step 4, there is no issue in clearing denominators if a positive parametrization was taken (Step 2), since in that case, the denominators are all positive. If taking a non-positive parametrization would we need to take saturation by the ideal generated by the denominators, as in [50]?*

We apply Procedure 6.6.4 to the ERK networks. From our investigation, we conclude that the mixed volume can go increase, decrease, or remain the same when a positive parametrization is used, so sspMV can be greater than, less than, or equal to augMV.

Example 6.6.8. Consider the full ERK network (defined in Section3.1) and the reduced ERK network (defined in Section 3.3). For each of these ERK networks, we compute the augMV (using

Definition 6.2.3), the umxMV (see Section 6.6.2), and the sspMV (using Procedure 6.6.4). We compute the sspMV under different choices of free variables selected in Step 0 of Procedure 6.6.4.

Table 6.4 collects our results. The `Macaulay2` input code used to compute the augMV, umxMV, and sspMV for each of the specified networks in this example is in Appendix C.

network	**augMV**	**sspMV (free variables)**	**umxMV**
full ERK (no effective steady state function)	7	8 (x_1, x_2, x_3)	13
full ERK (no effective steady state function)	7	6 (x_2, x_3, x_4)	13
full ERK (with effective steady state function)	7	8 (x_1, x_2, x_3)	13
full ERK (with effective steady state function)	7	8 (x_2, x_3, x_4)	13
red ERK (with effective steady state function)	3	3 (x_1, x_2, x_8)	9

Table 6.4: The mixed volume of ERK networks under the different definitions from Section 6.6. The `Macaulay2` code for the associated computations is in Appendix C.

Finally, we investigate another reduction: instead of choosing the augmented system (2.3) as the defining polynomial system for the network, we consider the augmented system (2.7) resulting from our choice of an effective steady-state function. Specifically, for the full ERK network, we use the effective steady-state function from Proposition 3.2.1, and for the reduced ERK network, we use the effective steady-state function from Proposition 3.3.1. We remark that the for the networks considered, the augMV and umxMV remain the same whether or not the steady-state function was first used to simplify the augmented system.

6.7 Discussion

Recall that our interest in the mixed volume of a reaction network comes from the fact that it bounds the maximum number of positive steady states. We saw in Section 6.3 that this bound is surprisingly good for certain signaling networks, and in Section 6.4 we again found that this bound performs well for small networks that are at-most-bimolecular. As networks arising in biological applications are typically at-most-bimolecular, we might expect the mixed-volume overcount to be low for biological networks of small to medium size.

Another future research direction pertains to one aim of our mixed volume work, which is to read off the mixed volume directly from a network. We now can do this for networks with just one reaction or one species (Section 6.4.1). As for at-most-bimolecular networks with two reactions and two species, the mixed volume is (with the exception of the 16 networks in Table 6.2) exactly the maximum number of positive steady states, which can be ascertained using results in [66]. We would like similar results for networks with more reactions or more species.

Continuing this line of investigation, we ask, *How do operations on networks affect the mixed volume (and thus the mixed-volume overcount)?* For instance, in Table 6.2, networks (1) and (7) can be obtained from each other by "stretching" one reaction (without changing the reactant or the direction of the reaction vector); and similarly for networks (2) and (4). Moreover, this operation does not affect the maximum nuber of steady states or the mixed volume, and thus does not affect the mixed-volume overcount. (This line of investigation therefore would be somewhat similar in spirit to the work of Rojas [85] and Bihan and Soprunov [10].) Indeed, having a list of operations and their effect on the mixed volume would greatly aid our classification of networks.

Finally, we analyzed different approaches to mixed volume from prior work on chemical reaction networks, and compared these to our definition of mixed volume. Motivated by key ideas from these results we defined a new procedure (Procedure 6.6.4) for incorporating steady-state parametrizations, with an intention to improve the mixed-volume bound. As discussed in Question 6.6.7, Procedure 6.6.4 depends on the choice of parametrization. Our goal for Section 6.6 was to investigate alternative procedures of mixed volume for chemical reaction networks. An underlying motivation is one well-defined notion of mixed volume for arbitrary chemical reaction networks such that the mixed-volume overcount is small.

7. NEWTON-OKOUNKOV BODIES OF CHEMICAL REACTION NETWORKS

This chapter contains new, unpublished material based on joint work with Elise Walker. We introduce a notion of a *Newton-Okounkov body* of a chemical reaction network. Specifically, our goals for this chapter are as follows. We motivate the need for a refined bound on the maximum number of positive steady states of a network, and in particular a bound that accounts for the algebraic dependencies among a network's defining polynomials (Section 7.1). Section 7.2 overviews the algebraic setup we use in this chapter. Section 7.3 overviews the basics of the theory of Newton-Okounkov bodies. In Section 7.4, we define a notion of Newton-Okounkov bodies for chemical reaction networks. Section 7.5 concerns the following question: When does the Newton-Okounkov body bound improve that of the mixed volume for chemical reaction networks? Finally, through examples, we compare the volume of the Newton-Okounkov body, the mixed volume (specifically, the augMV from Section 6.2), and the actual number of maximum steady states.

7.1 Motivation

The theory of Newton-Okounkov bodies is an exciting modern area of study that was originally developed in pure mathematics [67, 71], but has potential in applications, particularly in solving systems of polynomial equations. Newton-Okounkov bodies can be thought of as a generalization of Newton polytopes. In particular, the volume of Newton-Okounkov bodies generalizes the Bernstein-Khovanksii-Kushnirenko bound from Proposition 6.2.2; see Proposition 7.3.2. We refer the reader to the foundational works [67, 71] for more details.

Despite their noted potential, there are very few concrete examples of Newton-Okounkov bodies for polynomial systems arising from applications. Accordingly, here, we take a computational approach, as in [13]. Our focus is on defining a given chemical reaction network's associated Newton-Okounkov body, computing its volume, and assessing the resulting bound on the maximum number of the network's steady states.

7.2 Setup and overview

In this dissertation, we do not attempt to fully describe the vast, general theory of Newton-Okounkov bodies. Instead, we follow an algorithmic approach (cf. [13, Section 4.1]), and we take the following setup and assumptions.

Definition 7.2.1. Let A be a finitely generated subalgebra of a polynomial ring $k[x_1, \ldots, x_s]$, where k is a field. Fix a monomial term order $<$ on $k[x_1, \ldots, x_s]$.

For a nonzero $f \in k[x_1, \ldots, x_s]$, let $\text{in}_<(f)$ denote the leading term of f with respect to the term order $<$, that is, $\text{in}_<(f)$ is the term of f with nonzero coefficient which is greater than all other terms of f with nonzero coefficient. Let $\text{in}_<(A)$ be the k-vector space spanned by the set of monomials $\{\text{in}_<(f) \mid f \in A\}$. Then $\text{in}_<(A)$ is a subalgebra of A, called the initial algebra of A.

We call a subset $\mathcal{B}$ of a finitely generated polynomial subalgebra $A \subset k[x_1, \ldots, x_s]$ a SAGBI basis for A with respect to $<$ if the initial algebra $\text{in}_<(A)$ is equal to the k-algebra generated by the monomials $\text{in}_<(b)$ for $b \in \mathcal{B}$. In other words, $\mathcal{B}$ is a SAGBI basis for A with respect to $<$ if $\text{in}_<(A) = k[\text{in}_<(b) \mid b \in \mathcal{B}]$.

SAGBI bases for subalgebras are analogous to Gröbner bases of ideals; indeed the term SAGBI is the acronym for Subalgebra Analogue to Gröbner Bases for Ideals. Just as a Gröbner basis for an ideal generates the ideal, a SAGBI basis for a subalgebra generates the subalgebra [84, Proposition 1.16b]. That a SAGBI basis is a generating set follows from the *subduction algorithm*, which expresses a given subalgebra element as a polynomial in the elements of a SAGBI basis for the subalgebra:

Proposition 7.2.2 (Subduction Algorithm [95, Algorithm 11.1])**.**
Input: A SAGBI basis $\mathcal{B}$ for a subalgebra $A \subset \mathbb{C}[x_1, \ldots, x_s]$ and a polynomial $f \in A$.
Output: An polynomial expression of f in the elements of $\mathcal{B}$.
While f is not a constant in $\mathbb{C}$ do

1. *Find $b_1, b_2, \ldots, b_r \in \mathcal{B}$, exponents $i_1, i_2, \ldots, i_r \in \mathbb{N}$ and $c \in \mathbb{C}^*$ such that*

$$in_<(f) = c \cdot in_<(b_1)^{i_1} \cdot in_<(b_2)^{i_2} \cdots in_<(b_r)^{i_r} \ . \tag{7.1}$$

   (Recall that by definition, the leading terms of a SAGBI basis for A generates the initial algebra of A.)

2. *The leading terms of f and $p := c \cdot b_1^{i_1} b_2^{i_2} \cdots b_r^{i_r}$ are equal. Replace f by $f - p$, and repeat the process with f until f is a constant in $\mathbb{C}$.*

Remark 7.2.3. The subduction algorithm is the subalgebra analog of the *division algorithm* for ideals; the division algorithm takes a polynomial f in an ideal I and a Gröbner basis for I as inputs, and the output is an expression of f as a linear combination of the Gröbner basis elements.

Remark 7.2.4. In this chapter, we will only work with polynomial subalgebras that have finite SAGBI bases with respect to some term order. Under this assumption (namely, a finite SAGBI basis exists), we can compute a finite SAGBI basis $\mathcal{B}$ using the as-yet undistributed `Macaulay2` package `SubalgebraBases.m2` (based on [93]) – see Procedure 7.4.1.

However, deciding if a given finitely generated subalgebra A has a finite SAGBI basis with respect to some monomial term order $<$ is still an open question. In particular, there exist examples of finitely generated subalgebras with (i) no finite SAGBI basis with respect to any term order, (ii) SAGBI bases whose finiteness depends on the term order, and (iii) 'universal' finite SAGBI bases (the same SAGBI basis under any term order). We give an example of each below, and refer the reader to [84] for proofs. In what follows, k is a field.

(i) The following is [84, Example 1.20]. Consider the subalgebra A of $k[x, y]$ finitely generated (as a k-algebra) by $\{x + y,\ xy,\ xy^2\}$. There are only two term orderings on $k[x, y]$: either $x > y$ or $y > x$. If $x > y$, then any SAGBI basis of A must contain the infinite set $\{x + y,\ xy^n \mid n \in \mathbb{N}\}$. Similarly, if $y > x$, then A is also generated by $\{x + y,\ xy,\ x^2y\}$. Under this term order, any SAGBI basis of A must contain the infinite set $\{x+y,\ yx^n \mid n \in \mathbb{N}\}$. In either case, A has *no* finite SAGBI basis.

(ii) The following is [84, Example 4.11]. Let the ambient algebra be $k[x, y]$, and consider the subalgebra A finitely generated by $\{x,\ xy - y^2,\ xy^2\}$. If the chosen monomial term order has $y > x$, then this generating set $\mathcal{B} = \{x,\ xy - y^2,\ xy^2\}$ is a finite SAGBI basis for A. However, if the chosen monomial term order is $x > y$, then $k[xy^n \mid n \in \mathbb{N} \cup \{0\}] \subset \text{in}_>(A)$. In other words, any subset of A generating its initial algebra must contain infinitely many monomials. So, A does not have a finite SAGBI basis under this term order.

(iii) The following is [84, Example 1.13, Theorem 1.14]; see also [96, Section 1.1] for the proof when the chosen term order is degree lexicographic order. Let the ambient ring be $k[x_1, \ldots, x_n]$. Recall that a *symmetric polynomial* is a polynomial $p(x_1, \ldots, x_n)$ that remains the same if any variables are interchanged. In other words, for any permutation $\sigma \in \mathfrak{S}_n$ of the subscripts $1, 2, \ldots, n$, we have that $p(x_{\sigma(1)}, \ldots, x_{\sigma(n)}) = p(x_1, \ldots, x_n)$. Recall that the *elementary symmetric polynomials* $e_1, \ldots, e_n$ are symmetric polynomials defined by $e_i = \sum_{1 \leq j_1 < \ldots < j_i \leq n} x_{j_1} \cdots x_{j_i}$ for $i = 1, \ldots, n$. Then, the elementary symmetric polynomials are a SAGBI basis for the subalgebra of symmetric polynomials with respect to *any* term order.

Remark 7.2.5. As we saw in Remark 7.2.4 (i), a SAGBI basis is not unique and in particular can depend on the choice of the term order $<$. We discuss this complication further in Section 8.4.

Remark 7.2.6. Recently, [68] generalized the notions of Definition 7.2.1. In the general setting, the starting ingredients are an arbitrary finitely generated k-algebra A and a map $\nu : A \setminus \{0\} \to \Gamma \cup \{\infty\}$ called a *valuation* on A, where Γ is a group equipped with a total order and ν satisfies (1) $\nu(fg) = \nu(f) + \nu(g)$, (2) $\nu(f + g) \geq \min\{\nu(f), \nu(g)\}$, and (3) $\nu(f) = \infty$ if and only if $f = 0$. Through a more general construction, [68] describe a *Khovanskii basis* associated to (A, ν).

A SAGBI basis is a special case of a *Khovanskii basis*: specifically, a SAGBI basis is a Khovanskii basis where A is a subalgebra of a polynomial algebra $k[x_1, \ldots, x_s]$ and the valuation ν is a monomial valuation induced by a term order on $k[x_1, \ldots, x_s]$.

Remark 7.2.7. Another application of SAGBI bases to dynamical systems was that of [44]. There,

SAGBI bases were used a tool for exploiting algebraic structure in dynamical systems with symmetry.

We conclude this section with an overview of the next section.

In what follows, we will take the field $k = \mathbb{C}$, so that A is a finitely generated subalgebra of the polynomial algebra $\mathbb{C}[x_1, \ldots, x_s]$. Furthermore, we will fix a monomial term order $<$ such that A has a finite SAGBI basis $\mathcal{B} = \{p_1, \ldots, p_b\}$ with respect to $<$. Given A, $<$, and $\mathcal{B}$, we will construct a convex body $\Delta(A, <, \mathcal{B})$ called the *Newton-Okounkov body associated to* $(A, <, \mathcal{B})$[1], see Section 7.3.

As we will see in the next section, the normalized volume $\mathrm{vol}(\Delta(A, <, \mathcal{B})$ of this Newton-Okounkov body is used to count the number of isolated solutions of a polynomial system $f_1 = \cdots = f_s = 0$, where the f_i are in the linear span of $\mathcal{B}$ (see Proposition 7.3.2).

7.3 Background definitions

Now, we define a Newton-Okounkov body associated to a polynomial subalgebra with respect to a term order and finite SAGBI basis, following the presentation of [69].

Definition 7.3.1. Let A be a finitely generated polynomial subalgebra of $\mathbb{C}[x_1, \ldots, x_s]$ with a specified monomial term order $<$. Let $\mathcal{B} = \{p_1, \ldots, p_b\}$ be a finite SAGBI basis for A (Definition 7.2.1). Next, for each basis element of $\mathcal{B}$ we define an exponent vector via $<$ as follows: for each $p_i \in \mathcal{B}$, let α_i denote the largest monomial of p_i under the monomial term order $<$, so $x^\beta \leq x^{\alpha_i}$ for all monomials x^β of p_i. Then the set $\Delta(A, <, \mathcal{B}) := \mathrm{conv}\{\alpha_i \mid \alpha_i = 1, \ldots, \ell\}$ is the Newton-Okounkov body associated to $(A, <, \mathcal{B})$. We will use $\Delta(A)$ to denote the Newton-Okounkov body associated to $(A, <, \mathcal{B})$ when the term order and SAGBI basis are clear from context. Also, we will use $\mathrm{vol}(\Delta(\mathrm{A}))$ to denote the volume of the Newton-Okounkov body associated to $(A, <, \mathcal{B})$.

Finally, [67, 71] showed that the volume of the Newton-Okounkov body associated to $(A, <, \mathcal{B})$ counts isolated solutions of certain polynomial systems in A.

[1] We will see in Definition 7.3.1 that the definition of Newton-Okounkov body associated to $(A, <, \mathcal{B})$ depends upon the choice of SAGBI basis $\mathcal{B}$, and thus only weakly on A.

Proposition 7.3.2 ([67, 71])**.** *Let A be a polynomial subalgebra, fix a term order $<$, and let $\mathcal{B}$ be a SAGBI basis for A with respect to $<$. Let $\{f_1 = \cdots = f_s = 0\}$ be a system of polynomial equations, where each f_i is in the linear span of $\mathcal{B}$. Then $\{f_1 = \cdots = f_s = 0\}$ has $s! \operatorname{vol}(\Delta(\mathrm{A}))$ isolated solutions.*

The following proposition follows from the definitions of the various root counts that we consider in this dissertation (cf. [18]).

Proposition 7.3.3. *Let A be a polynomial subalgebra of $\mathbb{C}[x_1, \ldots, x_s]$, fix a monomial term order $<$, and assume $\mathcal{B}$ is a finite SAGBI basis for A with respect to $<$. Let $F := \{f_1 = \cdots = f_s = 0\}$ be a polynomial system in A, such that F is in the linear span of $\mathcal{B}$. Let $\#\ \mathbb{R}^+$-root denote the maximum number of positive-real solutions to F, let $\#\ \mathbb{C}^+$-root denote the maximum number of nonzero-complex-number solutions to F, let $\operatorname{vol}(\Delta(\mathrm{A}))$ denote the volume of the Newton-Okounkov body associated to $(A, <, \mathcal{B})$, and let $\operatorname{mv}(\operatorname{New}(f_1), \ldots, \operatorname{New}(f_s))$ denote the mixed volume of the Newton polytopes of the polynomials in F. Then the following inequalities hold:*

$$\#\,\mathbb{R}^+\text{-root} \quad \leq \quad \#\,\mathbb{C}^*\text{-root} \quad \leq \quad \operatorname{vol}(\Delta(\mathrm{A})) \quad \leq \quad \operatorname{mv}(\operatorname{New}(f_1), \ldots, \operatorname{New}(f_s))\,.$$

As described in this section, a Newton-Okounkov body is associated to a *subalgebra* of a polynomial algebra (really, to a *SAGBI basis*, see Footnote 1). However, our goal is to use the volume of a Newton-Okounkov body to give a bound on the number of steady states of a chemical reaction network. Accordingly, in the next section, we will define a Newton-Okounkov body of a *chemical reaction network*, and we will use Proposition 7.3.2 to get bounds on the network's maximum number of steady states.

7.4 Newton-Okounkov body of a chemical reaction network

In this section, we introduce a Newton-Okounkov body of a chemical reaction network. Following Definition 7.3.1, we will need to define a subalgebra A, monomial term order $<$, and SAGBI basis $\mathcal{B}$ associated to a chemical reaction system. Then we will define the Newton-Okounkov body of the chemical reaction system to be the Newton-Okounkov body of this associated triple

$(A, <, \mathcal{B})$. Procedure 7.4.1 describes our method for computing the volume of a Newton-Okounkov body of a given chemical reaction system.

First we begin by reminding the reader that the mixed volume of a chemical reaction network gives an upper bound on the maximum number of steady states. In this setting, we assume that there is no knowledge of the rate constants κ_i in the chemical reaction system (2.3). However, in certain applications, we may have some information about the rate constants. For instance, we may *a priori* know some relationship among the rate constants, such as equality. On the other hand, we may have specific values for some or all of the rate constants. The chemical reaction system from Example 7.5.1 has $\kappa = (1, 1, 5, 1, 1, 5, 1, 1, 1, 1, 1, 1, 1, 1, 5, 1, 5, 1, 1, 1)$, for example. We anticipate that the theory of Newton-Okounkov bodies for chemical reaction networks will improve bounds on the maximum number of steady states in these cases where we have some knowledge about the rate constants. We pursue this in Section 7.5.

Before presenting our procedure for computing a given chemical reaction network's Newton-Okounkov body, we briefly overview the method. Given a chemical reaction network with augmented system (2.3), denoted by F, choose a finite generating set of polynomials P such that any polynomial $f \in F$ can be written as a $\mathbb{C}$-linear combination of polynomials in P. The generating set P will be our candidate for a SAGBI basis for an algebra A. We will use the software package `SubalgebraBases.m2` to determine whether P is a SAGBI basis (in which case, we will take $\mathcal{B} := P$), and if it is not, a finite SAGBI basis $\mathcal{B}$ will be computed. The SAGBI basis generates a corresponding subalgebra A. Finally, the Newton-Okounkov body of the chemical reaction system is defined to be the Newton-Okounkov body $\Delta(A)$ of the associated $(A, <, \mathcal{B})$. The volume of this Newton-Okounkov body is an upper bound on the maximum number of steady states of the associated chemical reaction network.

We give a procedure for computing the Newton-Okounkov body $\Delta(A)$ of a chemical reaction system defined by polynomials $\{f_1, \ldots, f_s\}$, where $f_i \in \mathbb{C}[x_1, \ldots, x_s]$:

Procedure 7.4.1. *Input*: A chemical reaction system defined by polynomials $\{f_1, \ldots, f_s\}$, where $f_i \in \mathbb{C}[x_1, \ldots, x_s]$.

Output: The volume $\mathrm{vol}(\Delta(\mathrm{A}))$ of an associated Newton-Okounkov body $\Delta(A)$.

0. Choose a polynomial generating set P such that each f_i is a $\mathbb{C}$-linear combination of the polynomials of P.

1. Pick a monomial term order $<$.

2. Compute, using `SubalgebraBases.m2`, a SAGBI basis for the subalgebra generated by the set P of polynomials. The input to the `SubalgebraBases.m2` is the generating set P, and the output is a SAGBI basis $\mathcal{B}$.

3. Let A be the subalgebra generated by $\mathcal{B}$. Use Definition 7.3.1 to compute the Newton-Okounkov body $\Delta(A) := \Delta(A, <, \mathcal{B})$ associated to $(A, <, \mathcal{B})$.

4. Output the volume, $\mathrm{vol}(\Delta(\mathrm{A}))$; this is the volume of the Newton-Okounkov body of the chemical reaction system defined by the input $\{f_1, \ldots, f_s\}$.

Remark 7.4.2. In our examples, in Step 1 of Procedure 7.4.1 we will always select the monomial term order grevlex – graded reverse lexiographic term order. This is `Macaulay2`'s default term order. Then, for Step 3, the leading term for each element of the SAGBI basis $\mathcal{B}$ is its first term: by default, `Macaulay2` outputs monomials in order from greatest to least.

As we saw in Proposition 7.3.3, in general, the volume of the Newton-Okounkov body can improve the mixed volume bound on the maximum number of positive real solutions of a general polynomial system in the associated subalgebra by accounting for algebraic dependencies among the defining polynomials. The algebraic relationships among the polynomials of F will guide our choice of a generating set P from Step 0 of Procedure 6.6.4 for an algebra containing F.

At the moment choosing this generating set is a bit of an art. For instance, when the rate constants κ_i (i.e., the coefficients of each monomial in the system F) of a chemical reaction system are arbitrary, then we will take the generating set P to be the set of all monomials of the system F. We describe guiding principles for the choice of P when rate constants are fixed or some relationship between rate constants is imposed through the examples in Section 7.5.

7.5 Examples

In this section, we apply Procedure 7.4.1 to compute Newton-Okounkov bodies for chemical reaction systems. For each example, we investigate the bounds from Proposition 7.3.2, and we show that the volume of a network's Newton-Okounkov body gives a good bound on its maximum number of steady states.

Example 7.5.1. Networks with infinitely many positive steady states in a compatibility class were investigated in [11]. These networks were the first such weakly reversible networks discovered, and [11] showed that these networks have infinitely many positive steady states defined by a curve of steady states arising from a common factor of the individual ODEs. However, in general, the number of *isolated* (complex) solutions of these networks is small.

Consider the chemical reaction network in Figure 7.1 from [11, Example 4.1].

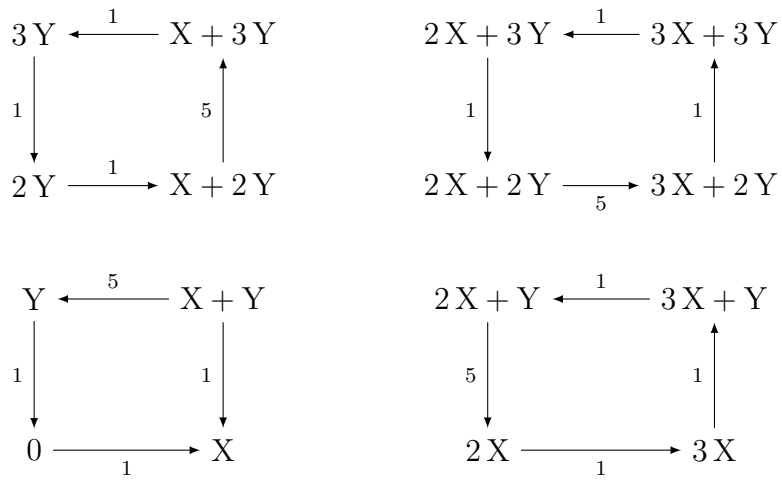

Figure 7.1: A chemical reaction network with infinitely many positive steady states.

The corresponding mass-action system is given by:

$$\begin{cases} \dot{x} = (x^2y^2 + x^2 + y^2 + 1 - 5xy)[1 - xy] \\ \dot{y} = (x^2y^2 + x^2 + y^2 + 1 - 5xy)[x - y] \, . \end{cases}$$

The set of positive steady states consists of the non-isolated points (x, y) on the curve $x^2y^2 + x^2 + y^2 + 1 - 5xy = 0$, and the only isolated solution that is positive is the steady state $(1, 1)$ ([11]). Notice that there is one more complex (non-positive) solution, namely $(-1, -1)$.

Let $p_1 := x^2y^2 + x^2 + y^2 + 1 - 5xy$ (the common factor of the two polynomials in the system), and let $p_2 := 1$, $p_3 := xy$, $p_4 := x$, $p_5 := y$ (these are the monomials in the factors remaining). Notice that $\dot{x} = p_1(p_2 - p_3)$ and $\dot{y} = p_1(p_4 - p_5)$.

Let $\mathcal{B} = \{p_1p_2,\ p_1p_3,\ p_1p_4,\ p_1p_5\}$, so that $\dot{x}, \dot{y} \in A$. Using `SubalgebraBases.m2`[2] we confirm that $\mathcal{B}$ is a SAGBI basis for A.

Taking exponent vectors of the leading terms with respect to grevlex (see Remark 7.4.2) of the elements of $\mathcal{B}$, we get $(2, 2)$, $(2, 3)$, $(3, 2)$, and $(3, 3)$. Then $\Delta(A)$ is a square with $2!\,\mathrm{vol}(\Delta(\mathrm{A})) = 2$, which is *equal* to the number of isolated (complex) solutions of the polynomial system. (Recall that by Proposition 7.3.2, $\mathrm{vol}(\Delta(\mathrm{A}))$ is an *upper bound* on the number of isolated complex solutions.) In contrast, by Definition 6.2.3, the augMV is 18. We already saw that the maximum number of isolated positive steady states is 1.

We summarize the bounds for this network in Table 7.1. The mixed volume bound is computed using PHCpack as in the proof of Proposition 6.3.4 and Procedure 6.4.12. The code used to compute the SAGBI basis $\mathcal{B}$ can be found in Appendix D.

max number steady states	max number $\mathbb{C}$-steady-states	mixed volume bound	Newton-Okounkov body bound
1	2	18	2

Table 7.1: The various root counts associated to the system in Example 7.5.1.

This is a great example of the volume of the Newton-Okounkov body achieving a tighter bound

[2]When computing a SAGBI basis using `SubalgebraBases.m2`, we get $p_1p_2,\ p_1p_4,\ p_1p_5$ and one more generator which is not equal to p_1p_3. However, since this last generator has the same leading term as p_1p_3, the resulting Newton-Okounkov body is identical.

than the mixed volume: the mixed-volume overcount is $18 - 1 = 17$, but the analogous *Newton-Okounkov overcount* is $2 - 1 = 1$.

Example 7.5.2. Consider the chemical reaction system defined by the following system of ODEs[3]:

$$\begin{cases} \dot{x} = k_1(x^2 + y^2) - k_2 x + k_3 \\ \dot{y} = k_1(x^2 + y^2) - k_4 y + k_5 \ . \end{cases}$$

where $k_i \in \mathbb{R}_{>0}$. We note here that some information is known about the rate constants: in particular, the coefficients of $(x^2 + y^2)$ in $\dot{x}$ and $\dot{y}$ are equal.

In this small example, we can explicitly compute the maximum number of complex solutions. Geometrically the system defines the intersection of two circles, so the system has at most 2 complex solutions. Moreover, we produce a witness for two positive, real solutions by taking $k_1 = 1,\ k_2 = 8,\ k_3 = 7,\ k_4 = 6,\ k_5 = 3$. In other words, the maximum number of steady states for the associated chemical reaction system is 2.

Let $\mathcal{B} = \{1, x, y, x^2 + y^2\}$ generate an associated subalgebra A. The exponent vectors of the leading monomials of the elements of $\mathcal{B}$ are $(0,0), (1,0), (0,1)$, and $(2,0)$. Then $\Delta(A)$ is a triangle, and $2!\,\mathrm{vol}(\Delta(\mathrm{A})) = 2$.

Notice that any system in A has the form

$$\begin{cases} \kappa_1(x^2 + y^2) + \kappa_2 y + \kappa_3 x + \kappa_4 = 0 \\ \kappa_5(x^2 + y^2) + \kappa_6 y + \kappa_7 x + \kappa_8 = 0 \ . \end{cases}$$

with $\kappa_i \in \mathbb{C}$. Thus, the mixed volume of a system in A is 4. However, any such generic system has exactly 2 solutions, since, the system defines the intersection of two circles. In other words, the maximum number of complex-number steady states is equal to the Newton-Okounkov body bound.

[3]This mass-action system can be obtained from a chemical reaction network since each defining polynomial is of the shape $f_\ell = p_\ell - x_\ell q_\ell$ for real polynomials $p_\ell,\ q_\ell$ with nonnegative coefficients [55].

We summarize the bounds for this network in Table 7.2. The mixed volume bound is computed using PHCpack as in the proof of Proposition 6.3.4 and Procedure 6.4.12. The code used to compute the SAGBI basis $\mathcal{B}$ can be found in Appendix D.

max number steady states	max number $\mathbb{C}$-steady-states	mixed volume bound	Newton-Okounkov body bound
2	2	4	2

Table 7.2: The various root counts associated to the system in Example 7.5.2.

7.6 Discussion

Theory dictates that the volume of the Newton-Okounkov body associated to a polynomial subalgebra bounds the number of isolated solutions to a general polynomial system in the linear span of a SAGBI basis for that subalgebra. However, in practice, very few examples of Newton-Okounkov bodies have been computed.

In this chapter, we defined the first notion of a Newton-Okounkov body of a chemical reaction system, and gave a procedure for computing this body (Procedure 7.4.1). Applying this procedure on concrete examples, we showed that the volume of the Newton-Okounkov body of a chemical reaction network improves the mixed volume bound (Section 7.5). These examples provide a proof-of-concept for our new method. In summary, the Newton-Okounkov body is a promising new tool for achieving our ultimate goal of tight bounds on the number of steady states of an arbitrary reaction network.

8. CONCLUSIONS AND FUTURE DIRECTIONS

In this chapter, we propose future research directions and projects arising from the results in this dissertation.

8.1 Oscillations in ERK networks

In Chapter 4, we showed that bistability and oscillations persist in certain subnetworks of the ERK network. However, the ERK network is just one of hundreds of models of the ERK pathway. Accordingly, we ask whether other models of the ERK pathway exhibit these dynamics. As a start, we propose to investigate oscillations.

Problem 8.1.1. *For which parameters and subnetworks are there oscillations in arbitrary models of the ERK pathway?*

The Newton-polytope method sets up a framework for constructing a Hopf bifurcation, if one exists (see Algorithm 4.3.4). However, even for the relatively simple full ERK network (Figure 3.1), the associated computation was infeasible to solve in its general state (too many variables and parameters). For this project, we propose to begin with the more modest goal of understanding all cone regions where the Newton-polytope method applies for select *subnetworks* of the ERK network, which makes the problem computationally tractable. Then, we need to develop conditions to "lift" our results to the full ERK network, following in the spirit of [49].

In theory, the Newton-polytope method is a general method for finding a positive solution to any system of polynomial inequalities, and hence can be used to apply any stability criterion described by a semialgebraic set, e.g., the Liénard–Chipart criterion [73]. Furthermore, this method currently requires preprocessing and multiple software programs. We propose to streamline this:

Problem 8.1.2. *(a) Improve the Newton-polytope method to include other stability criterion.*
(b) Implement the Newton-polytope method in a single software package.

The outcome of this implementation will be an efficient technique for solving Problem 8.1.1 for arbitrary ERK pathway models and arbitrary dynamics. The biological implication is a better

insight into and comparison of ERK pathway models. For instance, scientists will be equipped to uncover possible dynamics without the need for lab experiments. Also, knowing what dynamics a particular model is capable of can help scientists decide whether it is consistent with limited experimental data.

8.2 Global parameter space analysis

A comprehensive mathematical framework for studying pathway models must allow for noise, e.g., inexact or immeasurable parameters. Furthermore, biologists require methods for analyzing the massive multidimensional data sets from lab experiments on (parts of) the ERK pathway. Both challenges could be tackled by analyzing the global parameter space.

Recently, [54, 76] combined numerical algebraic methods with random sampling to understand how parameter space decomposes into regions having different possible dynamics, for a particular class of networks. Their focus was understanding the parameter geography with respect to multiple steady states, noting that the more refined question incorporating stability of steady states is more difficult. We pose this next, harder problem.

Problem 8.2.1. *Decompose parameter space of the ERK network (and its subnetworks) into regions by its corresponding dynamics. How does the resulting parameter geography inform the robustness of the dynamics?*

This project further answers the question of robustness of oscillations and bistability in the ERK network. The first part of this problem is precisely Problem 8.1.1, when we restrict to only considering Hopf bifurcations. Next, we propose to investigate the parameter geography by analyzing topological properties of various regions. Understanding the geometry and topology of a region will allow us to incorporate noise into a model and still accurately predict its dynamics: if perturbations of parameter values leave it in the same region, then the dynamics will be the same.

Discriminant locus methods [54] and the Newton-polytope method [78] both stratify the parameter space.

Problem 8.2.2. *Overlay the stratifications of parameter space for the ERK network under the*

discriminant locus method and Newton-polytope methods. What does this imply about the co-existence of multistationarity and Hopf bifurcations for this network (c.f., Section 5.3)?

Once we have a stratification, we propose an approach to investigate the parameter geography using topological properties of the stratified space.

One approach is to consider the real monodromy structure [56] – an invariant for a parametrized polynomial system that encodes the structure of its real solutions over parameter space – of ERK pathway models. In a toy example, we showed that this accurately tracks the change in the number of real steady states of a small reaction network as parameters vary. What can be said about the change in dynamics as we move through parameter space?

8.3 Mixed volume of polynomial dynamical systems

As discussed in Chapter 6, multistationarity has implications in cellular decision-making [42, 72, 80], and our new notion of a network's mixed volume is a parameter-free construction that gives good upper bounds on the number of steady states for select signalling networks. In particular, when a network's mixed volume is equal to the maximum number of steady states, the mixed volume precisely calculates this number and decides multistationarity.

Recall, from Definition 6.2.3, that we defined the mixed volume of a network G with respect to a conservation-law matrix W. We suspect that this definition can be relaxed:

Problem 8.3.1. *Show that mixed volume of a network G does not depend on the choice of conservation-law matrix W.*

For the ERK network, the mixed volume appeared to give a measure of complexity in the network: the mixed volume dropped as dynamical properties were lost (see Table 6.1). We ask whether this phenomena holds for other ERK models: how does mixed volume describe complexity of polynomial dynamical systems?

Problem 8.3.2. *Define and compute the mixed volume of general dynamical systems, e.g. using the fact that any system of ordinary differential equations can be linearized (by its Jacobian matrix).*

There are two immediate challenges: (1) the mixed volume computation complexity grows exponentially with the number of polynomials [52], and (2) there is no theory to discern how tight the mixed volume upper bound is on the number of steady states for arbitrary systems.

As mixed volume is efficient to calculate for small networks, we propose to begin here with small polynomial dynamical systems, as was [66]'s approach for multistationarity.

The next proposed problem aims to create a database of small networks with fixed mixed volume. We will then use this database to understand how network operations – like adding intermediate species or cross-talk – affect the number of steady states, an open question posed in [49].

Problem 8.3.3. *(a) Apply [2]'s classification of polytopes with a given mixed volume to create a mixed-volume poset of small chemical reaction networks. (b) How do network operations affect mixed volume and the number of steady states?*

For challenge (2), note that counting positive roots of (parametrized) polynomial systems is a hard problem in real algebraic geometry. One approach is to generalize Procedure 6.4.12 for lifting *positive real points* in the variety of the first elimination ideal to positive points in the variety defined by the polynomial system. The upshot of this generalized procedure is an efficient algebro-geometric method for counting (positive) steady states. However, this approach is computationally challenging, as it requires a generalization of Gaussian elimination for polynomial systems.

Finally, we recall from Section 6.6 the discussion of several related definitions of mixed volume for reaction networks. In particular, we would like a single unifying definition of mixed volume for reaction networks that incorporates steady-state parametrizations, so that a tight bound on the maximum number of steady states is achieved; see Procedure 6.6.4 and Question 6.6.7 that follows it.

8.4 Newton-Okounkov bodies of chemical reaction networks

In Chapter 7, we introduced a Newton-Okounkov body of a chemical of reaction network. Specifically, Procedure 7.4.1 detailed a method for computing a Newton-Okounkov body for a chemical reaction system. However, the resulting Newton-Okounkov body is not well-defined.

There are a number of choices (including choice of term order and choice of a generating set G for a SAGBI basis) made in Procedure 7.4.1 that can potentially yield different associated Newton-Okounkov bodies. The next problem concerns these choices. We would like one well-defined definition of a Newton-Okounkov body, or at least some detailed guiding principles for how best to define one to achieve the tightest bound.

Problem 8.4.1. *In Procedure 7.4.1,*

(a) How does the choice of term order $<$ affect the resulting Newton-Okounkov body of a chemical reaction system?

(b) Under which hypotheses on a generating set G does the associated Newton-Okounkov body give the tightest bound on the maximum number of steady states of a chemical reaction system?

REFERENCES

[1] D. ANGELI, P. DE LEENHEER, AND E. SONTAG, *A Petri net approach to persistence analysis in chemical reaction networks*, Springer-Verlag, Berlin, 2007, pp. 181–216.

[2] G. AVERKOV, C. BORGER, AND I. SOPRUNOV, *Classification of triples of lattice polytopes with a given mixed volume*, Discrete Comput. Geom., (2020).

[3] C. P. BAGOWSKI AND J. E. FERRELL, *Bistability in the JNK cascade*, Curr. Biol., 11 (2001), pp. 1176–1182.

[4] M. BANAJI, *Counting chemical reaction networks with NAUTY*, Preprint, `arXiv:1705.10820`, (2017).

[5] M. BANAJI, *Inheritance of oscillation in chemical reaction networks*, Appl. Math. Comput., 325 (2018), pp. 191–209.

[6] M. BANAJI AND C. PANTEA, *Some results on injectivity and multistationarity in chemical reaction networks*, SIAM J. Appl. Dyn. Syst., 15 (2016), pp. 807–869.

[7] ——, *The inheritance of nondegenerate multistationarity in chemical reaction networks*, SIAM J. Appl. Math., 78 (2018), pp. 1105–1130.

[8] D. N. BERNSHTEIN, *The number of roots of a system of equations*, Funct. Anal. Appl+, 9 (1975), p. 183.

[9] U. S. BHALLA, P. T. RAM, AND R. IYENGAR, *MAP kinase phosphatase as a locus of flexibility in a mitogen-activated protein kinase signaling network*, Science, 297 (2002), pp. 1018–1023.

[10] F. BIHAN AND I. SOPRUNOV, *Criteria for strict monotonicity of the mixed volume of convex polytopes*, Adv. Geom., 19 (2019), pp. 527–540.

[11] B. BOROS, G. CRACIUN, AND P. Y. YU, *Weakly reversible mass-action systems with infinitely many positive steady states*, Preprint, `arXiv:1912.10302`, (2019).

[12] P. BREIDING AND S. TIMME, *Homotopycontinuation.jl: A package for homotopy continuation in Julia*, in Mathematical Software – ICMS 2018, J. H. Davenport, M. Kauers,

G. Labahn, and J. Urban, eds., Springer, 2018, pp. 458–465.

[13] M. BURR, F. SOTTILE, AND E. WALKER, *Numerical homotopies from Khovanskii bases*, Preprint, arXiv:2008.13055, (2020).

[14] R. BUSCÁ, J. POUYSSÉGUR, AND P. LENORMAND, *ERK1 and ERK2 map kinases: Specific roles or functional redundancy?*, Front. Cell Dev. Biol., 4:53 (2016).

[15] D. CAPPELLETTI, E. FELIU, AND C. WIUF, *Addition of flow reactions preserving multistationarity and bistability*, Math. Biosci., 320 (2020), p. 108295.

[16] D. CAPPELLETTI AND C. WIUF, *Uniform approximation of solutions by elimination of intermediate species in deterministic reaction networks*, SIAM J. Appl. Dyn. Syst., 16 (2017), pp. 2259–2286.

[17] L. CHANG AND M. KARIN, *Mammalian MAP kinase signalling cascades*, Nature, 410 (2001), pp. 37–40.

[18] T. CHEN, R. DAVIS, AND D. MEHTA, *Counting equilibria of the kuramoto model using birationally invariant intersection index*, SIAM J. Appl. Algebra and Geom., 2 (2017).

[19] P. COHEN, *The regulation of protein function by multisite phosphorylation–a 25 year update*, Trends Bioch. Sci., 25 (2000), pp. 596–601.

[20] C. CONRADI, E. FELIU, AND M. MINCHEVA, *On the existence of Hopf bifurcations in the sequential and distributive double phosphorylation cycle*, Math. Biosci. Eng., 17 (2020), pp. 494–513.

[21] C. CONRADI, E. FELIU, M. MINCHEVA, AND C. WIUF, *Identifying parameter regions for multistationarity*, PLoS Comput. Biol., 13 (2017), p. e1005751.

[22] C. CONRADI, A. IOSIF, AND T. KAHLE, *Multistationarity in the space of total concentrations for systems that admit a monomial parametrization*, B. Math. Biol., 81 (2019).

[23] C. CONRADI, M. MINCHEVA, AND A. SHIU, *Emergence of oscillations in a mixed-mechanism phosphorylation system*, B. Math. Biol., 81 (2019), pp. 1829–1852.

[24] C. CONRADI, N. OBATAKE, A. SHIU, AND X. TANG, *Dynamics of erk regulation in the processive limit*, J. Math. Biol., 82 (2021), p. 32.

[25] C. CONRADI AND A. SHIU, *A global convergence result for processive multisite phosphorylation systems*, B. Math. Biol., 77 (2015), pp. 126–155.

[26] ——, *Dynamics of post-translational modification systems: recent progress and future challenges*, Biophys. J., 114 (2018), pp. 507–515.

[27] D. A. COX, J. LITTLE, AND D. O'SHEA, *Ideals, Varieties, and Algorithms: An Introduction to Computational Algebraic Geometry and Commutative Algebra, 3/e (Undergraduate Texts in Mathematics)*, Springer-Verlag, Berlin, Heidelberg, 2007.

[28] G. CRACIUN AND M. FEINBERG, *Multiple equilibria in complex chemical reaction networks: extensions to entrapped species models*, IEE P. Syst. Biol., 153 (2006), pp. 179–186.

[29] G. CRACIUN, Y. TANG, AND M. FEINBERG, *Understanding bistability in complex enzyme-driven reaction networks*, P. Natl. Acad. Sci. USA, 103 (2006), pp. 8697–8702.

[30] A. DHOOGE, W. GOVAERTS, AND Y. A. KUZNETSOV, *Matcont: A matlab package for numerical bifurcation analysis of odes*, ACM T. Math. Software, 29 (2003), p. 141–164.

[31] A. DICKENSTEIN, *Biochemical reaction networks: an invitation for algebraic geometers*, vol. 656 of Contemp. Math., American Mathematical Society, 2016.

[32] ——, *Biochemical reaction networks: An invitation for algebraic geometers*, in Contemp. Math., vol. 656, American Mathematical Soc., 2016, pp. 65–83.

[33] A. DICKENSTEIN, M. PÉREZ MILLÁN, A. SHIU, AND X. TANG, *Multistationarity in structured reaction networks*, B. Math. Biol., 81 (2019), pp. 1527–1581.

[34] J. DISTEFANO III, *Dynamic systems biology modeling and simulation*, Academic Press, 2013.

[35] M. EITHUN AND A. SHIU, *An all-encompassing global convergence result for processive multisite phosphorylation systems*, Math. Biosci., 291 (2017), pp. 1–9.

[36] G. EWALD, *Combinatorial convexity and algebraic geometry*, vol. 168 of Graduate Texts in Mathematics, Springer-Verlag, New York, 1996.

[37] M. FEINBERG, *Dynamics and Modelling of Reactive Systems*, Academic Press, 1980, ch. Chemical oscillations, multiple equilibria, and reaction network structure, pp. 59–130.

[38] M. FEINBERG, *Foundations of chemical reaction network theory*, vol. 202 of Appl. Math. Sci., Springer, Cham, 2019.

[39] E. FELIU, C. LAX, S. WALCHER, AND C. WIUF, *Quasi-steady state and singular perturbation reduction for reaction networks with non-interacting species*, Preprint, arXiv:1908.11270, (2019).

[40] E. FELIU AND C. WIUF, *Simplifying biochemical models with intermediate species*, J. R. Soc. Interface, 10 (2013).

[41] ——, *Simplifying biochemical models with intermediate species*, J. R. Soc. Interface, 10 (2013).

[42] ——, *Finding the positive feedback loops underlying multistationarity*, BMC Syst. Biol., 9 (2015), p. 22.

[43] A. S. FUTRAN, A. J. LINK, R. SEGER, AND S. Y. SHVARTSMAN, *ERK as a model for systems biology of enzyme kinetics in cells*, Curr. Biol., 23 (2013), pp. R972–R979.

[44] K. GATERMANN, *Applications of sagbi-bases in dynamics*, J. Symb. Comput., 35 (2003), pp. 543–575. Computer Algebra and Computer Analysis.

[45] M. GIAROLI, F. BIHAN, AND A. DICKENSTEIN, *Regions of multistationarity in cascades of Goldbeter–Koshland loops*, J. Math. Biol., (2018).

[46] M. GIAROLI, R. RISCHTER, M. PÉREZ MILLÁN, AND A. DICKENSTEIN, *Parameter regions that give rise to* $2\lfloor n/2 \rfloor + 1$ *positive steady states in the n-site phosphorylation system*, Math. Biosci. Eng., 16 (2019), pp. 7589–7615.

[47] D. J. GRABINER, *Descartes' rule of signs: Another construction*, Am. Math. Mon., 106 (1999), pp. 854–856.

[48] D. R. GRAYSON AND M. E. STILLMAN, *Macaulay2, a software system for research in algebraic geometry*. Available at http://www.math.uiuc.edu/Macaulay2/.

[49] E. GROSS, H. HARRINGTON, N. MESHKAT, AND A. SHIU, *Joining and decomposing reaction networks*, J. Math. Biol., 80 (2020), pp. 1683–1731.

[50] E. GROSS, H. A. HARRINGTON, Z. ROSEN, AND B. STURMFELS, *Algebraic systems*

biology: A case study for the Wnt pathway, B. Math. Biol., 78 (2016), pp. 21–51.

[51] E. GROSS AND C. HILL, *Steady state degree and mixed volume of chemical reaction networks*, Preprint, arXiv:1909.06652, (2019).

[52] E. GROSS, S. PETROVIC, AND J. VERSCHELDE, *PHCpack in Macaulay2*, The Journal of Software for Algebra and Geometry: Macaulay2, 5 (2013), pp. 20–25.

[53] O. HADAČ, F. MUZIKA, V. NEVORAL, M. PŘIBYL, AND I. SCHREIBER, *Minimal oscillating subnetwork in the Huang-Ferrell model of the MAPK cascade*, PLOS One, 12 (2017), pp. 1–25.

[54] H. A. HARRINGTON, D. MEHTA, H. M. BYRNE, AND J. D. HAUENSTEIN, *Decomposing the parameter space of biological networks via a numerical discriminant approach*, in Maple in Mathematics Education and Research, J. Gerhard and I. Kotsireas, eds., Cham, 2020, Springer International Publishing, pp. 114–131.

[55] V. HÁRS AND J. TÓTH, *On the inverse problem of reaction kinetics*, Colloq. Math. Soc. J. B, 30 (1981), pp. 363–379.

[56] J. D. HAUENSTEIN AND M. H. REGAN, *Real monodromy action*, Appl. Math. Comput., 373 (2020).

[57] J. HELL AND A. D. RENDALL, *Sustained oscillations in the map kinase cascade*, Math. Biosci., 282 (2016), pp. 162–173.

[58] R. D. HERNANSAIZ-BALLESTEROS, L. CARDELLI, AND A. CSIKÁSZ-NAGY, *Single molecules can operate as primitive biological sensors, switches and oscillators*, BMC Syst. Biol., 12 (2018), p. 70.

[59] Z. HILIOTI, W. SABBAGH, S. PALIWAL, A. BERGMANN, M. D. GONCALVES, L. BARDWELL, AND A. LEVCHENKO, *Oscillatory phosphorylation of yeast Fus3 MAP kinase controls periodic gene expression and morphogenesis*, Curr. Biol., 18 (2008), pp. 1700–1706.

[60] F. HORN, *Necessary and sufficient conditions for complex balancing in chemical kinetics*, Arch. Ration. Mech. An., 49 (1972/73), pp. 172–186.

[61] F. HORN AND R. JACKSON, *General mass action kinetics*, Arch. Ration. Mech. An., 47

(1972), pp. 81–116.

[62] H. HU, A. GOLTSOV, J. L. BOWN, A. H. SIMS, S. P. LANGDON, D. J. HARRISON, AND D. FARATIAN, *Feedforward and feedback regulation of the MAPK and PI3K oscillatory circuit in breast cancer*, Cell. Signal., 25 (2013), pp. 26–32.

[63] M. D. JOHNSTON, S. MÜLLER, AND C. PANTEA, *A deficiency-based approach to parametrizing positive equilibria of biochemical reaction systems*, B. Math. Biol., 81 (2019), pp. 1143–1172.

[64] B. JOSHI AND A. SHIU, *Atoms of multistationarity in chemical reaction networks*, J. Math. Chem., 51 (2013), pp. 153–178.

[65] ——, *A survey of methods for deciding whether a reaction network is multistationary*, Math. Model. Nat. Pheno., special issue on "Chemical dynamics", 10 (2015), pp. 47–67.

[66] ——, *Which small reaction networks are multistationary?*, SIAM J. Appl. Dyn. Syst., 16 (2017), pp. 802–833.

[67] K. KAVEH AND A. G. KHOVANSKII, *Newton-okounkov bodies, semigroups of integral points, graded algebras and intersection theory*, Ann. Math., 176 (2012), pp. 925–978.

[68] K. KAVEH AND C. MANON, *Khovanskii bases, higher rank valuations, and tropical geometry*, SIAM J. Appl. Algebra and Geom., 3 (2019), pp. 292–336.

[69] V. KIRITCHENKO, E. SMIRNOV, AND V. TIMORIN, *Ideas of newton-okounkov bodies*, Snapshots of modern mathematics from Oberwolfach, (2015).

[70] Y. A. KUZNETSOV, *Elements of applied bifurcation theory*, vol. 112, Springer Science & Business Media, 1995.

[71] R. LAZARSFELD AND M. MUSTA¸TĂ, *Convex bodies associated to linear series*, Ann. Sci. Ecole Norm. S., Ser. 4, 42 (2009), pp. 783–835.

[72] S. LEGEWIE, N. BLÜTHGEN, R. SCHÄFER, AND H. HERZEL, *Ultrasensitization: Switch-like regulation of cellular signaling by transcriptional induction*, PLOS Comput. Biol., 1 (2005), pp. 1–10.

[73] A. LIÉNARD AND M. H. CHIPART, *Sur la signe de la partie réelle des racines d'une*

équation algébrique, J. Math. Pure Appl., 10 (1914), pp. 291–346.

[74] M. MARCONDES DE FREITAS, E. FELIU, AND C. WIUF, *Intermediates, catalysts, persistence, and boundary steady states*, J. Math. Biol., 74 (2017), pp. 887–932.

[75] S. MÜLLER, E. FELIU, G. REGENSBURGER, C. CONRADI, A. SHIU, AND A. DICKENSTEIN, *Sign conditions for injectivity of generalized polynomial maps with applications to chemical reaction networks and real algebraic geometry*, Found. Comput. Math., 16 (2016), pp. 69–97.

[76] K.-M. NAM, B. M. GYORI, S. V. AMETHYST, D. J. BATES, AND J. GUNAWARDENA, *Robustness and parameter geography in post-translational modification systems*, PLOS Comput. Biol., 16 (2020), pp. 1–50.

[77] N. OBATAKE, A. SHIU, AND D. SOFIA, *Mixed volume of small reaction networks*, Involve: A Journal of Mathematics, 13 (2020), pp. 845 – 860.

[78] N. OBATAKE, A. SHIU, X. TANG, AND A. TORRES, *Oscillations and bistability in a model of ERK regulation*, J. Math. Biol., 79 (2019), pp. 1515–1549.

[79] K. L. ODE AND H. R. UEDA, *Design principles of phosphorylation-dependent timekeeping in eukaryotic circadian clocks*, Cold Spring Harbor Perspectives in Biology, (2017).

[80] S. PALANI AND C. A. SARKAR, *Synthetic conversion of a graded receptor signal into a tunable, reversible switch*, Mol. Syst. Biol., 7 (2011), p. 480.

[81] M. PÉREZ MILLÁN, A. DICKENSTEIN, A. SHIU, AND C. CONRADI, *Chemical reaction systems with toric steady states*, B. Math. Biol., 74 (2012), pp. 1027–1065.

[82] A. PLOTNIKOV, E. ZEHORAI, S. PROCACCIA, AND R. SEGER, *The MAPK cascades: signaling components, nuclear roles and mechanisms of nuclear translocation*, BBA-Mol. Cell. Res., 1813 (2011), pp. 1619–1633.

[83] S. RAO, *Global stability of a class of futile cycles*, J. Math. Biol., 74 (2017), pp. 709–726.

[84] L. ROBBIANO AND M. SWEEDLER, *Subalgebra bases*, in Commutative algebra, Springer, 1990, pp. 61–87.

[85] J. M. ROJAS, *A convex geometric approach to counting the roots of a polynomial system*,

Theor. Comput. Sci., 133 (1994), pp. 105–140.

[86] B. Y. RUBINSTEIN, H. H. MATTINGLY, A. M. BEREZHKOVSKII, AND S. Y. SHVARTSMAN, *Long-term dynamics of multisite phosphorylation*, Mol. Biol. Cell, 27 (2016), pp. 2331–2340.

[87] A. SADEGHIMANESH AND E. FELIU, *The multistationarity structure of networks with intermediates and a binomial core network*, B. Math. Biol., 81 (2019), pp. 2428–2462.

[88] ——, *The multistationarity structure of networks with intermediates and a binomial core network*, B. Math. Biol., 81 (2019), pp. 2428–2462.

[89] C. SALAZAR AND T. HÖFER, *Multisite protein phosphorylation – from molecular mechanisms to kinetic models*, FEBS J., 276 (2009), pp. 3177–3198.

[90] Y. D. SHAUL AND R. SEGER, *The MEK/ERK cascade: From signaling specificity to diverse functions*, BBA-Mol. Cell. Res., special issue on "Mitogen-Activated Protein Kinases: New Insights on Regulation, Function and Role in Human Disease", 1773 (2007), pp. 1213–1226.

[91] A. SHIU AND B. STURMFELS, *Siphons in chemical reaction networks*, B. Math. Biol., 72 (2010), pp. 1448–1463.

[92] F. SOTTILE, *Real Solutions to Equations from Geometry*, University lecture series, American Mathematical Society, 2011.

[93] M. STILLMAN AND H. TSAI, *Using sagbi bases to compute invariants*, J. Pure Appl. Algebra, 139 (1999), pp. 285–302.

[94] S. H. STROGATZ, *Nonlinear Dynamics and Chaos: With Applications to Physics, Biology, Chemistry and Engineering*, Westview Press, 2000.

[95] B. STURMFELS, *Grobner Bases and Convex Polytopes*, Memoirs of the American Mathematical Society, American Mathematical Society, 1996.

[96] B. STURMFELS, *Algorithms in Invariant Theory (Texts and Monographs in Symbolic Computation)*, Springer Publishing Company, Incorporated, 2nd ed.; vii, 197 pp.; 5 figs. ed., 2008.

[97] J. SUN, M. YI, L. YANG, W. WEI, Y. DING, AND Y. JIA, *Enhancement of tunability of mapk cascade due to coexistence of processive and distributive phosphorylation mechanisms*, Biophys. J., 106 (2014), pp. 1215–1226.

[98] T. SUWANMAJO AND J. KRISHNAN, *Mixed mechanisms of multi-site phosphorylation*, J. R. Soc. Interface, 12 (2015).

[99] X. TANG AND J. WANG, *Bistability of sequestration networks*, Discrete Cont. Dyn.-B, 26 (2021), pp. 1337–1357.

[100] M. THOMSON AND J. GUNAWARDENA, *The rational parameterisation theorem for multisite post-translational modification systems*, J. Theor. Biol., 261 (2009), pp. 626–636.

[101] A. TORRES AND E. FELIU, *Symbolic proof of bistability in reaction networks*, Preprint, `arXiv:1909.13608`, (2020).

[102] J. J. TYSON, R. ALBERT, A. GOLDBETER, P. RUOFF, AND J. SIBLE, *Biological switches and clocks*, J. R. Soc. Interface, 5 (2008), pp. S1–S8.

[103] D. M. VIRSHUP AND D. B. FORGER, *Keeping the beat in the rising heat*, Cell, 137 (2009), pp. 602–604.

[104] L. WANG AND E. SONTAG, *On the number of steady states in a multiple futile cycle*, J. Math. Biol., 57 (2008), pp. 29–52.

[105] C. WIUF AND E. FELIU, *Power-law kinetics and determinant criteria for the preclusion of multistationarity in networks of interacting species*, SIAM J. Appl. Dyn. Syst., 12 (2013), pp. 1685–1721.

[106] X. YANG, *Generalized form of Hurwitz-Routh criterion and Hopf bifurcation of higher order*, Appl. Math. Lett., 15 (2002), pp. 615–621.

[107] G. M. ZIEGLER, *Lectures on polytopes*, vol. 152 of Graduate Texts in Mathematics, Springer-Verlag, New York, 1995.

APPENDIX A

FILES IN THE SUPPORTING INFORMATION FOR CHAPTERS 4 and 6*

Table A.1 lists the files in the Supporting Information, and the result/proof each file supports. All files can be found at the online repository: `https://github.com/neeedz/ERK`.

Name	File type	Result
`ERK-Matcont.txt`	text file with `MATCONT` instructions	Figures 4.2 and 4.3
`irreversibleERK.mw`	`Maple`	Theorem 4.2.6
`reducedERK-noMSS.mw`	`Maple`	Proposition 4.2.5
`reducedERK-hopf.mw`	`Maple`	Theorem 4.2.3
`reducedERK-cones.sws`	`Sage`	Theorem 4.2.3
`ERK-mixedVol.m2`	`PHCPack`	Proposition 6.3.4
`ERK-MaxComplexNumber.nb`	`Mathematica`	Proposition 6.3.4

Table A.1: Supporting Information files and the results they support.

*The material in this appendix is reprinted from [78] by permission from Springer Nature Customer Service Centre GmbH: Springer *Journal of Mathematical Biology* "Oscillations and bistability in a model of ERK regulation", Nida Obatake, Anne Shiu, Xiaoxian Tang, and Angélica Torres, Copyright (2019).

APPENDIX B

FILES IN THE SUPPORTING INFORMATION FOR CHAPTER 5*

Table B.1 lists the files in the Supporting Information, and the result or section each file supports. All files can be found at the online repository: `https://github.com/neeedz/COST`

Name	File type	Result or Section
`minERK-MSS-bistab.mw`	`Maple`	Theorem 5.1.1
`minERK-MSS-bistab.mw`	`Maple`	Section 5.1.2
`redERK-Hopf.mw`	`Maple`	Theorem 5.2.1
`h5pos.nb`	`Mathematica`	Theorem 5.2.1
`nondegen-close-to-1.txt`	`Text*`	Theorem 5.2.1
`redERK-Hopf-all-pk-values.mw`	`Maple`	Proposition 5.2.5
`nondegen-all-process.txt`	`Text*`	Proposition 5.2.5
`min-bistab-ERK-Hopf-and-Bistability.mw`	`Maple`	Section 5.3.2
`maxNUMss.mw`	`Maple`	Section 5.4
`resultant.txt`	`Text`	Section 5.4

Table B.1: Supporting Information files and the results they support. Here, `Text*` indicates an output file from using the `Julia` package `HomotopyContinuation.jl` [12].

B.1 Procedure to study multistationarity numerically

Here we describe the procedure we used in Section 5.1.3 for numerically studying multistationarity in the minimally bistable ERK network at various processivity levels p_k and p_ℓ.

We begin by mirroring the analysis of Section 5.1.2. Specifically, we use the parameters given in (5.5) to study the critical function $C(\kappa, \hat{x})$ for $x_1 = x_2 = T$ and $x_3 = 1$. Due to this choice of κ and $\hat{c}$, the critical function is a (rational) function of p_k, p_ℓ, and T only, i.e., $C(\kappa, \hat{x}) \equiv C(p_k, p_\ell, T)$.

*The material in this appendix is reprinted from [24] by permission from Springer Nature Customer Service Centre GmbH: Springer *Journal of Mathematical Biology* "Dynamics of ERK regulation in the processive limit", Carsten Conradi, Nida Obatake, Anne Shiu, and Xiaoxiang Tang, Copyright (2020).

The numerator is the following polynomial:

$$\begin{aligned} q(p_k, p_\ell, T) = &-p_k\left((3-2p_\ell)p_\ell + p_k\left(1-3p_\ell+2p_\ell^2\right)\right) \\ &+\left(-5p_\ell^2 + p_kp_\ell(-9+11p_\ell) + p_k^3\left(-1+3p_\ell-2p_\ell^2\right) - p_k^2\left(3-3p_\ell+p_\ell^2\right)\right)T \\ &+\left(-8p_\ell^2 + p_kp_\ell(-13+9p_\ell) + p_k^3\left(-1+p_\ell-p_\ell^2\right) + p_k^2\left(-6+2p_\ell+7p_\ell^2\right)\right)T^2 \\ &+\left(-3p_\ell^2 - p_kp_\ell(5+8p_\ell) + p_k^3\left(-4+3p_\ell+p_\ell^2\right) + p_k^2\left(-3-10p_\ell+13p_\ell^2\right)\right)T^3 \\ &+p_k\left((5-8p_\ell)p_\ell + 3p_k\left(1-5p_\ell+p_\ell^2\right) + p_k^2\left(-7+4p_\ell+2p_\ell^2\right)\right)T^4 \\ &+p_k\left(3p_\ell + p_k^2\left(-3-3p_\ell+2p_\ell^2\right) - p_k\left(-2+p_\ell+4p_\ell^2\right)\right)T^5 - 2(-1+p_k)p_k^2p_\ell T^6 \end{aligned} \tag{B.1}$$

As $0 < p_k, p_\ell < 1$, the leading coefficient of $q(p_k, p_\ell, T)$ as a polynomial in T is positive. Next, the steady-state parametrization ϕ from Proposition 3.2.1 is as follows (cf. eq. (3.4)):

$$\begin{aligned} x_1 = T,\ x_2 = T,\ x_3 = 1,\ x_4 = \frac{p_kT^2(1+T)}{p_\ell + p_kp_\ell T},\ x_5 = -\frac{p_k(-1+p_\ell)T(1+T)}{p_\ell + p_kp_\ell T}, \\ x_6 = \frac{T-p_kT}{1+p_kT},\ x_7 = -\frac{(-1+p_k)T(1+T)}{1+p_kT},\ x_8 = -\frac{p_k(-1+p_\ell)T(1+T)}{p_\ell + p_kp_\ell T}, \\ x_9 = \frac{T-p_kT}{1+p_kT},\ x_{10} = -\frac{p_k(-1+p_\ell)(1+T)}{p_\ell + p_kp_\ell T},\ x_{11} = T^2,\ x_{12} = \frac{p_k(1+T)}{p_\ell + p_kp_\ell T} \end{aligned} \tag{B.2}$$

To numerically study multistationarity for p_k, $p_\ell \to 1$, we proceed as follows:

(i) Pick values of $0 < \tilde{p}_k, \tilde{p}_\ell < 1$ and $\tilde{T} > 0$ such that $q(\tilde{p}_k, \tilde{p}_\ell, \tilde{T}) > 0$ (recall eq. (B.1)).

(ii) Substitute into (B.2) the values of $\tilde{p}_k$, $\tilde{p}_\ell$, and $\tilde{T}$ from the previous step to obtain a steady state $\tilde{x}$.

(iii) Compute, using (3.15), the total amounts $\tilde{c}_1$, $\tilde{c}_2$, and $\tilde{c}_3$ at $\tilde{x}$.

(iv) Use `Matcont` with initial condition near $\tilde{x}$ and bifurcation parameter c_2, to obtain a bifurcation curve.

(v) To compare curves corresponding to distinct $\tilde{p}_k$ and $\tilde{p}_\ell$, compute relative concentrations $\frac{x_i}{\tilde{c}_1}$ and $\frac{c_2}{\tilde{c}_2}$ that relate x_i and c_2 to the $\tilde{x}$ and $\tilde{c}_2$ computed in steps (ii) and (iii).

Step (v) is crucial for interpreting the numerical results obtained by the above procedure, because certain total amounts differ by orders of magnitude as p_k, $p_\ell \to 1$, and so it is more meaningful to compare values relative to the reference point $\tilde{x}$ obtained in step (ii).

	Figure 5.3			
p_k	0.1	0.1	0.1	0.1
p_ℓ	0.1	0.5	0.9	0.999
T	2.21958	3.72221	4.98625	5.28023

	Figure 5.4				
p_k	0.5	0.75	0.8	0.85	0.9
p_ℓ	0.9	0.9	0.9	0.9	0.9
T	4.80723	8.59917	10.6576	14.1522	21.2341

Table B.2: Values of p_k, p_ℓ, and T used in Figures 5.3 and 5.4.

	Figure 5.5			
p_k	0.9	0.95	0.98	0.99
p_ℓ	0.9	0.95	0.98	0.99
T	21.2341	43.2027	109.186	219.18

Table B.3: Values of p_k, p_ℓ, and T used in Figure 5.5.

APPENDIX C

SUPPORTING COMPUTATIONS FOR CHAPTER 6

We provide the `Macaulay2` input code to compute the augMV, umxMV, and sspMV for the *full ERK network* from Example 6.6.8.

```
restart;
loadPackage "PHCpack"
---full ERK without effective steady state function
---first the augMV mixed volume for full ERK
---without effective steady state function
R = CC[x1,x2,x3,x4,x5,x6,x7,x8,x9,x10,x11,x12];
f1 = x2+x7+x8+x11-1;
f2 = x3+x4+x5+x6-1;
f3 = x1+x4+x5+x6+x7+x8+x9+x10+x11+x12-1;
f4 = x1*x2-2*x11;
f5 = x10*x2-2*x8;
f6 = x12*x3-2*x4;
f7 = x3*x9-2*x6;
f8 = x10*x3+x4-2*x5;
f9 = x2*x9+x11-2*x7;
f10 = -x10*x2-x10*x3+x5+x8;
f11 = -x12*x3+x4+x7+x8;
f12 = -x2*x9-x3*x9+x6+x7;
mixedVolume({f1,f2,f3,f4,f5,f6,f7,f8,f9,f10,f11,f12})
--- augMV = 7
---Next, the umxMV for full ERK
```

```
---without effective steady state function

F = matrix{{f1,f2,f3,f4,f5,f6,f7,f8,f9,f10,f11,f12}};
F = transpose(F)
M = random(CC^12,CC^12);
F' = M*F;
E = entries F';
mixedVolume(toList(12:E#0#0)) --- umxMV = 13
---Now the sspMV for full ERK without eff ss func
---with x1, x2, x3 free
R = CC[x1,x2,x3];
f1 = 3*x1*x2^2+3*x1*x2*x3+2*x2^2+4*x2*x3-2*x2-4*x3;
f2 = 3*x1*x2^2+3*x1*x2*x3+2*x2*x3+4*x3^2-2*x2-4*x3;
f3 = 6*x1*x2^2*x3+6*x1*x2*x3^2+4*x1*x2^2+7*x1*x2*x3
        +4*x1*x3^2-2*x2*x3-4*x3^2;
mixedVolume({f1,f2,f3}) --- MV = 8
---Now the sspMV for full ERK without eff ss func
---with x2, x3, x4 free
S = CC[x2,x3,x4];
f1 = 2*x2*x3+3*x2*x4+x3^2+3*x3*x4-2*x2-x3;
f2 = 2*x2*x3+3*x2*x4+x3^2+3*x3*x4-2*x2-x3;
f3 = 6*x2^2*x3*x4+6*x2*x3^2*x4-2*x2^2*x3+4*x2^2*x4
        -x2*x3^2+7*x2*x3*x4+4*x3^2*x4;
mixedVolume({f1,f2,f3}) --- MV = 6

---full ERK with effective steady state function
---all rate constants and effective parameters are taken to be 1
```

```
---first the augMV mixed volume of the full ERK system
R = CC[x1,x2,x3,x4,x5,x6,x7,x8,x9,x10,x11,x12];
f1 = -x5+x7;
f2 = x11-x6-x7;
f3 = x4-x5-x8;
f4 = x2+x7+x8+x11-1;
f5 = x3+x4+x5+x6-1;
f6 = x1+x4+x5+x6+x7+x8+x9+x10+x11+x12-1;
f7 = x1*x2-x11;
f8 = x10*x2-x8;
f9 = x12*x3-x4;
f10 = x3*x9-x6;
f11 = -x10*x3+x5-x8;
f12 = -x2*x9-x6+x7;
mixedVolume({f1,f2,f3,f4,f5,f6,f7,f8,f9,f10,f11,f12})
--- augMV = 7
---Now the umxMV for fullERK with effective steady state function
R = CC[x1,x2,x3,x4,x5,x6,x7,x8,x9,x10,x11,x12];
M = random(CC^12,CC^12);
fullERK = matrix{{f1,f2,f3,f4,f5,f6,f7,f8,f9,f10,f11,f12}};
fullERKmat = transpose(fullERK);
P = M * fullERKmat;
randpoly = (entries P)#0#0
mixedVolume(toList(12:randpoly)) --- umxMV = 13
---Next sspMV using the steady state parameterization
---with x1, x2, x3 free
R = CC[x1,x2,x3];
```

```
f1 = 3*x1*x2^2+3*x1*x2*x3+x2*x3+2*x3^2-x2-2*x3;
f2 = 3*x1*x2^2+3*x1*x2*x3+x2^2+2*x2*x3-x2-2*x3;
f3 = 6*x1*x2^2*x3+6*x1*x2*x3^2+2*x1*x2^2+4*x1*x2*x3
        +2*x1*x3^2-x2*x3-2*x3^2;
mixedVolume({f1,f2,f3}) --- MV = 8
---Now sspMV using the steady state parametrization
---with x2, x3, x4 free
R = CC[x2,x3,x4];
f1 = 2*x2^2+x2*x3+3*x2*x4+3*x3*x4-2*x2-x3;
f2 = 2*x2*x3+3*x2*x4+x3^2+3*x3*x4-2*x2-x3;
f3 = 6*x2^2*x3*x4+6*x2*x3^2*x4-2*x2^2*x3
        +2*x2^2*x4-x2*x3^2+4*x2*x3*x4+2*x3^2*x4;
mixedVolume({f1,f2,f3}) --- MV = 8
```

The following code supports the computations of the augMV, umxMV, and sspMV for the *reduced ERK network* in Example 6.6.8.

```
restart;
loadPackage "PHCpack"

---reduced ERK with effective steady state function
---first the augMV mixed volume for the red ERK with eff ss func
S = CC[x1,x2,x3,x4,x5,x6,x7,x8,x9,x10];
f1 = x3-2*x4;
f2 = x4-x10;
f3 = x9-2*x10;
f4 = x2+x3+x4-1;
f5 = x8+x9+x10-1;
f6 = x1+x3+x4+x5+x6+x7+x9+x10-1;
```

```
f7 = x1*x2-2*x10;
f8 = -x2*x7+x10;
f9 = x5*x8-2*x10;
f10 = -x6*x8+x10;
mixedVolume({f1,f2,f3,f4,f5,f6,f7,f8,f9,f10}) --- augMV = 3

---Next the umxMV for red ERK with eff ss func
F = matrix{{f1},{f2},{f3},{f4},{f5},{f6},{f7},{f8},{f9},{f10}}
M = random(CC^10, CC^10);
F' = M*F;
E = entries F';
randpoly = E#0#0;
mixedVolume(toList(10:randpoly)) --- umxMV = 9

---Now the sspMV for red ERK with eff ss func
---with x1, x2, x8 free
R = CC[x8,x1,x2];
f1 = 3*x8*x1*x2 + 3/2 * x1 * x8 - x8 + 3/2* x2*x1;
f2 = 3/2 * x2*x1 + x2 -1;
f3 = 3/2 * x2*x1 + x8 -1;
mixedVolume({f1,f2,f3}) --- sspMV = 3
```

APPENDIX D

SUPPORTING COMPUTATIONS FOR CHAPTER 7

We provide the `Macaulay2` input code to compute the volume of the Newton-Okounkov body and augMV for the chemical reaction system from Example 7.5.1.

```
--- xdot = p1(p2-p3)
--- ydot = p1(p4-p5)

restart
needsPackage "SubalgebraBases"
needsPackage "Polyhedra"
R = QQ[x,y];
p1 = x^2*y^2 + x^2 + y^2 + 1 -5*x*y;
p2 = 1;
p3 = x*y;
p4 = x;
p5 = y;

-- compute volume of Newton-Okounkov body
G = {p1*p2, p1*p3, p1*p4, p1*p5} --choose to be generating set G
SAGBIbasis = sagbi(matrix {G})
NObody = convexHull(transpose matrix (flatten for i in G
                                      list exponents leadTerm(i)))
volumeNObody = (numgens R)!*volume(NObody)

-- compute mixed volume of system (augMV)
```

```
needsPackage("PHCpack")

R = CC[x,y];

f1 = G#0-G#1;

f2 = G#2-G#3;

mixedVolume({f1,f2})
```